Investigation into low power active electromagnetic damping for automotive applications

A thesis

submitted in fulfilment

of the requirements for the degree

of

Doctor of Philosophy in Engineering

at

The University of Waikato

by

Alista Fow

THE UNIVERSITY OF

WAIKATO

Te Whare Wānanga o Waikato

2015

Dedication

This thesis is dedicated to my brother Charlie Watson.
You're with us in our dreams and memories.

Acknowledgements

I would like to thank Doctor Mike Duke for his supervision and introducing me to the world of engineering. This work has been the result of several years of study and he has kept me on track through this entire period.

Also, I would like to thank those who study and teach engineering and physics who have assisted me through this period. And to those who have shared my office space with not just myself, but also a vibration rig and all the noise that ensued. And I must not forget the technical support who have gone above and beyond, in their assistance. Thank you. Plus a big thanks to the University of Waikato for their academic assistance and Wintec for their financial assistance.

Thanks to all my family and friends that have stood by and helped, or at least stopped me going to pieces. It has been a long and sometimes difficult journey to get to this point. I could not have done it without you.

Abstract

Automobile suspension systems carry out two important functions; road handling and passenger comfort. Hydraulic passive dampers are the most common system employed on vehicles, yet it is well known that passive suspension systems are less effective on lightweight vehicles. Modern damper technologies such as semi-active and active dampers, offer potential benefits when used in these vehicles. An active electromagnetic (e.m.) damper could offer these same benefits with lower power consumption and with less mechanical complexity than existing active suspension systems. This research investigates the effectiveness of e.m. passive and active damping on the performance of lightweight electric vehicles and develops a novel, fully integrated model of the e.m. damper in both passive and active modes.

The proposed e.m. damper consisted of one or more cylindrical permanent magnets that travelled axially through one or more cylindrical solenoids. A magnet/solenoid damper system was modelled for both the passive and active modes. The magnets were modelled as a current carrying solenoid and from Maxwell's Laws the magnetic field was determined. For the passive damper, the magnetic field was used with Faraday's Law to determine the forces generated. In the case of the active damper the magnetic field and the current in the damper solenoid were used to calculate the magnetic force.

Both a passive and active e.m. damper were modelled for a small, one degree of freedom experimental system. The active e.m. damper was modelled as a pure Skyhook damper. There was a good correlation between the modelled and experimental data for the magnet, the passive and the active Skyhook dampers. The passive damper model was scaled up as a two degree of freedom system using realistic values for a road legal lightweight electric vehicle and demonstrated that sufficient passive damping could be achieved for automotive uses, but at the price of excessive mass. For the scaled up active damper model, sufficient force could be achieved with a mass similar to a commercial hydraulic damper. The power consumption was less than 5 % of an equivalent active hydraulic suspension system.

This demonstrated that the passive damper was currently impractical for lightweight electric vehicles, but the active electromagnetic damper was of sufficiently low weight and power consumption: had enough authority and offered sufficient passenger comfort benefits to include in future lightweight electric vehicle designs.

Contents

List of Figures

List of Tables

Glossary

Active Damper :   A damper that can introduce energy into a suspension system under a controller.

E.M. :   Electromagnetic.

E.R. :   Electrorhelogical.

LVDT :   Linear Variable Displacement Transducer.

M.R. :   Magnetorheological.

Passive damper :   A damper that has no external supply of energy or external control.

REALTIME :   A VISSIM package that allows realtime input, processing and output of control signals.

Regenerative Damper :   A damper that converts the motion of damper travel into electricity for vehicle use.

Semi-active damper :   A passive damper that has external control, but does not introduce energy into the system.

SIMULINK :   A MATLAB simulation software package using a graphic interface.

VISSIM :   An engineering simulation software package using a graphic interface.

Chapter 1

Introduction

1.1   Introduction

In automotive design the suspension system is of high importance in providing a comfortable ride and in providing safety when the automobile is accelerating, braking, travelling or cornering. With conventional passive systems these two design considerations can be mutually exclusive. A third consideration in the design of the automobile and its suspension is the amount of suspension travel. The designer of such an automobile therefore has usually to reach a compromise solution between the safety, comfort and travel of the suspension. In the past the only solution available to the designer was to use passive damping using an oil filled damper or similar. In recent years advances in technology have allowed the use of semi-active and active damping.

In the field of automotive suspension passive oil damper systems have been developed to a very high degree. It is unlikely that any major advances will be made in totally passive dampers in the foreseeable future. Semi-active systems such as magnetorheological dampers using a Skyhook algorithm have become a mature technology that is now commercially available on a number of production automobiles. These systems have many of the advantages of an active system and achieve much the same performance without the requirement of inputting power into the suspension system. However the addition of power to the damper can achieve significant increases of performance of both the passive and semi-active dampers. Such active systems in the past have primarily been hydraulic using kilowatts of power, but with advances in modern technology an investigation is being into the use of such dampers in lightweight electric vehicles using electromagnetic systems.

If a low power active damping system were able to be produced this would be of utility in most automobiles, but particularly it would benefit lightweight electric vehicles. Most electric vehicles are designed to be of lightweight so as to make the most efficient use of the energy stored on-board. However the lightweight of these vehicles makes the use of a passive dampers less effective in increasing ride

comfort and providing safety to the vehicle. If a low power active suspension can be developed this may produce a net benefit to the vehicle in safety, comfort and power consumption. Due to the energy density of current energy storage devices the less power utilised in an active suspension, the more power is available for propulsion. This would thereby extend the range of the vehicle over other types of active suspension systems.

While there are several automotive manufacturers conducting research on active suspension systems, much of this research is proprietary and not available to the academic community. Of those that are known few have been placed into production. This is partly due to the use of hydraulic systems or problems that have been faced in implementing a fully active electromagnetic suspension. Previous research has primarily focused on the use of regenerative electromagnetic suspension systems which are designed to recover the energy that is normally dissipated by a suspension system or they are designed for automobiles of average weight. The University of Waikato has a history of research into electric vehicles and their students have designed and constructed a road legal electric car from scratch. The suspension on this vehicle uses commercial oil dampers. One of the questions asked was "is it possible to design an electro-magnetic suspension system that would be suitable for use on this car?" This would be able to recover energy to the battery or if an active system it would be able to provide a good response to the road surface therefore improving comfort, road contact and possibly energy.

Research was therefore done into modelling an active and a passive electromagnetic damper from first principles. This was to determine the damping that could be provided to a system and ultimately, when scaled up, it would determine if such a system would be of use to a lightweight car. The steps involved in this included modelling of the magnet and the suspension system. When the model has been verified, then this model is itself used in a model of a passive damper. This magnet model is also used separately in another model that represented an active damper. The passive and active model then had to be verified by using a single bump response in the time domain and also using a continuous pseudo-sine wave to test both the time domain and frequency domain response of the modelled dampers.

The aim of the proposed research is to determine if it is possible to model a passive electromagnetic and an active electromagnetic damper for use in the University of Waikato electric vehicle fleet. With a model of an electromagnetic damper it would be possible to determine whether the a damper with enough authority to successfully damp the electric automobile will also have a sufficiently small mass so as not to be detrimental to the vehicles performance.

1.2   The Report

The first part of this report, Chapter 2, is a survey of previous work that has been conducted in this field. An examination is made of the damping strategies that are currently available, namely passive, semi-active, regenerative and active damping. Further research is conducted into the use of these strategies using electromagnetic elements in the suspension system. The authority of the system, the mass of the dampers and the power consumption are noted as these are of crucial design importance. At the end of chapter 2 the research aims for this thesis are specified.

Based on the finding of the Literature Review, Chapter 3 proposes a strategy to model, test and validate the passive and active dampers proposed for this research.

In Chapter 4 a magnet model is developed from Maxwell's equations. This model is then used to simulate the magnet magnetic fields generated by the permanent magnet. The model of the magnet is validated by comparing the predicted magnetic field of prototype magnet with the measured fields.

Chapter 5 is an examination of modelling a passive damper. A passive e.m. damper model is required to simulate a semi-active damper or regenerative damper. A modelled damper is then compared with a prototype damper and the model is then scaled to produce a model of a damper suitable for use in automotive applications.

The Active damper is examined in Chapter 6. A model of the active damper system is created and the modelled behaviour of the system is compared to a prototype system. The model active damper is then scaled to determine the suitability in automotive applications.

Discussion of the results and conclusions are given in Chapter 7. There are also recommendations for further research.

Chapter 2

Literature Review

2.1   Introduction

Overview

The sources used in this review included journals, conference papers, patents, text and reference books as well as internet sources. Most sources were from journal and conference papers. A search was conducted for material dealing with electromagnetic dampers and damping; electromagnetic suspension, regenerative suspension, active suspensions, semi-active suspensions and energy requirements of suspensions.

Key Sources

In the area of active control and semi-active control there were thousands of papers. This text examines papers that were important or of relevance to the subject of the thesis. Some indicative papers were also introduced to show trends in the relevant fields of study

Of individual authors, Dean Karnopp has made significant advances in the field of vehicle dynamics, with particular emphasis on active damping and his development of Skyhook damping for semi-active systems. He also proposed electromagnetic systems for automotive damping using both passive and active elements.

Key Journals in this field were "Vehicle System Dynamics", "International Journal of Vehicle Design and "Journal of Sound and Vibration".

For searching in Google Scholar and the Engineering Village many key words used in combination. In all searches dealing with electro-magnetic elements several versions of the term were used. These included 'electro-magnetic'. 'electromagnetic', 'EM' and 'magnetic'. In the following keywords, EM was used for searches that used all four variations. Key word searches included 'EM damping', 'EM suspension', active suspension', 'semi-active suspension', 'skyhook' and 'automotive damping'. It should be noted that when using the key words 'EM suspension', many of the entries returned were for magnetic levitation systems.

Overview of Types of Automotive Damping Systems

The University of Waikato possesses a small fleet of electric vehicles. These include: a commercial electric motor scooter: A Suzuki Carry van that has been converted on site for electrical propulsion: the Ultracommuter (figure 2.1a) which was built at the University of Waikato to original plans and the BEV (figure 2.1b), which is a one person electric vehicle which was wholly designed and built at the University of Waikato. As these vehicles are lighter than most comparable automobiles, commercial dampers are less effective than on heavier automobiles. This facilitates a need to investigate alternative suspension technologies for these vehicles.

(a) The University of Waikato Ultracommuter

(b) The University of Waikato Battery Electric Vehicle (BEV)

Figure 2.1: Electric vehicles built by the University of Waikato.

This thesis will examine the four types of damping used in the damping of automotive motions, namely Passive, Semi-Active, Regenerative and Active. A particular emphasis was placed on the performance of these damping strategies with regards to lightweight electric vehicles of similar type and weight as the University of Waikato electric fleet.

Definitions of the types of damping used in vehicles would be defined as follows.

Passive Suspension   The most common suspensions used are passive suspension systems. This damping is usually achieved by moving a mechanical element through a liquid, turning the energy of motion into heat. The force generated by the damper is always opposite to the relative velocity of the sprung mass and the unsprung mass. Generally a passive suspension has no energy input and no requirement for any control inputs other than the relative motion.

Semi-Active Suspension   A semi-active suspension is usually based upon a passive damper. It was observed at various times through a cycle of motion of a passive system that the action of the damper could be detrimental to the final damping. By being able to switch off the damper during these periods, the damping performance can be improved. The ability to turn on and off the force element at the command of a controller is the prime characteristic a semi-active suspension. A semi-active suspension requires energy to switch the damper on and off, but no energy is used to

directly oppose the motion of the sprung mass. Commercial semi-active suspension systems for automobiles use electrorheological and magnetorheological dampers. In a semi-active suspension system the force of the damper either opposes the motion of the relative velocity or is ideally equal to zero.

Active Suspension   An active system contains an element that can generate a force in the suspension system independent of the relative motion. This force can either oppose or act in concert with the motion of the relative velocity of the mass. The force can be generated by various means including; mechanical, electromagnetic or hydraulic. Energy is required to be supplied to the system to provide the damping force. In addition a controller is required to ensure the most efficient use of the forces thus generated. For this thesis an active suspension was any system that can create a force that was independent of the motion. This includes force actuator–spring and force actuator only systems.

Regenerative Damping   Another type of system that is being researched is the regenerative suspension. This is usually based upon a passive element. Instead of converting the kinetic energy of the motion of the sprung mass into heat, it is instead converted to electrical energy or other energy that can be stored or transmitted to other systems in the automobile. This regeneration can be switched on and off as a semi-active suspension. Alternatively the energy regenerated can be stored and then used to supply energy to active elements in the suspension system. To quote Sharp and Hassan (1986) "If an automotive suspension system is well endowed with working space relative to the road roughness, good active systems offer modest performance advantages over good passive systems, and semi-active (dissipative) systems employing passive springs to support the body mass and rapidly variable dampers can almost be as good as fully active systems. As the suspension working space becomes more restricted, the advantage of active over passive systems increases, and in extreme cases will be substantial. The performance of the semi-active damper lies between that of the passive damper and the active damper. Obtaining the best performance from any particular type of suspension over a variety of operating conditions, involving road roughness and vehicle speed variations and a fixed working space, requires the adjustment of suspension parameters though wide ranges. Fully active systems are capable, in principle, of such adjustment, and through avoiding the need to compromise can be made much better than fixed parameter passive systems."

Measuring the performance of different control strategies.   To determine the best control strategies for a suspension system there should be some quantitative means of determining the relative performance of the various damping strategies. Work by Sharp and Hassan (1986) proposed using the parameters of passenger

discomfort, suspension working space and the dynamic tyre parameters. These were measured using ISO weighting parameters.

2.1.1 History of Vehicle Dampers

Early suspensions dealt with horse drawn carriages traversing the rough roads of the mid nineteenth century. The better carriages of that period had long bent leaf springs called semi-elliptics. When placed back to back they form a full elliptic suspension. This provided a very soft ride and damping was achieved solely by the inherent friction between the leaves in the springs. This system was easy to manufacture and possibly worked tolerably well for the speeds of the period and the quality of the roads. Dixon (1999)

With the invention of the horseless carriage, the fitting of dedicated damping devices to vehicle suspensions followed rapidly. Up until 1910 dampers were hardly used at all. Then from 1910 until 1925, mostly dry friction dampers (snubbers) were used for suspension. Early friction suspension consisted of two sliding disks operated by two arms. As the arms moved, they slid the disks against each other creating friction. An early suspension of this sort was the Truffault-Hartford Suspension. The amount of friction force, F_s was, given by 2.1

$$F_s \geq \mu_s F_n \tag{2.1}$$

where μ_s was the co-efficient of static friction and F_n was the normal force being applied. The amount of damping was determined by the normal force applied to the disc and in later systems, such as the Hartford Telecontrol damper, the damping could be changed by altering the normal force. This type of damper provided Coulombic damping only. Dixon (1999)
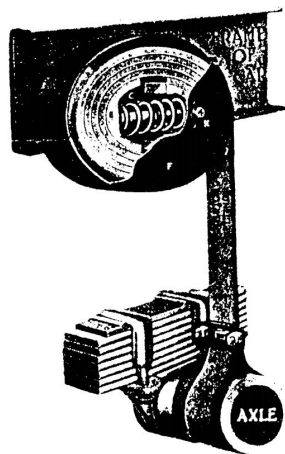
Figure 2.2: The Gabriel Snubber (1915); This used a leather strap around sprung metal or wooden blocks to give restraint in the rebound. [Source Dixon (1999), originally from Simanaitis. (1976)]

The dry-friction block and belt snubber was invented in 1915 by Claud Foster. This was manufactured in large numbers by his Gabriel Company and was usually known as the Gabrielle Snubber. Sales were probably based on reliability and low cost rather than performance. Spring loaded blocks were mounted on the body or chassis rails, with a leather belt wrapped around the blocks and then fixed to the wheel upright or axle as in figure 2.2. In upward motions, the snubber had no effect; the spring-loaded blocks taking up any slack. The downward motion was opposed by the friction of the belt tightening about the blocks. This produced a fully asymmetric Coulombic damping, with damping only occurring on the downward movement of the wheel. Dry-friction snubbers were in wide spread use into the 1930s. Dixon (1999)
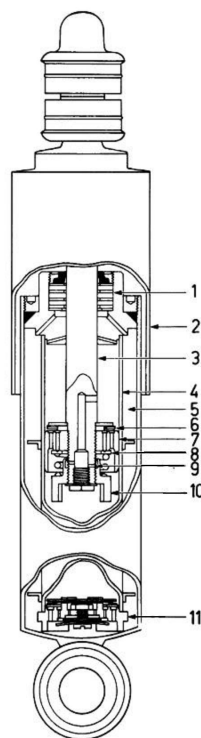
Figure 2.3: A double tube damper, circa 1950. The key to the damper: 1. Seal. 2 shroud; 3 rod; 4 inner cylinder; 5 annular foot and gas chambers; 6 piston compression valve; 7 piston; 8 extension valve; 9 parallel hole feed; 10 adjuster; 11 foot valve. [Source Dixon (1999), originally from Koni]

Even though early dampers used Coulombic friction as their main damping mechanism, Coulombic friction was undesirable in a suspension, because it locks the suspension when there were small forces and gave a poor ride on smooth surfaces. This was called boulevard jerk. In modern times, in order to optimise ride quality every effort is made to reduce Coulombic friction. An alternative to Coulombic friction for damping was hydraulic viscous damping. Viscous friction is proportional to the flow rate of the working fluid and was thus ideal for damping. Unfortunately viscous damping is very sensitive to temperature. Fluid dynamic damping, caused by energy

dissipation from turbulence, is proportional to the square of the flow rate. While it produces forces that were too large at high speeds and too small at low speeds, the resulting damping was dependant upon the fluid density and not the viscosity, so was less dependant upon temperature. In 1901, C.L. Horock patented a telescopic hydraulic damper unit, which laid the foundation for the modern type. In 1905 Renault patented an opposed piston hydraulic damper and patented improvements to Horocks damper, establishing substantially the design used today. Renault used the piston type damper on his racing cars but not his production cars. In 1910 oil filled dampers came into use on aircraft under-carriages and in 1928 hydraulic dampers were first supplied as standard equipment on cars in the United States. The Armstrong telescopic damper was patented in 1930 and in 1934 Monroe began manufacture of telescopic dampers. Koning introduced adjustable telescopic dampers in 1947 as in figure 2.3. And in 1950 the gas pressurized single-tube telescopic damper was invented and manufactured by de Carbon. During the 1950s telescopic dampers became more widely used on passenger cars. Although other types were used, the telescopic hydraulic damper was accepted as the norm for cars and motorcycles. Dixon (1999)

While the telescopic hydraulic damper is the dominant system, there have been other types over the years. The Moulton rubber suspension system was used on the Morris Mini for 34 of its 41 year production run. Dr. Alex Moultan originally wanted the Mini to have Hydrolastic suspension, which was used on the Morris 1100. Hydrogas suspension was an evolution of the hydrolastic suspension. Famously it was used on the 1986 Porsche Rally car that entered the Paris-Dakar Rally and today is in the MGF Roadster. Since the early 1950s, Citroën have been using hydropnuematic suspension. This was a whole car system that can include the brakes and steering. Longhurst (2006)

In 2006, Audi launched the new TT model and one of the innovations was magnetic semi-active suspension. It is a form of damping technology developed from Delphis Magneride system. Delphi used to be a division of General Motors and developed the first version of the Magneride in conjunction with LORD Corp. The initial version was used in the 2002 Cadillac Seville STS. The dampers were similar to normal hydraulic dampers except that they were filled with a magnetorheological fluid. This fluid is synthetic hydrocarbon oil containing fine magnetic particles held in suspension. Longhurst (2006)

Active suspension systems have been applied to racing cars, notably in the FIA Formula One cars 1983 Lotus 92, the 1987 Lotus 99t and most successfully in the 1991/2 Williams FW14B. After the 1993 season Active suspension system systems were banned from FIA Formula One racing. The First Full Active suspension on a commercially produced private automobile was the 'a' model of the 1990 Nissan Infiniti Q45. This featured a hydraulic active suspension in addition to springs to carry the weight of the vehicle.

2.1.2   Components of Suspension

In most modern automobiles the suspension is comprised of three elements: a wheel, with pneumatic tyre, which connects the wheel to the ground: the spring which carries the main weight of the car and the damper which removes unwanted oscillations from the sprung mass. In figure 2.4 a typical system is illustrated with a tube in tube damper in parallel with a spring.
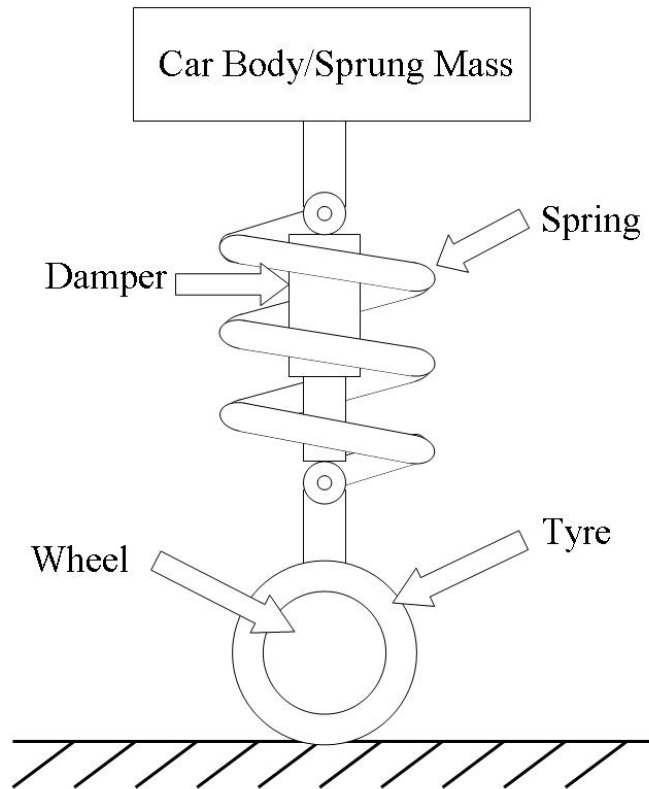
Figure 2.4: The components of a two degree of freedom suspension system.

Tyres   Pneumatic tyres were originally developed in 1888 by John Boyd Dunlop. They act, in conjunction with the wheel, as a second order low pass filter. This attenuates most frequencies above 10 Hz such as those created by small road irregularities. The tyres also provide friction with the surface for acceleration, braking and when cornering. Duke (1997).

The Spring   In a commercial car the main body of an automobile is isolated from shock by the use of a spring system. For most modern vehicles they consist of a metal helical coil spring or a leaf spring. Some systems such as 'hydrolastic' systems use a compressed gas as a spring. There are many ways that the spring and wheel can be connected to the body of the vehicle, such as MacPherson strut, double wishbone, trailing arm and De Dion to name just a few. These are well covered in

books such as Dixon (1999) and Gillespie (1992).

The spring acts as a second order low pass filter with a break frequency of between 1 Hz and 2 Hz for typical road vehicles. The spring also acts as an energy storage device. It compresses when the vehicle travels over a bump in the road and stores the energy as strain energy. When the bump has passed, the energy is released by the extension of the spring. It is well known that for most vehicles a lower spring stiffness produces better ride comfort for the passenger. However there is a lower limit to the spring stiffness that is useful in an automobile. If the spring stiffness is set to low and the spring fully compresses, then no damping will be achieved. Duke (1997).

The natural undamped frequency of oscillation of the vehicle depends upon the spring stiffness and the mass of the sprung mass. By reducing the spring stiffness, the resonant frequency decreases. For very low spring stiffnesses, the weight of the passengers can dramatically affect the ride height equilibrium position. If enough passengers enter the vehicle then the suspension would then end up resting on the bump stops. Bump stops are normally blocks of rubber or other elasticated material that sit at the ends of the suspension travel. These are designed so that in severe conditions they act as an emergency spring system and prevent metal to metal contact. Therefore the selection of the spring stiffness is a compromise between the ride comfort of the passenger and the suspension travel.

The Damper   In vehicles, the function of the damper is to reduce the oscillations that occur in a sprung weight travelling over a road surface that provides random vertical forces. The most common damper used in mass produced vehicles is the hydraulic damper of the tube in tube type. This works by converting the kinetic energy of the sprung mass into heat energy that is then dissipated. With a telescopic tube damper, when it is compressed, oil is forced through small orifices in the piston causing friction between the oil and the inside of the damper. In this type of damper the damping is dependent upon the density of the fluid rather than the viscosity of the liquid. This ensures a consistent damping response over a wide range of temperatures. When combined with the spring, on a bump the spring stores on the compression and the damper dissipates the energy on the extension of the spring. It is common on road vehicles that the compression (bound) and extension (rebound) damping values were different. Hence when a vehicle hits a vertical bump, the damping rate is lower to reduce the force transmitted to the chassis and the passenger cabin. On the rebound there is a much higher damping rate as the car settles back to the equilibrium position. Duke (1997). As is illustrated in figure 2.5 the force was different for a positive velocity and a negative velocity.
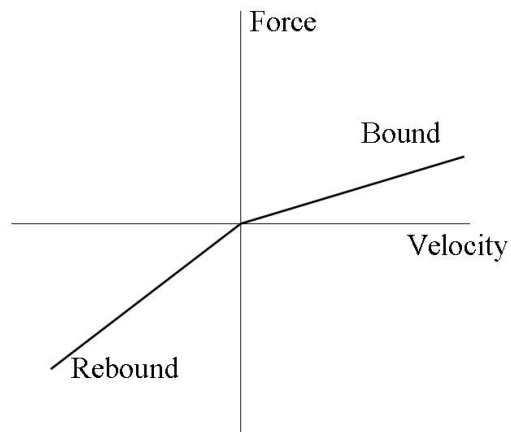
Figure 2.5: Force vs. velocity for the bound and rebound of a suspension system.

2.1.3   Suspension Design Considerations.

When trying to determine the relative performance of different control strategies there should be some quantitative measurements that can be used to determine the relative performances. Sharp and Hassan (1986) give three measurable requirements in modern suspension systems: passenger comfort, road holding and rattle space. In the design of a suspension system these three factors are often contradictory. With conventional passive systems, improving one of these factors is usually at the expense of one or both of the other factors. In sports cars the road handling is usually optimised and the passenger comfort can be a secondary consideration. In luxury cars the ride comfort is accentuated at the expense of road handling. In off road vehicles the rattle space is often an important consideration due to the possible range of motions. One of the possible benefits of an active suspension system is that a compromise does not have to be made between these three factors.

Passenger Comfort   A common measure of passenger comfort is given by the standard ISO 2631/1 (1997). This uses a weighted value of the root-mean-square (r.m.s.) vertical accelerations to determine the level of discomfort a passenger feels. The higher the accelerations, then the higher the level of discomfort that is experienced by the passenger. When designing a suspension, the aim is to reduce the r.m.s. acceleration that a person experiences to the smallest possible amount. While the ISO 2631/1 standard deals with both vertical and lateral accelerations, it is usual amongst researchers to model a quarter car suspension system as a two degree of freedom system and they therefore only use the vertical accelerations.

Road Holding   This is determined by the constancy of the force between the tyre and the road surface. Forces are generated between the vehicle and the surface of the road by the vehicle accelerating, decelerating and cornering. The maximum

friction force available is directly related to the friction coefficient of the surface and the normal force supplied by the wheel. If there is variation in this force then the limiting friction force available becomes the minimum force available for ground holding during one oscillation of the vehicle.

Rattle Space   Rattle space or suspension deflection is a third important concern for a suspension designer. As cars have become more compact and more streamlined, the amount of working space for the suspension system has reduced. This rattle space is the vertical height that the suspension travels when in normal operations. When a tyre travels a greater distance than the rattle space available, then damage to the suspension can occur. To prevent this some designers use springs with variable spring rates. As the travel approaches the limits the spring rate increases. Just about all automotive suspension systems also have bump stops, which are rubber blocks designed to stop damage to the vehicle if the vertical travel distance exceeds the rattle space available.

Modelling of Suspension Systems

It was common for researchers who were investigating suspension systems and wanting to model the behaviour of the suspensions theoretically to use a Single Degree of Freedom system or a Quarter car model. Both of these models are illustrated in figure 2.6.

For the Single Degree of Freedom model in figure 2.6(a), the ground surface motion was represented by z_0. This travels up in down only in the z direction. The car body was represented by the sprung mass, m_1 and this has a displacement of z_1. Between the ground and the sprung mass were a spring, with a spring rate of k and a damper with a damping coefficient of c. In this model movement was only permitted in the z direction.

However in reality most road vehicles also have a pneumatic tyre. This tyre, with its associated suspension components on acts as an unsprung mass which was independent of the road surface and of the sprung mass. Also the pneumatic tyre acts as a spring and as a damper. Usually the tyre acted as a spring with a spring constant up to an order of magnitude greater than the main suspension spring. In the Quarter Car model illustrated in figure 2.6(b), z_0 remains the same as previously, m_1 is now the unsprung mass, z_1 was the displacement of the unsprung mass, m_2 was the sprung mass and z_2 was the displacement of that mass. The spring rate and damping coefficient of the tyre were given by k_1 and c_1 and for the main suspension k_2 and c_2. Often the damping coefficient of the tyre was considered low and was then ignored.

In modelling of real world vehicles, Gysen *et al.* (2008b) gives nominal parameters of a typical automobile as :

k = 30 kN/m
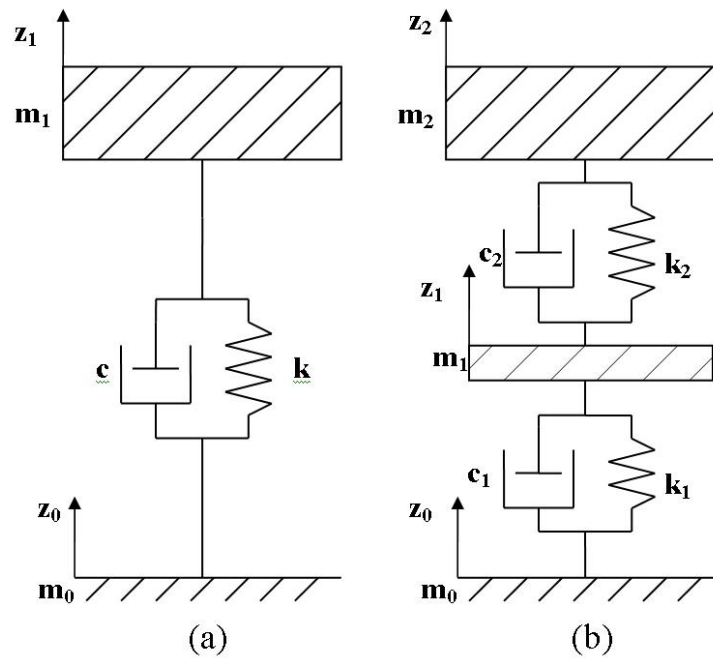
Figure 2.6: (a) A Single Degree of Freedom model and (b) a Quarter Car model.

$k_1 = 160$ kN/m

c (a), c_2 (b) $= 1,200$ Ns/m

m_1(a), m_2(b), $= 450$ kg

m_1(figure b) $= 40$ kg

.

2.2 Passive Suspension Systems

In examining passive damping, this study can be divided in to two separate components. There was the physical damper itself and the equations that cover the motion and control of the damper. The hydraulic damper is the most common type used in private automobiles and has been described previously. The action of this damper gives a force that was only resultant upon the relative velocity of the elements of the damper. However, modern research was exploring whether the damper can be given a non-linear response or a response that is determined by other factors. The basic equations governing the motion of the passive damper in the automobile are covered in Dixon (1996), Dixon (1999) and Gillespie (1992).

In relation to low weight vehicles the accelerations and road harshness experienced by the occupants increase as the weight decreases. For a classical one degree of system using a passive damper, as illustrated in figure 2.6 (a), the force equation is given by 2.2

$$m\ddot{z} + c(\dot{z}_2 - \dot{z}_1) + k(z_2 - z_1) \tag{2.2}$$

where m is the sprung mass, $\ddot{z}$ is the acceleration of the sprung mass, c is the damping coefficient, $\dot{z}_2 - \dot{z}_1$ is the relative velocity of the sprung mass and the ground surface, k is the spring constant and $(z_2 - z_1)$ is the relative displacement of the sprung mass and the surface. Taking the relationship between the damping coefficient which is 2.3

$$c = 2\zeta\sqrt{mk} \tag{2.3}$$

,

where ζ is the damping ratio, which is the ratio of the damping coefficient of the damper to the critical damping coefficient of $2m\sqrt{k/m}$. Then 2.3 can be substituted into equation 2.2 and then equation 2.2 can be rearranged to give 2.4.

$$\ddot{z} = \frac{2\zeta\sqrt{mk}(\dot{z}_2 - \dot{z}_1) + k(z_2 - z_1)}{m} \tag{2.4}$$

.

Looking at the relationship between damping and mass, this can be seen to be given in 2.5.

$$\ddot{z} \ \alpha \ \frac{1}{\sqrt{m}} \tag{2.5}$$

.

From this relationship it can be seen that as the mass of the vehicle decreases the acceleration and consequently the ride harshness felt by the passengers will increase, as is the case for the University of Waikato's electric vehicle, the Ultracommuter. This vehicle has half the weight of many commercial sedans which means for the same damping ratio and experiencing the same velocities and displacements, the occupant of the Ultrcommuter will be experiencing accelerations over 40% larger than the occupant of the heavier vehicle,

2.2.1   New Concepts in Passive Damping

Modelling as a mechanical circuit.

Much of the early work on the dampers was purely experimental. However a theoretical model of the damper in a system was required so as to predict the behaviour of the unsprung mass, the spring and the damper combined. This was of further relevance when determining the motions of a two degree of freedom system. One well known model that has been of use was using the mechanical elements of the spring, damper and unsprung mass as an analogue of an electrical circuit.

In 1933 F.A. Firestone considered a mechanical system as an analogue of an electrical circuit. "By considering each mass in a linear mechanical system as having two terminals, one fixed in the mass and one fixed to the frame of reference, every

linear mechanical system was reduced to a multiplicity of closed mechanical circuits to which force and velocity to Kirchoff's Laws may be applied." Firestone (1933)

The oldest Electrical-Mechanical analogy was the Force Voltage Analogy where force was analogous with voltage and velocity was the analogue of current. Through the work of Darrieus in France in 1929, Haehnle of Germany in 1932 and Firestone (1933) they each independently proposed a Force-Current analogy. In this the Current represented the Force, the Voltage was the analogue of the velocity and the mechanical ground was analogous to the electrical ground of the circuit. Using these analogies the damper was the mechanical equivalent to a resistor in that it dissipates energy Smith (2003).

This was developed into the well known electrical-mechanical anology where force represents the voltage, velocity the current, displacement the charge, the damper is the resistor, the spring is the capacitor and the sprung mass is the inductor. This has proved a useful description for mechanical damping circuits for many years.

However, for work on a new suspension element, research was conducted where the spring was used as the equivalent to the inductor, in that it stores energy and the sprung mass represented a capacitor where one end was grounded. Smith (2003) However due to having a capacitor with one end grounded, the mechanical system was not a direct analogue of the electrical circuit. This imposed a restriction on the class of passive mechanical impedances which could be physically represented. Another problem was that the suspension strut needed to have a small mass compared to the vehicle body and wheel hub. This itself imposed further restrictions on the class of mechanical impedances that could be practically realised using the classic spring-mass-damper. Smith and Wang (2004)

The Inerter

M.C. Smith of the University of Cambridge proposed a new theoretical suspension element that would be the equivalent of an ungrounded capacitor. He defined this new element, which he called an 'Inerter', as "a mechanical one port device such that the equal and opposite force applied at the nodes was proportional to the relative acceleration between the nodes." This inerter was a new mechanical element in addition to the damper, but which could be tuned to work in conjunction with the damper. By the use of the two elements together there was a potential increase in the performance of the suspension system The force generated by the inerter element was given by 2.6

$$F = b(\dot{v}_2 - \dot{v}_1) \tag{2.6}$$

.

where F was the damper force, b was the inertance of the inerter in kg and $\dot{v}_2 - \dot{v}_1$ was the velocity of the sprung mass relative to the ground surface. He then asked
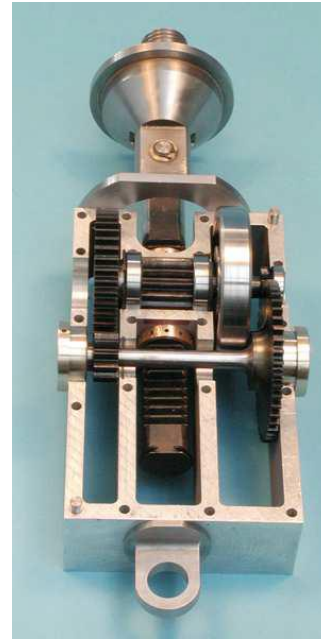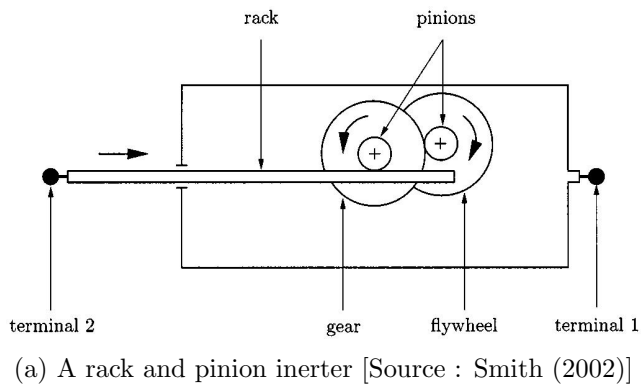
(b) Rack and pinion proto-type [Source : Papagergiou and Smith (2005)]

(a) A rack and pinion inerter [Source : Smith (2002)]

(c) A rotary inerter [Source : Smith (2003)]
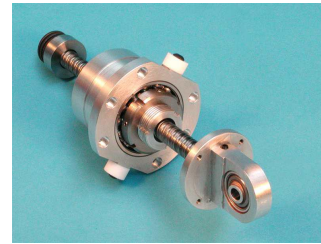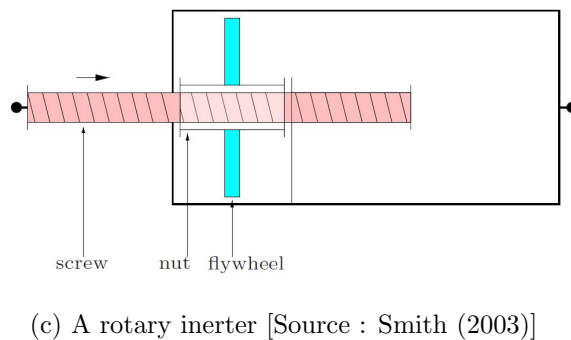
(d) A rotary prototype [Source : Papagergiou and Smith (2005)]

Figure 2.7: Inerter designs by M.C. Smith

the question "Is it possible to construct a physical device such that the relative acceleration between its end points was proportional to the applied force?" Smith (2003). By 2003 he had two different mechanisms that achieved these ends. These are illustrated in figure 2.7. Both used mechanical systems to store energy. The total energy being stored was dependent upon the inertance and the change in velocity. The energy, E, was given by 2.7

$$E = \frac{1}{2}b(\dot{v}_2 - \dot{v}_1)^2 \tag{2.7}$$

Experimentation demonstrated an 8.17% improvement in ride quality with an inerter in parallel with the damper and a 9.26% improvement when in series. There was no improvement in tyre loads with the inerter in parallel, but a 6.53% improvement when in series, Smith and Wang (2004). Further research has shown that there

were regions of non-linear behaviour which were detrimental to the performance of the inerter except in cases of very low spring rates, Wang and Su (2008). Smith et al had noticed non-linear spiking in their research and noted that this could be overcome by adding a buffer network to the inerter system Smith and Wang (2004). While the original inerter designs have been purely mechanical in nature, further research by Wang *et al.* (2011) has produced a hydraulic inerter.

The Inerter is a very important area of research in the modern suspension system. It allows an improvement in the ride comfort and tyre loading with a purely passive element. This allows for better design of dampers. This increase of performance did not require active elements, a controller or a power input.

Dead Band Damping

A more advanced form of passive damper was one where the construction was designed to give non-linear damping. This non-linear damping coefficient was built into the device and was not changeable once installed. Research was conducted by Duke and Fow (2012) into non-linear damping of a passive damper for a tractor seat. In tractors there was no spring/damper to absorb sudden shocks produced by the road surface. The only suspension involved was the tyre and the tractor seat. Work was done to determine if the use of passive, non-linear spring and damping units could offer an improvement in ride performance compared to linear steel springs. Two elements were explored: The use of non-linear spring elements, which allowed for a 'soft' spring rate in the mid range of the motion and a 'stiff' spring range at each extreme of the motion. It is well known that a soft spring rate better attenuates the higher frequency vibrations, so this was considered desirable in the equilibrium position. Also it is known in passive systems that low damped mass-spring-damper systems were also better at attenuating higher frequencies. A "dead band" was introduced in and around the equilibrium position of the tractor seat, this region of motion produces no damping. During the travel of the seat damping occurred at the extremes of motion and was turned off as it travelled near the mid position. The force generated by such a damper is shown in figure 2.8. Simulations were conducted which demonstrated that the non-linear damper out performed the linear damper in reducing RMS acceleration. The experimental results also confirmed that the dead band damping could reduce the RMS acceleration experienced by the operator. The trade off was that the system was much more sensitive to harsh bumps, often with the seat hitting the end stops.

This experiment was conducted using a switchable damper, so was in effect a semi-active system whose control algorithm was based upon the displacement of the damper. However there was no reason that this can not be achieved purely mechanically. In the case of an e.m. damper the dead band can be created by the placement of the coils or the placements of the metal being used to generate eddy
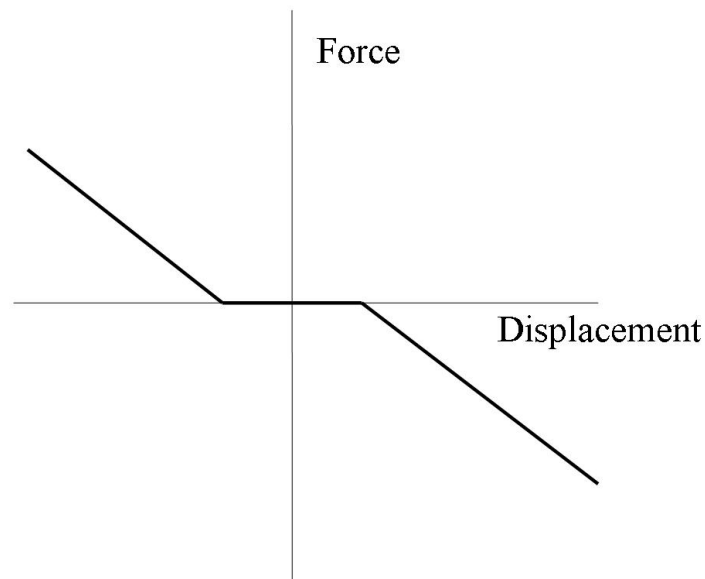
Figure 2.8: Force vs. Displacement for a deadband damper.

currents. By careful design this may provide a totally 'passive' damper that may show an improvement of performance over existing forms of e.m. Passive dampers.

2.2.2   Passive E.M. Damping – Eddy Currents

Physically, the eddy damper is the least complicated e.m. damper to construct. In its simplest form it consists of a magnet (often cylindrical) that moves relative to a metal plate or inside a metallic tube. The motion of the magnet creates a change in the local magnetic field which causes the mechanical energy to be converted into electrical energy in the form of eddy currents which circulate in the metal plate or tube. The resistance of the metal then converts the electrical energy into heat energy which was then transferred to the environment through radiation and convection. The control of an eddy current damper was usually fully passive.

Kanamori *et al.* (1994) noted that the advantages of the eddy current damper include that the damping force was produced without any physical contact. This reduced friction, abrasion and fatigue. This type of damper also did not produce secondary damping effects due to friction which would produce the less desired Coulombic damping. Kanamori also noted that this system required no lubrication so was suitable for use in vacuum situations. This would also make this technology applicable to modern aircraft which must endure extremes of temperature and pressures. The simplicity of the design and the stability of the damping were also noted.

In their research Kanamori et al used the finite element method to model the damper. Physically this was constructed with two rectangular magnets on either side of a flat aluminium plate as in figure 2.9. The damping coefficient of this damper was given by 2.8

$$C_{obj} = 1/\rho C_o B^2 t S_p \qquad\qquad (2.8)$$

where C_{obj} was the damping coefficient of the damper, ρ was the resistivity of the conducting slab, C_o was a dimensionless damping coefficient that is determined from the ratio of the area of the magnet's pole and the area of the conducting plate, B was the magnetic field in Tesla, t was the thickness of the plate in meters and S_p was the area of one magnetic pole in m^2. Typical values of C_o range from 0.625-0.775 for when the area of the plate was 3 to 5 times the size of the magnetic pole. Using an experimental rig the equation was verified and a damping coefficient of 60 $N\,s\,/m$ was achieved.
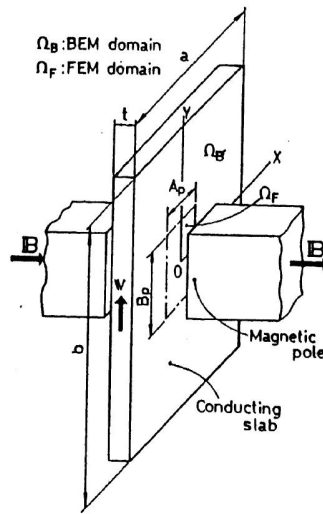
Figure 2.9: An eddy current damper. [Source : Kanamori *et al.* (1994)]

Kanamori *et al.* (1994) examined a damper made of a magnet and a slab of metal, the research being to determine the optimum shape of each element. It was determined that the optimal shape for the slab was a convex-concave shape similar to an optical lenticular lens. The optimal shape of the pole was a convex-plano shape that fitted into the concave side of the slab as illustrated in figure 2.10. It was also determined that the damping coefficient increases with the decrease of the magnetic pole area to conducting slab area ratio. Using the techniques developed a design for an optimal damper and experimentally verified it.

Simeu and Georges (1996) modelled an eddy current 'brake' that consisted of a copper or aluminium disc that was driven in a rotary motion through the air gap in an electromagnet. As the disc rotates, eddy currents were generated by the disc by the magnet. These eddy currents generate their own magnetic field which in turn induces eddy currents in the pole of the magnet. These eddy currents were created so that they oppose the magnetic field of the magnet and will therefore reduce the pole strength of the magnet. In this system, three different behaviour regions were observed
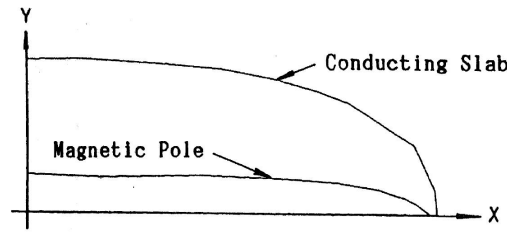
Figure 2.10: The optimal shape of eddy current damper [Source : Kanamori *et al.* (1994)]

1) At low speeds the magnetic induction in the magnet caused by the eddy currents in the plate was negligible. Most braking will occur in this region.

2) The critical speed region where the braking force generated was the maximum. At this speed the eddy currents induced in the magnet were no longer negligible and caused the magnetic strength to be decreased.

3) At higher speeds the eddy currents induced in the magnet will increase until, theoretically, at infinite speed they will totally cancel out the magnetic field produced by the magnet.

The power dissipated by this damper in the 'ideal' case was given by

$$P_d = \pi/(4\rho)D^2 dB^2 v^2 \tag{2.9}$$

where P_d was the power dissipated, ρ was the resistivity of the disc, d was the disc thickness, D was the diameter of a circle with the same area as the pole, B was the magnetic field and v was the velocity of the disc measured at the mid-point of the pole face. The force generated was given by

$$F_d = \pi/(4\rho)D^2 dB^2 v \tag{2.10}$$

where F_d was the force generated by the damper. In the low speed region the eddy current brake acted as a linear damper where the braking force was proportional to the speed. By varying the current to the electromagnet this brake can vary the force being applied.

In an eddy current damper the damping was related to the relative velocity of the components, with higher damping occurring at higher velocities. Matsuoka and Ohmata (2002) proposed magnifying the velocity of the magnet relative to the copper conducting plate by using a lever arrangement. This consisted of two levers, three connecting rods and 8 pins (all of the pins being ball bearings). In addition to increasing the velocity of the magnet relative to the plate, it also increased the friction in the entire system. The actual prototype constructed, magnified the displacement by a factor of 8.72 and was tested at integer frequencies between 1 and 5

Hz. While this damper showed an improvement over no damping at all, there was no comparison to a damper using the same magnets and the same copper conducting plate. While the extra displacement should show an increase in damping over a more traditional eddy current damper, it would do so at the expense of complexity and moving parts that were in contact with each other. The increased displacement will also increase the rattle space required for the damper. Further, it introduces a component of Coulombic damping which may be sufficient to introduce undesirable characteristics to the overall suspension package and the ride comfort of the passengers.

Sodano *et al.* (2006) developed a passive damping system for buildings that utilised eddy currents in a moving conductor to reduce the vibrations in a beam. The damper was passive, and was therefore robust to parameter changes, required no external energy and was easy to apply to a structure. Also it was a non-contact damper, therefore the properties and the dynamics of a structure were unaffected even when large amounts of damping were being applied.

Zheng *et al.* (2006) proposed an eddy current damper with an eight pole electromagnetic rotor rotating inside a cylinder of conducting material. This was tested at frequencies of 90-115 Hz. This showed a reduction of vibration at the resonant frequency of the system tested.

In Ebrahimi *et al.* (2008) it was noted that the spring in a spring–damper system can be the magnetic repulsion between two rare earth permanent magnets. The damping in a suspension system can be supplied by the eddy currents generated by the movement of permanent magnets. Therefore it was proposed that the spring and damper can consist of a single unit that consisted of a pair of magnets where one was connected to the wheel/ground and the other was affixed to the sprung mass. These travelled through a ring of aluminium. The movement in the magnets relative to each other produced an alternating magnetic field which induced eddy currents in the aluminium ring. A dipole moment model was developed to calculate the flux density at a distance. This model gave a discrepancy of 7.5% r.m.s. when compared to experimental results. The prototype damper produced up to 40 Ns/m damping coefficient. The difficulties of such a damper would include a low amount of suspension travel due to the short range of the magnets involved, especially with the pre-loading of the car. Also, the damper would have a strongly non-linear characteristic. Improvements to this system would include the use of a 'stack' of magnets whose poles alternate so as to produce repulsion between each pair of magnets, placed inside a copper tube. The multiple magnets will extend the range of motion. The tube would ensure that the eddy current material was close to the magnetic fields and the copper had a lower resistivity which would increase the current generated and the damping ratio.

Ebrahimi *et al.* (2009b) has modelled, simulated and tested an eddy current damper for automobiles. This was different to his previous designs. The damper,

illustrated in figure 2.11, consists of a conductor as the outer tube and array of axially magnetised ring shaped permanent magnets separated by iron poles as a mover. The series of annular magnets were assembled onto a non-ferromagnetic rod. The magnets were mounted so they face in opposite directions and there was an iron pole piece between each pairing of magnets. It was noted that axially magnetised permanent magnets in the mover result in a higher specific force capability than using radially magnetised magnets.
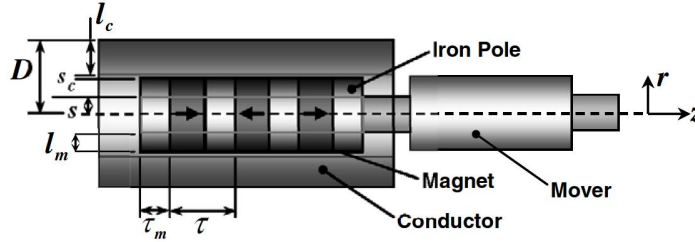
Figure 2.11: An eddy current damper for an automobile [Source : Ebrahimi *et al.* (2009b)]

From the Lorentz Force Law, the relative motion between the conductor and the magnets caused eddy currents to be induced in the conductor. From Lenz's law, these eddy currents created a magnetic flux which opposed the external flux density resulting in a damping force for each pole piece that was given by 2.11.

$$\mathbf{F} = \int_{\Gamma} \mathbf{J} \times \mathbf{B} d\Gamma \qquad (2.11)$$

Where Γ was the conductors volume, $\mathbf{J}$ was the induced current density and $\mathbf{B}$ was the magnetic flux density. The induced current density can be determined from 2.12

$$\mathbf{J} = \sigma(v \times \mathbf{B}) \qquad (2.12)$$

Where σ was the conductors conductivity and v was relative velocity between the magnetic flux density and the conductor. The final force generated along the z axis, being the axis of motion, was obtained by combining 2.11 and 2.12. The final force being 2.13

$$F_z = -\sigma(\tau - \tau_m)v_z \int_0^{2\pi} \int_{r_{inside}}^{r_{outside}} r B_r^2(r, z_0) dr d\theta \qquad (2.13)$$

Where B_r was the radial component of the magnetic flux, r_{inside} was the conductors inside radius and $r_{outside}$ was the outside radius. F_z was the force in the z direction.

A model was created and showed a good correlation between experimental and theoretical results as shown in figure 2.12. In a one degree of freedom system a damping ratio of 0.28 and a damping coefficient of 53 Ns/m was achieved.
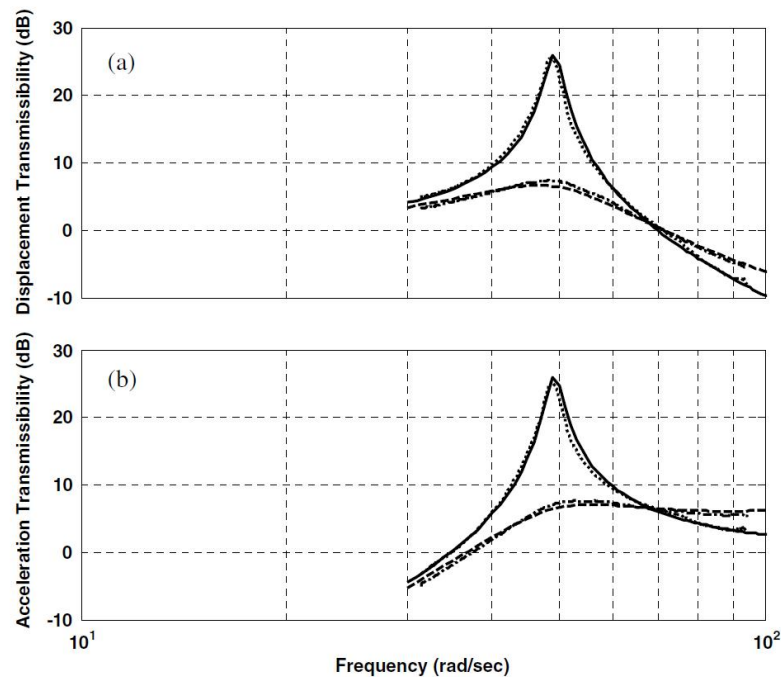
Figure 2.12: (a) Displacement and (b) acceleration transmissibilities of the 1 DOF vibration isolation system for an eddy current damper: –.– experimental with damping, - - - - simulated with damping, ...experimental without damping and ——— simulated with damping [Source : Ebrahimi *et al.* (2009b)]

In Ebrahimi *et al.* (2009a)the damper in Ebrahimi *et al.* (2009b) was developed further. Using the same damper design a model was developed for automotive use. It was concluded that the weight and cost of an Eddy Current Damper were not appealing, but the performance may be of interest. The advantages noted were that the damper was oil free, non-contact and could offer high reliability and durability, partially through its very simple design.

2.2.3 Passive E.M. Damping – Induction

The basic theory behind electromagnetic induction goes back to the time of Michael Faraday. In Karnopp (1989) it was conjectured that this induction could be used for damping in automobiles. Karnopp notes that when an electrodynamic actuator coil was shorted or connected to an external resistor, then the device acts as a linear mechanical damper. When the coil was shorted, the damping coefficient reaches its maximum value. He also notes that because the resistance can be varied rapidly electronically, then it can also act as a semi-active damper.

For an electromagnetic damper that consists of a coil travelling through a constant magnet field as illustrated in figure 2.13, Karnopp determined that the maximum force generated by the damper was given by 2.14.

(a) The magnets (above) and coil (below) [Source : Karnopp (1989)]

(b) The plan view of the magnetic magnets and pole pieces [Source : Karnopp (1989)]
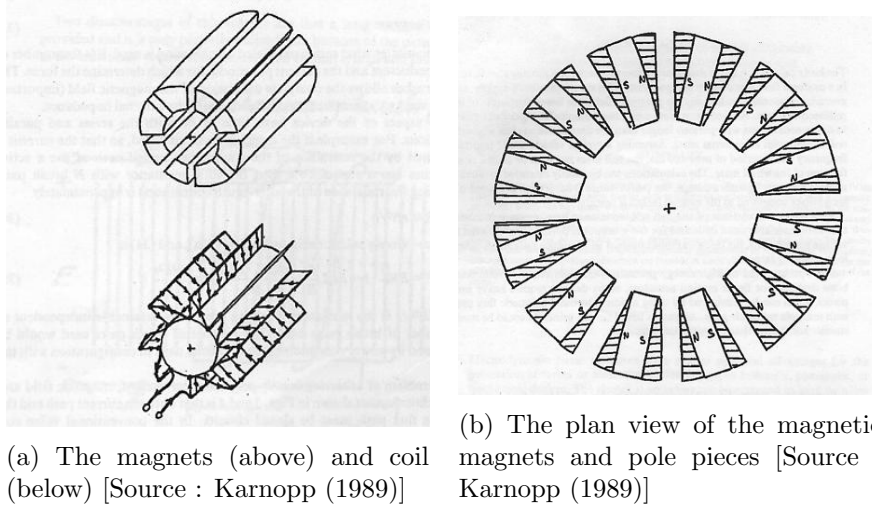
Figure 2.13: The Karnopp Electro-Magnetic Damper

$$F_{max} = \frac{B^2 \cdot M_c}{\sigma \rho} \cdot \dot{X} \qquad (2.14)$$

where F_{max} was the maximum force generated in N, B was the magnetic field in Tesla, M_c was the mass of copper in the coil in kg, σ was the resistivity of copper in $\Omega \cdot m$ and ρ was the density in kg/m^3. The damping coefficient of the damper can be given by $c = F_{max}/\dot{X}$. Substituting this into 2.14 and rearranging gives 2.15.

$$c = \frac{B^2 \cdot M_c}{\sigma \rho} \qquad (2.15)$$

.

Rearranging 2.15 for M_c determines the mass of the copper wire required in a damper to produce the required damping and is given in 2.16

$$M_c = \frac{\sigma \rho c}{B^2} \qquad (2.16)$$

.

The damping coefficient for a typical sedan can be determined from 2.17

$$c = 2\zeta\sqrt{mk} \qquad (2.17)$$

.

where ζ was the damping ratio, m was the mass supported by one wheel of the vehicle and k was the spring rate. Typical values of ζ range from 0.3 - 0.6, Dixon (1999). Taking a low value of 0.3, a mass of 500 kg and a spring rate of 20,000 N/m, this gave a required damping coefficient of 1,000 Ns/m. Using 2.17 and the Samarium-Cobalt magnets of time, the mass of copper required was 2.2 kg. Taking into account the weight of the magnets, end pieces and the coils this weight could be

trebled or quadrupled. Using the more powerful Neodymium permanent magnets now available, the mass of copper required was reduced to a weight of 0.78kg, giving a total damper weight of 3–4 kg or, with sufficient design, less.

To determine the physical limitations of the passive e.m. damper Karnopp, determined the time constant of the coil by itself. This was the fastest rate of decay possible for the system given the properties of the materials. The time constant of the coil alone is given by 2.18

$$\tau_{mech} = \frac{\sigma \rho}{B^2} \tag{2.18}$$

Using copper as the conducting material and using the Samarium-Cobalt magnets available to Karnopp, the time constant for the damper alone was approximately 1 ms. To determine the time constant of the damper system it was required to know the mass of the conducting wire and the sprung mass, M_{ext} and using this in 2.19 determines the time factor of the system.

$$\tau_{ext} = \tau_{mech} \times \left(1 + \frac{M_{ext}}{M_c}\right) \tag{2.19}$$

In the case where $M_{ext} = 100 \times M_c$ the time constant would be approximately 100 ms. To get large damping ratios the natural period of the sprung mass must be considerably larger than the time constant. Using the Samarium-Cobalt magnets available to Karnopp, a minimum of about 3% of the car mass was required to damp frequencies up to several Hertz. Using more modern Neodymium magnets this figure could be reduced by one third.

However this mass of the damper was just the mass of the electrical conductor. In the case of the damper proposed by Karnopp there was also the use of pole pieces, which were added to the magnets to help produce a uniform magnetic field. The pole pieces greatly increase the weight of the final damper. The work was sufficient to demonstrate the principle, but probably not a commercial design. Karnopp showed that the damping produced by a moving shorted coil in a uniform field does not depend upon the geometry of the coil. Also, a passive e.m. damper could be useful in the frequency ranges of typical automotive applications.

Mirzaei *et al.* (2001) created a Flexible Electromagnetic Damper by replacing the permanent magnet inside the coil with an electromagnet. As the electromagnet vibrates this induces a current in the damper coil, thus producing damping. The advantage that was proposed by such a system was that by varying the voltage at the primary coil, this produced a variable damping coefficient in the damper. This design was investigated with a focus on semi-active damping using a switchable passive damper. While this research verified the concept of electromagnetic damping, it did nullify the major benefits of passive damping, namely the simplicity of the design and that no energy was supplied to the damper. This approach would be competitive with magnetorheological damper devices or as an active suspension which also must

consume power to produce damping.
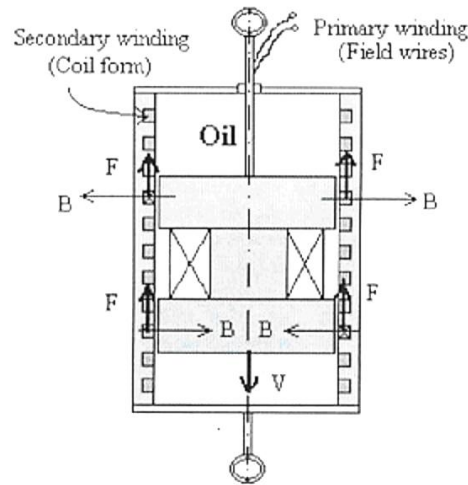
Figure 2.14: A hybrid e.m. damper.[Source : Mirzaei (2007)

Mirzaei (2007) continues the work from Mirzaei *et al.* (2001). In the earlier work the damper was constructed so that magnet moved in response to the input signal. This magnet travelled inside the damper which contained air at atmospheric pressure. In the later damper design the same linear e.m. damper was used, but the space between the electromagnet and the coil wall was now filled with a magneto-rheological liquid as in figure 2.14. This meant that when the electromagnet was activated to provide damping, it simultaneously acted as a magneto-rheological damper and an induction damper. One of the proposed advantages of this system was that in the event of a total failure of the e.m. system, there was still passive damping from the oil component of the damper. Adding the liquids used in the magneto-rheological damper adds more mechanical elements. While simpler than a fully active damper it was still more complex than a passive e.m. damper comprising of magnets and a coil or conducting slab. As a pure passive damper it would be easier to use a permanent magnet as this does not require any power supply. The advantage of this damper would be in semi-active applications. Whether it offers long term or power advantages over a pure magnetorheological damper was yet to be investigated.

Gupta *et al.* (2003) constructed an e.m. passive damper. Ultimately it may be intended for regenerative damping, but was mainly examined as a passive damper. The damper itself was constructed so that there was an inner magnet stack that was surrounded concentrically by a larger outer magnet stack. Each stack, inner and outer, consisted of three ring magnets that were axially magnetised. Between the magnets and on each end of each stack were iron pole pieces. The magnets were of the Neodymium type and were orientated so that the North poles face each other and the South poles also face the South poles of the adjoining magnets. By this arrangement the pole pieces between the magnets had a field intensity of

approximately one Tesla and the ends of the stacks would have a field of about 0.5 Tesla.

There were two coil stacks, the smaller that went between the magnet stacks and the larger which surround the magnets. Each coil was divided into four separate coils with alternating polarities. These four coils were centred upon the four pole pieces of the magnet stacks. The advantages of this set up were that large uniform magnetic fields were generated. Due to this uniform field Gupta determined that the theoretical force generated by the damper was as given by 2.20

$$F = \frac{K^2 v}{R_l + R_c} \tag{2.20}$$

where K was a constant given by $K = nhB$ with n being the number of turns of the coil per mm, h was the height of the coil in mm and B was the strength of the magnetic field in Tesla; R_l was the external load in ohms and R_c was the resistance of the coils, also in ohms. The total predicted power P, was given by 2.21

$$P = \frac{K^2 v^2 R_c}{(R_l + R_c)^2} \tag{2.21}$$

where v was the velocity m/s. The damper was then tested using a load resister to simulate charging a vehicle or electrical apparatus. This apparatus was tested over a range of frequencies from 10 Hz to 100 Hz. However it should be noted that most automotive dampers operate in the 1-10 Hz range. Above 10 Hz the tyre acts as a low pass filter that stops most high frequency vibration except in extreme cases or vibration generated on the sprung mass itself. What was clearly demonstrated in this paper was that the resistance of the damper greatly affects the power dissipated.

Ebrahimi *et al.* (2007) developed a passive e.m. damper that used a stack of ring magnets, with spacers between, that travelled inside a stack of oppositely polarised coils as illustrated in figure 2.15. Each coil sat around one magnet. These coils therefore acted as a linear motor/generator. The magnets were moved relative to the coils and current was generated. The damper was modelled using Finite Element Modelling. A good relationship was achieved between the modelling and measurement. This linear motor could be used for power generation in regenerative systems. However, most of the testing was done with an amplitude of 0.004 m and a frequency of 25 Hz. As has been noted earlier, 25 Hz should be a frequency that was already attenuated by the tyre, so it was hard to determine the actual practicality of this damper as the primary damper, though it could have utility in damping engine motion and other secondary automotive damping.

The most common design for an electromagnetic damper was the 'speaker' design. This is illustrated in figure 2.16a. A major advantage of this design was that it produces a uniform magnetic field through the coil therefore making the behaviour of the system easily predictable. The forces generated were very linear. The
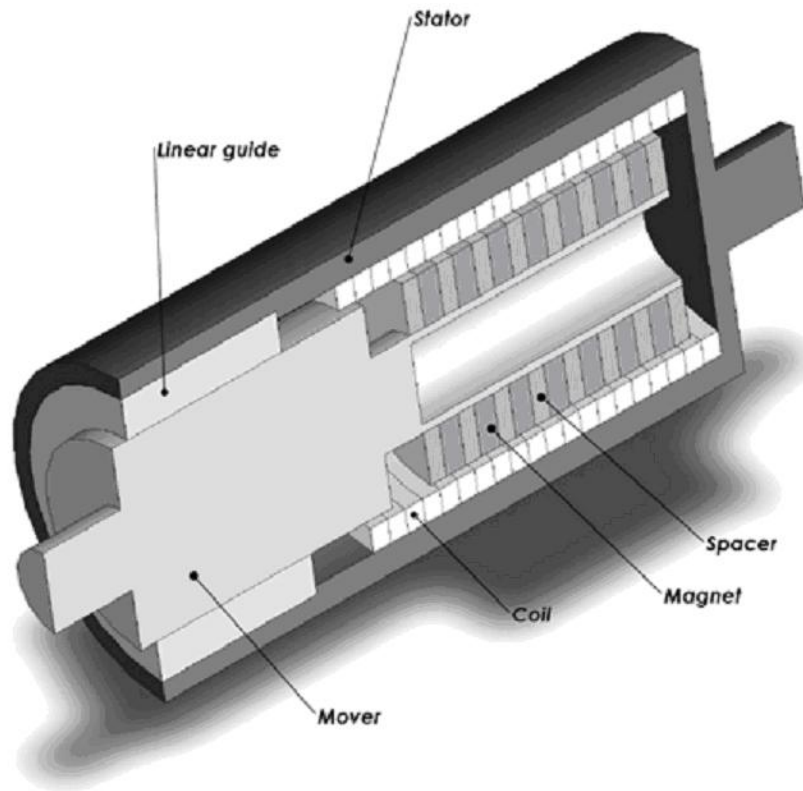
Figure 2.15: Proposed electromagnetic damper [Source : Ebrahimi *et al.* (2007)]
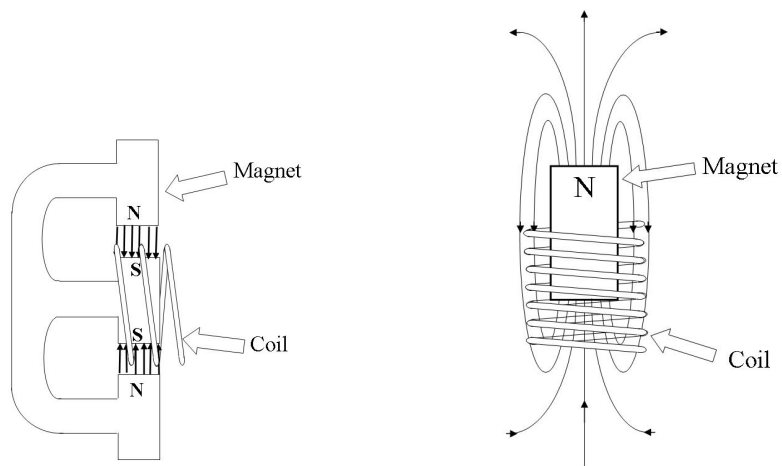
(a) A speaker type damper

(b) A linear magnet and coil damper

Figure 2.16: Two types of passive damper design.

disadvantage was the large mass of the magnet relative to the coil. Yet, conceptually, the simplest damper design was a single cylindrical axially aligned magnet that travelled through a cylindrical coil, as in figure 2.16b. This design was hard to model analytically, but Agutu (2007) characterised this type of damper. The advantage of this damper was the much lighter magnet involved. However modelling such a damper was mathematically much more complex as it was a non-linear system.

For a simple magnet–coil damper the damping force was proportional to the current generated, which was in turn proportional to the voltage generated by the coil. By experimentation Agutu observed that the maximum induced voltage occurred at half the radius above the end of the coil and half the radius of the coil below the coil. Other properties that Agutu observed were that the coil should be made from thick wires. This will reduce the resistance of the coil and therefore increase the current and the power of the coil. Also reducing the external resistance did increase the damping force. Finally, he observed that when there was more than one coil, then they should be connected in series, rather than in parallel. As noted earlier, this work was characterising the basic damper rather than modelling it.

Conclusions concerning passive dampers.

The traditional passive damper is well developed and is currently in widespread use. This has not stopped further research into the area. In particular, referring to the lightweight vehicle, the passenger acceleration is a function of the inverse root of the mass. Therefore a passenger in a light weight vehicle will experience greater accelerations than if in a larger vehicle. While new techniques such as the inerter and dead band damping can improve the passenger comfort, this will not greatly advantage light weight vehicles in comparison to the heavier vehicles.

The use of passive e.m. dampers may increase the reliability of dampers due to the lack of physical contact required for the operation of passive dampers. There were two types of passive e.m. damper available: eddy current dampers and induction dampers. Eddy current dampers have been modelled and the exhibit great simplicity. However they have not been demonstrated to show the same damping ability as a conventional hydraulic damper of similar weight. Induction dampers have been able to demonstrate effective damping, but at the levels required for automotive applications the mass of the complete damper will exceed current hydraulic dampers.

In the specific application of the e.m. damper to a light weight vehicle, by themselves, they offer no performance advantage over hydraulic dampers as they still use the same control strategy as a hydraulic damper. Thus the acceleration of the vehicle is still inversely related to the inverse root of mass. However, the e.m. damper may be a partial solution when used in conjunction with other control strategies such as semi-active damping.

2.3   Semi-Active Suspension Systems

Introduction

A modern innovation in suspension was the introduction of the semi-active damper. Most semi-active dampers are based upon passive dampers. The difference between the two systems is that the semi active damper can turn the damping on and off, or vary it, under the control of some control algorithm that receives information about the state of the vehicle, as shown in figure 2.17. An absolute velocity signal from the sprung mass is used in a control algorithm and the semi-active damper can be turned off at times when the damping would be disadvantageous. The semi-active damper usually requires less energy than a fully active damper, yet can return a significant increase in performance over a passive system However the semi-active controller needs a control system, usually a micro-computer, as well as signal inputs such as accelerometers, Linear Variable Displacement Transducers (LVDTs) or similar and a mechanism for turning the damper on and off.
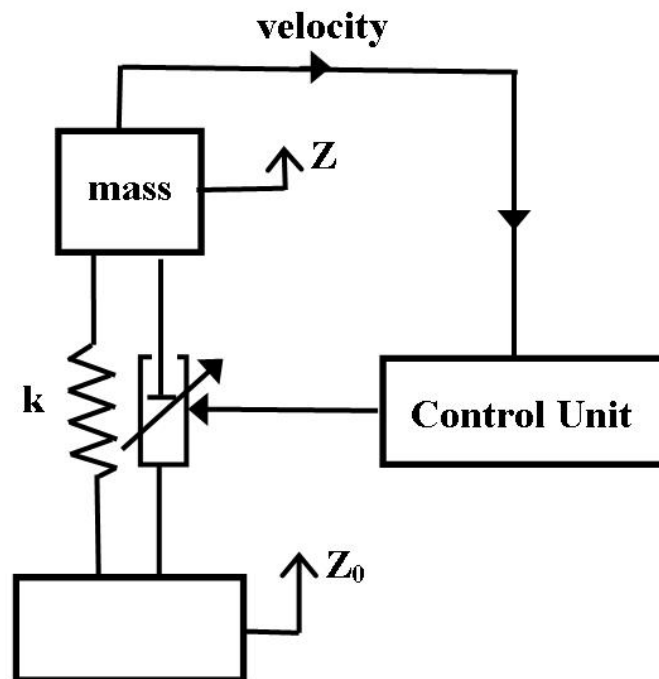
Figure 2.17: A genneral representation of a Skyhook damper.

"The idea of varying vibration control system parameters rapidly has a long history. As early as the 1920s patents were issued for shock absorbers in which a seismic mass was supposed to activate hydraulic valving directly or through the use of electrical contacts." Karnopp *et al.* (1974)

Sophisticated active systems for controlling vibrations were not developed until the 1950s and 60s. Active controllers were used to deal with problems such as heli-

copter rotor isolation, flexible aerospace vehicle bending mode control, and isolation of fighter pilots from aircraft motion. While an active isolation control system could be constructed which had better performance than the best possible passive systems or which could accomplish tasks that were not even possible with passive means, it should be noted that active systems in general were more costly, more complex and therefore often less reliable than passive systems. Karnopp *et al.* (1974)

Semi-active Skyhook dampers were first proposed by Karnopp in 1973 and more comprehensively in 1974. At present such dampers are available on more expensive commercial automobiles. Due to the relative simplicity of switching current as compared to hydraulic fluids, most passive induction style e.m. dampers can be converted into semi-active dampers by the addition of a control circuit and a current switching device. Technically, even eddy current dampers could be considered switchable if a mechanism was produced that allows the distance between the magnet and the plate can be varied rapidly and under control. So it is probable that any commercially developed e.m. damper will be rapidly adapted to semi-active control.

This section will firstly examine the control systems used in semi-active dampers with particular focus on Skyhook dampers as first proposed by Karnopp in 1974. The second part will examine the actual dampers and their performance.

2.3.1 Control Strategies

For a passive damper in a Single Degree of Freedom system, the force generated is directly proportional to the relative velocities of the unsprung mass and the sprung mass. This can be expressed as 2.22

$$F = c(\dot{x} - \dot{x}_o) \tag{2.22}$$

where F is the force in Newtons, c is the damping coefficient given in Ns/m, $\dot{x}$ is the velocity of the sprung mass in m/s and $\dot{x}_o$ is the velocity of the road surface, also in m/s.

Karnopp *et al.* (1974) proposed a Skyhook' damper. In this, the position of the body of the car was not measured relative to the level of the ground, rather the position of the sprung mass was fixed to an external inertial reference point. This was usually considered as an infinitely removed point and was the 'sky' that the name Skyhook was referencing. Using this external reference the equation for the force in the system at any given time was given by 2.23.

$$F_c = b\dot{x} + k(x - x_o) \tag{2.23}$$

where k was the spring constant, b was the damper constant, x was the displacement and $\dot{x}$ the velocity of the sprung mass and x_o was the the displacement of the unsprung mass. In an ideal Skyhook system, such as in figure 2.17, the force

generated by the damper was given by

$$F_D = b\dot{x} \tag{2.24}$$

However to achieve this ideal damping would require an input of energy at points in the cycle rather than just dissipating it. When the damper entered a regime where energy had to be supplied, then the damper was switched off so as to provide no force. This is given in 2.25

$$C = \begin{cases} \dot{x}(\dot{x} - \dot{x}_o) > 0 & F = b\dot{x} \\ \dot{x}(\dot{x} - \dot{x}_o) < 0 & F = 0 \end{cases} \tag{2.25}$$

Karnopp proposed a semi-active damper and as this was a demonstration of the control strategy only, he implemented this control strategy using an active hydraulic damper as the prototype. By use of control algorithms the active damper would act as a semi-active damper. His simulations showed that the semi-active damper with Skyhook control was more effective than a passive system at all frequencies. While less effective than a fully active damper, the performance was much better than the passive system. As the frequency approached 10 Hz the performance of the active and semi-active suspension systems became almost identical.

However, the performance of a semi-active damper while approaching that of an active damper, cannot exceed it. The reasons for this were given in Crosby and Karnopp (1973). "Compared to fully active elements, the [semi-]active damper has the following limitations:
1. The [semi-]active damper can produce a force only when a relative velocity is present across the attachment points.
2. There will be time intervals when the direction of the available force from the [semi-]active damper is opposite to the direction of the desired force. During these intervals the [semi-]active damper must be controlled to produce zero force.
3. If the commanded force exceeds that which can be produced with a finite damping coefficient, the damper is controlled to a locked up or rigid link mode. In this mode, the maximum force which can be produced is limited to the inertial forces derived from accelerating the attached masses less than the algebraic sum of other forces acting on the masses."

The Skyhook damper was issued US Patent No. 3,807,678 on April 30th, 1974 in the name of the Lord Corporation. Krasnicki (1980), working for Lord Kinematics, built a physical damper that would confirm Karnopp's earlier research. Using an active damper first built in 1972, Krasnicki showed that a physical semi-active damper using a Skyhook algorithm did surpass the performance of a passive damper at all frequencies tested, Krasnicki (1980).

Kransnicki continued this work by constructing a semi-active damper and in-

stalling it on an off road motorcycle. The damper used two states, operating with 'on' and 'off' as being the only settings. A bump course was constructed consisting of eight 4 inch by 4 inch (10 cm x 10 cm) beams spaced 15 feet (4.5 meters) apart. The performance of the modified motorcycle was compared with a stock motorcycle using passive dampers on the same course. The vehicles were driven over the course at 15 mph (6.667 m/s). Large amounts of data were collected during the test runs. However , due to the limited processing power of the times, specific details were not dealt with, rather the general interpretations. Krasnicki concluded that in the lower frequency ranges, 0–10 Hz, the acceleration peaks for given frequencies were significantly lower, and at times substantially, reduced compared to the passive dampers trialled. Further, no extra rattle space was required for the operation of the semi-active damper.

It is usually assumed that the fully active system is some sort of ideal and other systems are a compromise or lesser in their abilities. However, even with complete state variable feedback an active system is not capable of reasonable, ideal filtering behaviour. A passive system with adjustable parameters or a semi active system in which some damping force components are generated actively or semi actively can perform, in essence, as well in filtering roadway disturbances as any then state of the art active suspensions, Karnopp (1986).

In Karnopp (1987) it was noted that there were many forms of resistive element that were controllable. It was also noted that there were many possible ways to create semi-active dampers or control elements. A comparison was undertaken between the use of hydraulic dampers and the new concept of using an electromagnetic damper in a semi-active application. Certain problems were noted with each of these dampers. In the case of the hydraulic damper small damping forces were a problem in a damping system. Even with fully open control valves on a semi-active damper there will always be some residual hydraulic resistance that will produce a force. In practice this means that a hydraulic system may not be able to produce forces sufficiently small for optimal damping. However, in the case of the e.m. damper, when the resistance was very high there was almost no force generated. Moreover, even with an open circuit there was a limit on the possible amount of damping available for an e.m. damper. This meant that the e.m. damper may not have sufficient authority to control extreme accelerations. Bond graphs were used by Karnopp to demonstrate that e.m. dampers were still feasible.

One drawback of the Skyhook damper was the need to have an inertial frame of reference. For standard commercial applications, the fineness of measurement for control of small vibrations was often not obtainable for early Skyhook dampers. Therefore Alanoly and Sankar (1987) proposed a control algorithm using the relative velocity and relative displacements of the sprung mass and the surface. Instead of the original algorithm given in 2.25 , this was modified to 2.26

$$C = \begin{cases} (\dot{x} - \dot{x}_o)(x - x_o) < 0 & F = b(x - x_o) \\ (\dot{x} - \dot{x}_o)(x - x_o) > 0 & F = 0 \end{cases} \qquad (2.26)$$

and this would then act in a similar manner to 2.25. The primary advantage of this was that the instrumentation can be reduced to a single measurement device such as a Linear Variable Displacement Transducer (LVDT). The LVDT directly gives the relative displacement and by differentiation it also gives the relative velocity. This lead Alanoly to conclude "The new concept in semi-active vibrational control [...] is shown to give performance comparable to that of a fully active isolator. The control scheme's main attraction is that it uses only relative velocity and relative displacement measurements, both of which were easily measured in vehicle suspensions. This can not be extended into fully active dampers".

Besinger *et al.* (1991), investigated a damper for use on lorries supplied by the Lord Corporation. The damper had 22 damper settings which was achieved using a 900 Hz stepper motor. This allowed a change from minimum to maximum damping in 25 milliseconds. This performance allowed this damper to have a performance close to a continuously variable damper. This work confirmed previous work showing that the switching time from off until on should be less than 25 ms and this resulted in a 15-20% reduction in body acceleration. Besieger et al also found little improvement if the damper switching time was faster than this, however the active system rapidly deteriorated with slower switching times. At 50 ms switching time the active system had a body acceleration 10% worse than a passive system.

Another disadvantage of the Skyhook damper was that in the ideal system the only input to the system was the inertial reference of the sprung mass. However in practical applications there were two masses attached to the suspension spring, one at each end. There was the cabin of the vehicle at one end of the spring and the wheel was attached to the other. The rubber tyre on the wheel acts as an additional damper and spring system. This produced a secondary vibration for which the original Skyhook damping scheme did not provide any control signals. M. Valášek and M. Novák proposed in 1996 a new scheme to control the wheel hop, which they called "Ground Hook".

Using the quarter car model as illustrated in figure 2.18, the equations of motion of the two masses were given by 2.27 and 2.28

$$m_1\ddot{z}_1 + k_{10}(z_1 - z_0) = b_{10}(\dot{z}_1 - \dot{z}_0) - k_{12}(Z_2 - z_1) + F_d = 0 \qquad (2.27)$$

$$m_2\ddot{z}_2 + k_{12}(z_2 - z_1) - F_d = 0 \qquad (2.28)$$

where m_1 was the unsprung mass, m_2 was the sprung mass, k_{12} was the stiffness of the main suspension spring, k_{10} was the spring constant of the tyre, b_{10} was the damping coefficient of the tyre, F_D was the force supplied by the damper and z_0, z_1 and z_2 were the displacements of the ground, the unsprung mass and the sprung
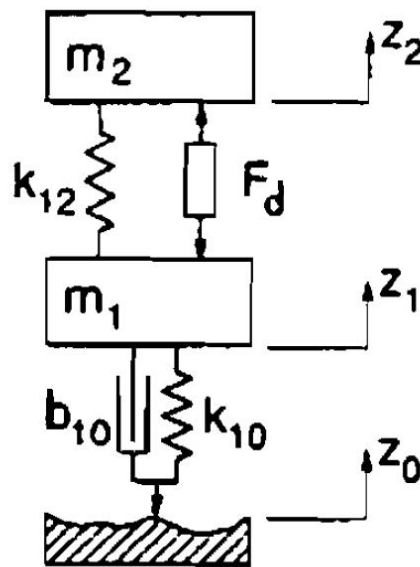
Figure 2.18: An ideal Groundhook Damper.[Source : Valášek *et al.* (1997)]

mass respectively. Valášek *et al.* (1997) extended the concept of the Ground Hook damper to give a force as given by 2.29.

$$F_{10} = k_{10}(z_1 - -z_0) + b_{10}(\dot{z}_1 - \dot{z}_0) \tag{2.29}$$

This force was then added to the damper force to generate the final damper force required, Valášek *et al.* (1997).

The Groundhook approach directly deals with the wheel hop that occurs when a suspension system only has an inertial frame of reference. It was an important step in developing a control system that gave the optimal performance of both passenger comfort and minimising the tyre contact forces. This approach can be used in fully active systems and semi-active systems where the amount of damping was variable. It was of less use when the damper has an 'on-off' control system instead of a continuously variable control system. Another issue concerning semi-active dampers noted by Williams (1997) was the tendency of the damper to produce vibrations at high frequencies which were not present in the passive dampers which they replace.

Due to the benefits of the semi-active damper over the traditional passive damper in providing increased ride comfort in private automobiles, the use of semi-active dampers has been investigated for other vehicles, including heavy vehicles Kitching *et al.* (2000) and tractors Ibrahim and El-Demerdash (1999). Research in this field is still active. In Simon and Ahmadian (2002) control strategies were investigated for the use of semi-Active dampers in Sport Utility Vehicles (SUVs).

Of the three major requirements of an automotive suspension system: Passenger

Comfort, Road Contact Force and Rattle Space, the semi-active damper proposed by Karnopp in 1973 was designed to optimise passenger comfort. To optimise road forces, Valášek and M. Novák proposed the Ground Hook Damper. However there is still research being conducted to optimise the previous two factors and the rattle space needed for the damper to operate.

For example, due to the cost of processing power and the limiting frequency of the hydraulic dampers available, strategies such as Redfield (1991) were suggested to reduce the bandwidth for the damper. This allowed equipment with a response frequency of 5-10 Hz to be used. Adaptive Skyhook damping was suggested by Yi and Song (1999) which used a damper that could be adjusted in real time for 19 different damping coefficients. Elbeheiry (2001) applied a generalised quadratic performance index to minimise the variances of the system state variables, the broadband control input and the damping factors of the semi-active dampers in an effort to apply suboptimal bilinear control methods to suppress the vehicle vibrations. Dixit (2001) applied Sliding Mode Observation and Control to semi-active dampers. A new model using Gain Scheduling and Hardware-in-the-Loop tuning was proposed by Hong *et al.* (2002b). Simultaneous optimisation techniques were used by Mailat *et al.* (2004) to improve the vibration behaviour in automotive applications. The use of H∞ controllers was investigated by, amongst others, Sammier *et al.* (2003). Model free controllers, such as neural networks, with respect to semi-active dampers were investigated by Lauwerys *et al.* (2004). The use of linear systems with constraints was investigated by Paschedag *et al.* (2006). Fuzzy logic controllers have also been designed using genetic algorithms Hashiyama *et al.* (1995), Yan and Zhou (2006). Comparative studies of various semi-active dampers were carried out by Jalili (2002) and Mailat *et al.* (2004) In Liu and Liu (2006) a damper was constructed using an e.m. mechanism that could adjust the damping rate of the damper so as to achieve semi-active damping. In this damper a permanent magnet was mounted between the two poles of a 'C' shaped electromagnet. The use of a single semi-active linear mount for vibration attenuation of a natural multi-degree-of-freedom was modelled by Kim and Lee (2003) using a new control law.

The Karnopp Skyhook semi-active damper has been demonstrated to be useful in practical applications. As the pure Skyhook algorithm only suppresses the motion of the sprung mass, another algorithm such as Valášek's Ground Hook is used to maintain the wheel contact. These have been shown to produce a significant performance improvement over commercial hydraulic dampers. While hydraulic passive dampers can be controllable by the insertion of an electronically variable valve, there are alternative technologies that can also achieve semi-active damping.

ER & MR Dampers

Semi-active dampers have achieved a practical realisation through the use of Electrorheological (ER) and Magnetorheological (MR) fluids in a hydraulic damper. By changing the viscosity of the fluid under computer control, it is possible to change the damping coefficient of the damper.

Electrorheological fluids were first reported in Winslow (1949). It was noted by Winslow that with particles suspended in a fluid that the application of a strong electric field changes the shear resistance of the fluid and it could produce negative shear resistances. When used in a damper, by switching the electrical field the resistance of the damper can be changed from a maximum to a minimum and therefore acts as a switchable or even continuously variable damper which was suitable for use with Semi-active control strategies. This work has been applied to automotive damper designs in Choi *et al.* (1996) and Choi and Kim (1999). A typical design of an electrorheologial damper is illustrated in figure 2.19
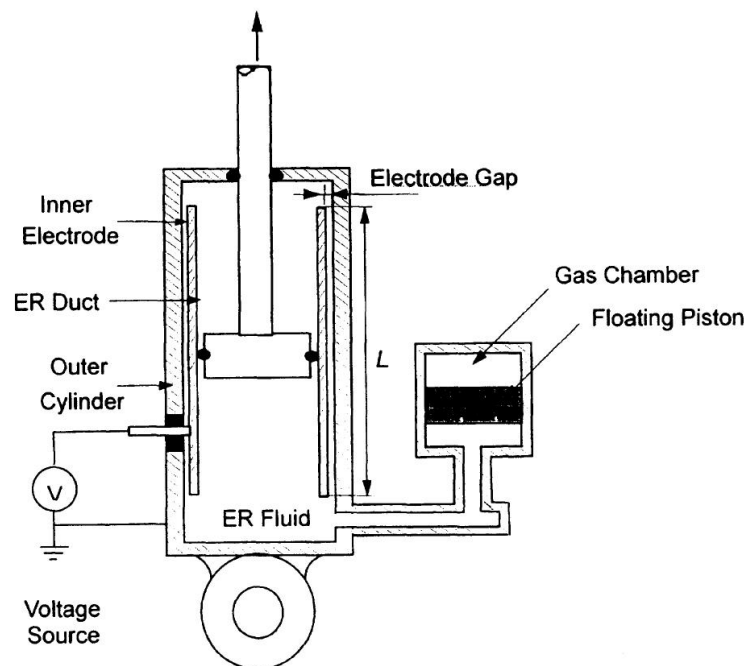
Figure 2.19: Parts of an electro rheological damper [Source : Kim (1999)]

Magnetorheological dampers were first patented by Jacob Rabinow in 1954 "My invention relates to a variable viscosity magnetic material, the physical properties of which can be changed under the influence of a magnetic field. For example, the fluidity, or apparent viscosity can be altered by varying the strength of a permeating magnetic field, in such a manner that the material can be changed between a iiuid-lilre [liquid] consistency and a substantially solid consistency, depending on the instantaneous strength of the field. The ability of the material to adhere to a paramagnetic or ferromagnetic material is also controllable by varying the permeat-

ing magnetic field. The ability of the material to oppose mechanical penetration and to retain a given shape or conformation is also controllable by application of a magnetic field. It is a primary objective of my invention to provide such a material and means for controlling it at the will of an operator." Rabinow (1954). Since then work has been done on MR dampers by Delphi Automotive Corporation and Lord Corporation. A typical MR damper is very similar to the ER damper illustrated in figure 2.19, the main difference is the substitution an electromagnet instead of the electrodes illustrated.

Contemporary MR fluids are of 1-10 μm ferromagnetic and ferrimagnetic particles suspended in an organic or aqueous carrier fluid. While many materials have been tried the most common useful magnet material was high purity iron powder. When in the 'off' state the fluids have an apparent viscosity of 0.1 to 1 Pa-s, at low flow rates. When switched on the MR fluids could develop an apparent yield stress of up to approximately 100 kPa. While higher yield stresses were achievable, the cost and availability of suitable materials often ruled them out. In damping systems one of the major attributes was the response time of the fluid. For MR fluids this tended to be in the range of 10-20 ms depending upon the device and the magnetic circuit design, Phule (2001).

After Rabinow reported and patented MR fluids, they essentially disappeared from the consciousness of this field. The reasons for this are not entirely known. ER fluids seem to have generated a higher level of interest. There may have also been issues with keeping the fine iron particles in suspension. So it was only since the 1990s that there has been a revival of interest in this research, Phule (2001). This includes research into both the damper design Yao *et al.* (2002), Hong *et al.* (2002a) and Sapinski (2008); as well as the control properties and algorithms associated with these dampers, Lee and Choi (2000) and Turnip *et al.* (2008). A significant body of work has now been established in this field.

Delphi Automotive systems have developed a semi-active MR fluid based damper called Magneride^{TM}. This consists of a plunger that travels in a cylinder and through a MR fluid. There were channels cut into the plunger so as to allow fluid to pass from the top of the plunger to the bottom of the plunger. Inside the plunger and wrapped around the axis is an electromagnetic coil that alters the viscosity of the fluid in the plunger, thereby providing damping, Systems (2008). This is now commercially available on a variety of automotive platforms.

2.3.2 E.M. Semi-active dampers

While there were many papers published on semi-active e.m. dampers, most of these dealt with the damper as a component of a regenerative damping system. This was in part due to the semi-active damper being developed from the passive damper, the primary difference being the use of a control algorithm and the ability to control

the amount of damping generated by the damper. Also, much of the research into passive and semi-active e.m. dampers has been in regards to regenerative damping and those examples will be dealt with in a later section. The remaining list of stand alone semi-active dampers was therefore very limited.

Conclusion

The use of semi-active damping allows for a high degree of vibration control. The Skyhook damper as proposed by Karnopp provides a sound basis for the development of such a damping system. The Skyhook damper primarily improved passenger comfort, so to complement this a Ground Hook strategy was also useful for optimising the ground handling properties of the system. Currently, semi-active dampers are a well researched field and are in production. At the time of writing the vehicles available with Skyhook suspension include, but is not limited to, the Chevrolet Corvette and Camaro: Cadillac ATS and CTS-V: Ferrari 599, F12 Berlinetta and California: Holden HSV GTS, Senator and W427: Audi R8 and TT: Acura MDX and ZDX and Range Rover Evoque. All commercially available systems are based on hydraulic passive dampers where the damping coefficient can be switched off or continuously varied as required by use of rheological fluids and an electromagnet. Most research into e.m. Semi-active Dampers has been done in conjunction with regenerative damping and will be explored in that section.

2.3.3 Regenerative Suspensions

In recent years there has been much discussion about recovering energy from the suspension system. Regenerative braking has been used successfully for many years on vehicles such as trains and trams and in modern electric vehicles. It was a logical thought that the energy dissipated in automotive dampers could be converted into other forms, such as electrical, so as to be reused in the main propulsion system or in secondary systems such as lighting, heating or the windscreen wipers.

Browne and Hamburb (1986) investigated the amount of energy dissipated by dampers in automobile dampers. Two different methods were used to determine the amount of energy dissipated. The first method used the amount of thermal change in the damper to determine the amount of energy dissipated when the vehicle travelled over a rough surface. This method was only partially successful and only provided a lower bound on energy dissipation rates and would yield gross trends. The second method involved measuring the axial components of the applied force and the relative velocity between the two end attachments of a conventional shock absorber. The product of the force measurements and the instantaneous velocity provided the instantaneous rate of energy dissipation. Measurements were recorded from two different test vehicles. These were driven over different test tracks, under normal traffic conditions on highways as well as urban and rural main arterial roads. The

energy loss rate per damper as determined by the above method was 3 to 57 Watts, depending upon the surface. Typical dissipation rates for normal road surfaces were 10 to 15 Watts per damper. For a typical four wheel vehicle travelling on good to average surfaces the total amount of energy dissipated by the dampers would be 40 to 60 Watts.

From their investigation Browne and Hamburb (1986) concluded that it was not practical to regenerate suspension energy for use in the vehicles major systems, and any regenerated power would have little effect on fuel economy. They did speculate that the regeneration of this power could be of use of electric vehicles, or could be stored for systems that only required energy on an intermittent basis, such as windscreen wipers or defrosters.

In a conventional petrol or diesel powered sedan, 60 Watts of power represents less than 10% of the power output of a conventional AC alternator. In an electric vehicle this amount of power was less than 1% of the power driving the wheels at motorway speeds. To recover this power, electromagnetic dampers, control systems and power regulators were required. With current technology this represents an increase in the weight of the suspension system and it becomes problematic whether the power generated exceeds the increased power requirements of the now, heavier vehicle. Also there was an added level of complexity for what was a very small return. While this is a small amount of power compared to that actually used in a modern vehicle, it has not stopped researchers trying to develop systems to recover this energy.

Wendel and Stecklein (1991) proposed an active hydraulic suspension system with a hydraulic pump to regenerate some of the energy for use in an active actuator. They then explored this concept and discussed pump configurations and pump strategies.

Fodor and Redfield (1993) stated that the primary function of a regenerative damping element was to transfer vibration energy to an energy-storage device as efficiently as possible while maintaining acceptable vibration control. Their research emphasised matching the impedance between the storage device and the energy source to maximise the regeneration efficiency. Fodor and Redfield developed a Variable Linear Transmission (VLT) for vibrational energy regeneration. The VLT used a mechanical method of vibration energy regeneration, using a mechanical lever and a movable fulcrum mechanism as shown in figure 2.20.

Bond graphs were used to mathematically model the system. The VLT was analysed with a two degree of freedom, quarter car model and it was shown that in the ideal case the VLT had the ability to store all the power that was otherwise dissipated. Further it provided linear damping and required no power to drive the fulcrum actuators. For a non-ideal fulcrum actuation mechanism there were limitations. For the ideal actuator, the VLT acted as a viscous damper. However for low bandwidth actuator operation the VLT acted as a Coulombic damper. Fodor
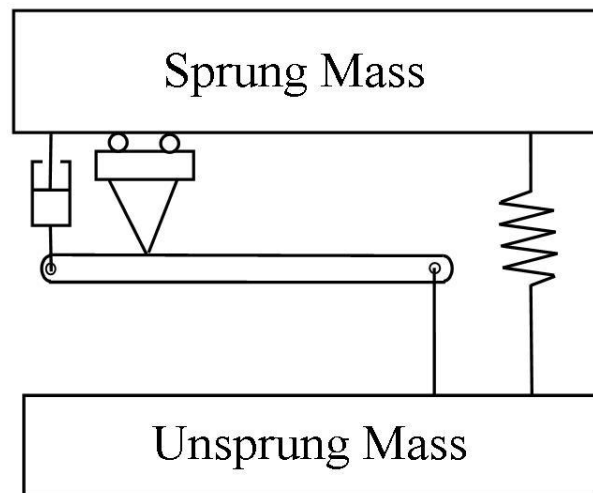
Figure 2.20: The Variable Linear Transmission as proposed by Fodor and Redfield (1993).

also concluded that analysis indicated that an actuation bandwidth similar to the vibration being damped results in a regenerative damper which closely approximates a passive viscous damper. The actuation bandwidth required for this system in motor vehicles was given as 20 to 30 Hz.

The non-ideal VLT model was also analysed with respect to the operating efficiency of the damper. The proposed VLT was modelled as a two degree of freedom system with input power being provided in each degree of freedom. The VLT was analysed for a typical vehicle with non-ideal actuators and random input. In this scenario the VLT consumed more power than it generated. Fodor et al suggested that a more advanced fulcrum control strategy was required. Otherwise reducing the fulcrum motion from two to one degrees of freedom would also increase the efficiency.

Jolly and Margolis (1997) investigated the use of regeneration of energy in an active hydraulic damper. They noted several issues that make practical implementation of regenerative hardware difficult. These factors included the parasitic damping of all dynamic systems, and the impossibility of regenerating all of the available power. Also noted was that, in general, the effort/flow relationships of a specified control scheme was not consistent with the behaviour of the energy storage elements. This made the ability to maintain damping performance, while efficiently managing energy, very difficult.

It was proposed by Jolly that a regenerative damper would require four elements: an energy storage element to temporarily store energy that was generated: an energy transformer: an energy management system and also a controller and sensors to determine the required damping.

Suda and Shiba (1996) investigated a regenerative damping system which con-

verted vibrational energy into electrical energy using a rotating DC motor. The principle used was that the motion caused a change in magnetic flux density through a closed electrical circuit. This produced a Lorentz force that affected the mass in the same way as if it were an ordinary viscous damper.

Suda and Shiba showed there was a direct trade off between energy regeneration efficiency and the system damping coefficient. The damping coefficient was affected by the internal resistance of the DC machine and the external resistance of the circuit. By using a larger gear ratio in the DC machine, the damping coefficient was also increased. However, this also led to an increase of the moment of inertia of the rotational motor and an increase in the friction of the system.

Suda and Shiba then made an experimental damper from which they determined the proposed damper had an adequate damping effect. Their calculated damping coefficient was 110 N s/m which nominally correlated with the theoretical damping coefficient of 99.44 N s/m. In their experiment the maximum regeneration efficiency was close to the theoretical maximum. In this experimental set up the result was 24.3% of the energy was recovered. At higher frequencies the efficiency was shown to reduce due to the small amplitude of motion which lead to large machinery losses.

Further research by Suda *et al.* (1998) incorporated the use of a regenerative damper with an active Skyhook damping algorithm. In this research a linear DC motor was used instead of a rotational DC motor, to generate energy from the motion of the wheel. The generated energy was stored in a condenser and was supplied on demand from the condenser into the DC motor, which now acted as an actuator.

Suda's damper was designed to achieve two conditions: First the actuator should require little energy and second the damper should work even if there was no energy in stored the damper. The damper therefore acted as a two state skyhook damper as given in 2.30

$$C = \begin{cases} \dot{z}_0 \dot{z}_1 > 0 & c = passive \\ \dot{z}_0 \dot{z}_1 < 0 & c = active \end{cases} \tag{2.30}$$

where c was the damping coefficient, $\dot{z}_0$ was the velocity of the ground and $\dot{z}_1$ was the velocity of the sprung mass.

This damper was successfully constructed and showed improved damping performance over a standard passive damper or a semi-active damper, especially at higher frequencies.

Kim (1999) investigated the use of energy regeneration in an electrorheological (ER) damper. In this evaluation a semi-active ER damper is manufactured with a mechanism that also converted some of the linear motion of the damper into rotary motion. This rotary motion was then amplified through gears and was used by an AC generator to produce electrical energy. This energy was stored in a battery at 12 V. A transformer was used to step up the output of the generator to charge the battery. A voltage amplifier was then required to supply the high voltages needed to

generate the electric fields that increased the viscosity of the ER fluid in the damper. The voltage amplification factor was 1000 times from the base input voltage of 0–5 V. A micro-computer was used to control the damper. Kim et al reported an increased isolation through the use of the ER damper. They also state "it was known that the power produced by the proposed regenerator mechanism is enough to operate the ER suspension system for a passenger car." It should be noted that they were conducting their testing with an excitation amplitude of ±20 mm at a frequency of 1.4 Hz. The amplitude of motion tested was not typical for most road passenger vehicles. They also stated that it takes 20 Watts to activate a typical ER damper for passenger vehicles.

From Browne and Hamburb (1986), it was observed that the normal power dissipation of a damper was 3–57 W with 10–15 W being generated under most conditions. Even though the electric field in the ER damper was not generated all the time, the energy demands were not trivial. Allowing for efficiency losses from converting linear motion to rotational motion, the amplification of the rotational energy, the conversion to electrical energy, the storage of the electrical energy, the stepping up of the voltage, the generation of the electric field and the energy cost of using a microprocessor system, this would indicate that the system will only regenerate enough energy for use in only the most extreme cases of vibration.

Graves *et al.* (2000b) suggested that while the energy regenerated from electromagnetic dampers may be considered insignificant in modern automobiles, he suggested that it may be of use in electric vehicles where the total energy consumption is lower and energy efficiency is a primary concern.

Graves examines the previous work of Karnopp, in particular his 1989 paper. He showed that if a damper was made of multiple elements, the damping coefficient generated does not depend upon if the elements were in parallel or in series or a combination of both. In these cases the damping coefficient was

$$C_v = B^2 L^2 \times \frac{1}{(R_{INT} + R_{EXT})} \tag{2.31}$$

where C_v was the coefficient of damping, B was the magnetic field in Tesla, L was the length of the conducting elements, R_{INT} was the resistance of the damper and R_{EXT} was the external load on the damper. An investigation was also carried out for rotating compared to linear dampers. It was noted that the main advantage of a rotating system such as a rack and pinion, was the ability to mechanically amplify the displacement relative to the damper. This was offset by the rotating inertia of the damper affecting the suspension system dynamics. In a damper the transmissibility of vibration was of importance, with zero transmission of road surface vibration being the ideal. Graves noted that in a linear damper the transmissibility approached zero for high frequencies while for a rotational damper the transmissibility does not approach zero. For a rotational damper, to keep the high frequency transmissibility

low, the rotating inertia must also be kept low.
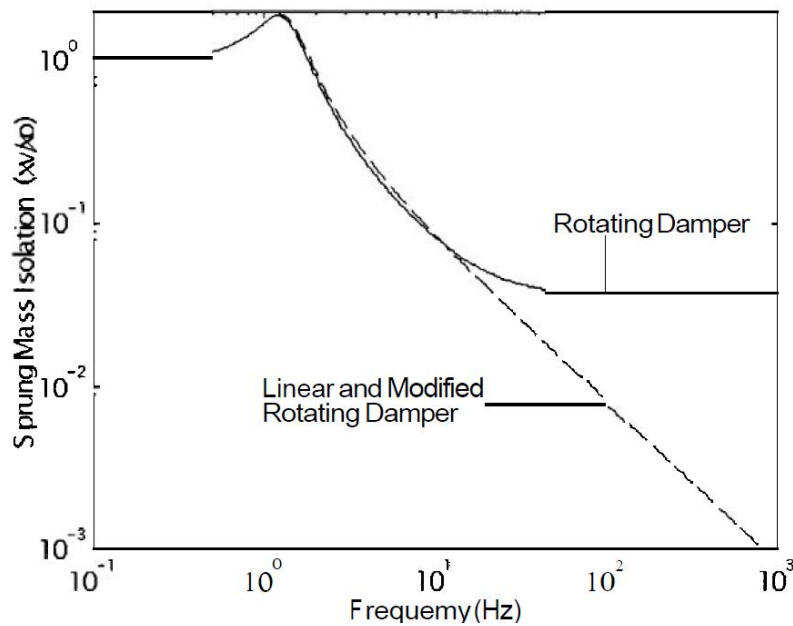
Figure 2.21: Isolation response of a modified rotating damping system. [Source : Graves *et al.* (2000a)]

As is shown in figure 2.21, for a single degree of freedom rotational damper the transmissibility becomes asymptotic. In a real world application the car tyre acts as a low pass filter. This helps isolate the damper from high frequency vibrations. When the damper was modelled with the tyre as a two degree of freedom system the high frequency performance improved, while in the 5 –12 Hz range the performance of the rotating damper degraded and allowed greater accelerations in the sprung mass than the linear damper.

To restore the performance of the rotary damper to that of a one degree of freedom linear damper, a second damper and spring element was added in series to the rotary damper. By matching the damping coefficient of the damper and the spring constant to a zero pole theory this was demonstrated, by numerical modelling, to exhibit the behaviour of a linear damper. While this reduced the transmissibility of the system at high frequencies it also reduced the effectiveness of a regenerative damper as some energy was lost in the new damper.

Goldner and Zerigian (2001) conducted an investigation into a power dissipation eddy current damper with the final aim of replacing this with a method of regenerating this energy. They concluded that a 2,500 lb (1,140 kg) car travelling at 20 m/s (72 kph), travelling over one mm bumps would generate 1,915 W. When travelling over 3 mm bumps they conclude that they can generate 17,400 W. When compared to the same car travelling over a smooth surface consuming 7,500 W of energy the percentage of engine energy recovered from the dampers would be 20%

and 70% respectively for the two cases given. However, in the final case, the power dissipated by the dampers was 2.3 times the power produced for forward propulsion on a smooth surface. This seems highly improbable as the dampers on current road vehicles would require cooling systems similar in size and thermal transfer capacity as the main power source of the vehicle. The figures given by Goldner were two orders of magnitude greater than given by Browne and Hamburb (1986). The proposed power generated at 20 m/s can be summarised as 2.32.

$$P = (Height\ of\ bump\ \times\ 44,000)^2 \qquad (2.32)$$

From this it can determined that the energy required for a car to travel at 20 m/s over a corrugated road with a bump height of 1 cm would be 193.6 kW. This power would be much greater than was actually used by vehicles in this situation and contradicts the findings of other authors. A Patent was granted to Goldner et al for a regenerating damper in 2005 Goldner and Zerigian (2005).

Kim and Okade. (2002) noted that one of the major issues with a regenerative damper was that the damper often produced a Back Electro Motive (BEM). This often reduced the damper output voltage so that it was smaller than the voltage required to charge the battery. This in turn produced a dead zone in the dampers performance. One method examined earlier to overcome this issue, was the use of mechanical amplification of the motion of the damper, thereby producing higher voltages. A different method proposed by Kim and Okada was to use a step up chopper between the damper and the charging unit. The damper used in this paper was a linear d.c. motor. The use of step up chopper was to convert the lower voltages into a higher voltage suitable for use with the battery. The traditional step up voltage chopper had a constant pulse width modulation of 50%. This reduced the dead zone, but does not eliminate it. To overcome this limitation a pulse width modulated step up chopper was developed. Using this control technique the duty cycle was increased when the velocity and therefore the voltage generated by the damper was low. Experimentation by Suda and Okada confirmed that energy was regenerated even when the voltage produced directly by the damper was less than the voltage of the battery. They also confirmed that continuous damping was produced and that the previous dead band had been eliminated. By changing the duty ratio, the damping characteristics of the damper could be altered.

Gupta *et al.* (2003) constructed an electromagnetic regenerative damper using Neodymium magnets. Gupta provided no illustration of the device but described the damper as "The magnet assembly consists of an inner magnet stack surrounded concentrically by a larger diameter outer magnet stack. Each stack consists of three axially magnetised ring magnets separated by separated by two iron pole-rings and two additional iron pole rings located at the ends of the stack. [...] The polarity of the magnets was chosen such that radial magnetic flux emanated from both sides of

each iron pole and the flux of the inner pole adds to that of the outer rings." With this configuration it was estimated that the flux through the two pole rings was half that of the flux through the interior pole rings. For estimating performance a value of 1 Tesla was used for the interior rings and 0.5 Tesla for the end poles.

The coil assembly as described consisted of two coils; an inner coil and a larger diameter outer coil. the second coil surrounded the inner coil concentrically. Each of the coils consisted of four continuously wound layers of #25 magnet wire and were of approximately 800 turns. Each coil was separated into fours sections by the use of insulators. Each of the four coils sections was centred on a different iron pole ring. The polarity of each section was reversed in each adjacent section.

A first order approximation of the voltage generated by the damper was determined using 2.33

$$V = nhvB_i \tag{2.33}$$

where V was the voltage generated in Volts, n was the number of turns in the coil per mm, h was the height of the coil section in mm, v was the velocity of the coil and B_i was the magnetic field in Tesla.

In the case of a regenerative damper the total force generated by the damper was given by 2.34

$$F = K^2 \frac{v}{RI + R_c} \tag{2.34}$$

where F was the force in Newtons, K was a constant determined by the construction of the damper, RI was the external load and R_c was the resistance of the coil, both in Ohms. Gupta then claimed that the power of the circuit was given by 2.35,

$$P = K^2 v^2 \frac{R_c}{(RI + R_c)^2} \tag{2.35}$$

however there was no derivation given and the power equation was not consistent with the more common derivations.

Gupta then stated that the maximum force generated was when RI = 0, but the maximum power was generated when RI = R_c. How this was justified from the equations given previously was left unexplained. The power equation again showed that maximum power would occur when RI = 0.

In a practical demonstration of the damper, the damper had an internal resistance of 31Ω and the external load was varied from 0.1Ω, 30 Ω, 50 Ω and an open circuit. Using the results using a 33 Ω external resistor, as this was the closest to the 'ideal' resistance, the maximum power generated was at 10 Hz, with a displacement of 1.757mm r.m.s and a r.m.s velocity of 110.38 mm/s. This generated a r.m.s voltage of 3.082 Volts and a r.m.s power of 0.2878 Watts. However when compared to the previous equations there appears to be no correlation between the theoretical

and measured values and no comparison was offered by the authors. While this research should be of value, this value was negated by these inconsistencies.

Zhang *et al.* (2007) and Zhang *et al.* (2008) noted that problems with active hydraulic suspension suspensions were the complexity, the high energy consumption and the slow response rate. Zhang et al developed an e.m. damper using a permanent magnet DC motor that was driven by a ball screw and thread. This was later used as the rear suspension of a test automobile at the University of Shanghi. It was confirmed that the damper regenerated electricity.

Gupta *et al.* (2006) designed two different e.m. dampers to turn the energy dissipated in shock absorbers in to electrical energy. The first, Mark 1, model was a linear motor using a moving coil. The second, Mark 2, was a rotary motor attached by linkages. The Mark 1 assembly consisted of an inner magnet stack surrounded concentrically by a larger diameter outer magnetic stack. Each stack had three axially magnetized ring magnets separated by two iron pole rings and two additional pole pieces on the ends of the stacks. The permanent magnets were sintered anisotropic NdFeB. For purposes of estimating performance, a 1T radial flux density was assumed to emanate from the interior pole rings while 0.5 T emanated from the end rings. The coil assembly consisted of an inner coil surrounded by an outer coil. Each coil had 800 turns and was broken into four sections, separated by insulators, each of which was centred on a different iron pole ring. The winding direction was reversed in the adjacent section of each coil to accommodate the reversal in radial flux of adjacent pole rings. Thus, the induced voltages in each section of the coil have the same polarity.

The Mark 1 was tested on an electrodynamic shaker. The open circuit voltage generated was 0.71 V and at 33 Ω the power was 3W for a velocity of 0.01 m/s. For 0.05 m/s the voltage was 3.44 V and again at 33 Ω resistance the power was 54 W. This unit was mounted on a quad bike and the bike was driven over a 4x4 beam generating a maximum power of 7.4 W. The Mark 2, rotary damper, was tested and the damping coefficient was determined to be 38 N/m/s. Mounted on the same quad bike as the Mark 1 damper and crossing the same 4x4 beam, 88.8 W of power were generated.

While much effort has been expended in the research and design of regenerative suspension systems, it was highly questionable whether the low power generation capacity of such systems, even at 100% efficiency, was worth the extra weight and vehicle complexity, therefore this area will not be examined further.

2.4   Active Suspension Systems

Active damping provides a way to improve the performance of the suspension system in passenger comfort, road handling and rattle space. By use of hydraulic or electromagnetic systems it is possible to input energy into the suspension, thus providing

force at times that passive and semi-active dampers cannot. Passive and semi-active systems have no energy input into the system, so can only provide optimal damping for a portion of the cycle of motion. This extra power and force of an active system allows the damping to occur over the full cycle of motion and provides more effective damping than a pure passive or a semi-active system. Due to the control algorithms and information gathering employed on a vehicle it is possible to create a coordinated strategy for all four wheels of an automobile. Thus it is possible for the suspension to adjust for dive when under braking, to resist squat when under acceleration and counter roll while the vehicle is cornering. By use of a road 'preview' the active damper does not have to react solely from the road input through the tyre, but can actually predict what the motion of the tyre will be and thereby enable prediction of the required forces to be applied to the dampers. The use of active dampers offers the greatest likelihood of being able to overcome the limitations of a lightweight vehicle.

Active suspension systems have been in development for vehicles since the 1930s. However most of the significant advances have occurred since the 1950s. Along with the development of high performance feedback control servo mechanisms, a parallel development of active suspension systems has occurred. Mechanopneumatic suspensions for automobiles were developed in the 1950s along with low frequency load levelling suspensions for several types of vehicles. In the 1960s there was effort made to increase the speed of intercity transport, which lead for a desire in advancements of active suspension systems for trains and for automobiles, Hedrick and Wormley (1975).

In the late 1950s automobile manufacturers investigated the feasibility of active mechanopneumatic suspension systems. An active system was developed by Westinghouse Laboratories that used hydraulic actuators to replace the shock absorbers. The input signals were provided by an accelerometer that was offset from the vehicle centre of mass. This was used to activate both the vertical and horizontal suspension functions. However, the early use of active suspension was superseded generally by the further development of passive suspensions and the smoothness of interstate highways in the USA, Hedrick and Wormley (1975).

In the 1970s the Lord Corporation and others investigated hydraulic active systems for cars. While these have had some success on the race track, there has only been a very few models of commercial automobiles with full active suspension that has been sold to the general public.

In practice, most fully active dampers can be divided into two types: those derived from Karnopp's Skyhook damper and those derived from Lotus' Modal Control, Williams and Haddad (1997).

From Gysen *et al.* (2008a) it was noted that all commercial body control systems use hydraulics to provide the active suspension system to improve vehicle ride control and roll behaviour. The advantages he lists for the hydraulic active suspension were

the very high force density of a hydraulic system, the ease of control, the ease of design, the commercial availability of parts, the reliability of modern systems and the commercial maturity. However, the disadvantages of such a system were the inefficiency due to the continuously pressurized system, the relatively high time constant caused by pressure loss and flexible hoses and environmental pollution if toxic fluids escape. The later issue was probably of little or no consequence when comparing the toxic fluids in the dampers with the quantities of toxic materials carried in the remainder of the vehicle. The major advantage of such a system when compared with magnetorheological dampers was that hydraulic systems were capable of introducing energy into the damper system.
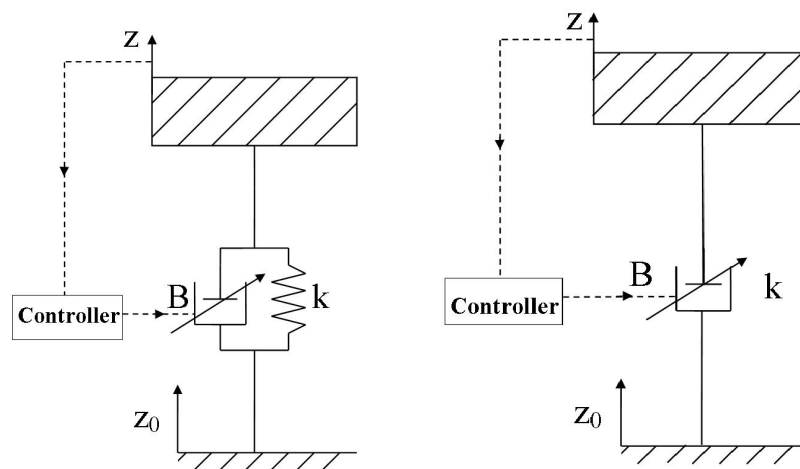
(a) A single degree of freedom active suspension with a spring element

(b) A single degree of freedom active suspension without a spring element

Figure 2.22: A single degree of freedom active suspension with and without a spring element. Key : z is the displacement of the sprung mass, z_0 is the displacement of the surface, b is the damping coefficient and k is the spring constant.

Another consideration was the use of a spring in the suspension system. Systems such as the Lotus Modal System and the BOSE suspension system both use a suspension system without a spring element. While this allows for direct application of the control algorithms to the system, it also requires the active element in the damper to have much higher power requirements than an active system with a spring element. In figure 2.22 a single degree of freedom system with and without a spring element is illustrated.

For a lightweight vehicle the potential performance improvement of an active system was of interest. The potential advantage was improved passenger comfort while still maintaining ground holding capacities. Potential disadvantages would include additional weight over a passive system and for an electric powered vehicle the power consumption was also a prime concern. The power considerations make the use of a damper with a spring element a more attractive proposition than the a

system without a spring.

2.4.1 Control Strategies and Hydraulic Active Systems.
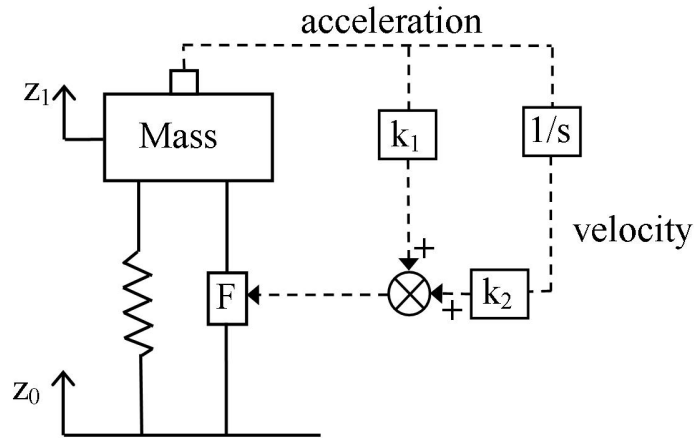
Figure 2.23: An actively isolated system as proposed by Crosby and Karnopp (1973).

From Crosby and Karnopp (1973), in the case of a single degree of freedom system, as illustrated in figure 2.23, with a passive damper in parallel with a spring, taking the Laplace transform of the equations of motion for the system yielded the transfer function of the sprung mass, X, to the motion of the surface, X_0 was given by 2.36

$$\frac{X}{X_0} = \frac{BS + K}{MS^2 + BS + K} \tag{2.36}$$

where S was the independent variable after it has been through the transform, in this case S was given by $\omega\sqrt{-1}$ where ω was the frequency in rad/s, B was the damping coefficient, M was the sprung mass, K was the spring constant, X was the displacement of the sprung mass and X_0 was the displacement of the surface. The undamped natural frequency of the system ω_n was $\sqrt{(K/M)}$ and the damping ratio ζ was $B/2\sqrt{(KM)}$. Plotting the amplitude ratio, X/X_0 vs. frequency as a log-log graph will yield the familiar transmissibility graph (as illustrated in figure 2.24).

Crosby and Karnopp (1973) gave the transfer function for a fully active isolation system as 2.37.

$$\frac{X}{X_0} = \frac{K}{(M + k_1)S^2 + k_2S + K} \tag{2.37}$$

In this system the force generator was in parallel with the spring and the force generator was controlled by the acceleration of the sprung mass and the velocity of the sprung mass. k_1 represented the gain on the acceleration signal and k_2 represented the gain on the velocity signal. The undamped natural frequency of this system

Transmissibilty Function
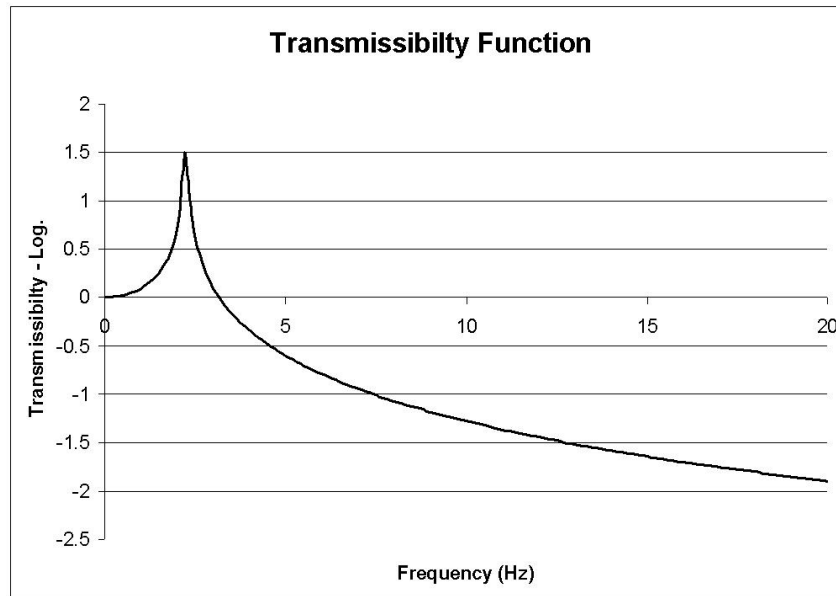
Figure 2.24: The transmissibilty of a suspension system with no damping , a mass of 2,000kg and a spring constant of 10,000 N/m.

was $\sqrt{K/(M + k_1)}$. Because $k - 1$ can be set at any desired value within the force elements ability, both positive and negative, this meant that the natural frequency could be adjusted to any value desired by the controller. For a low natural frequency the value of k_1 will be set an s positive number.

The damping ratio of the active system was given by $k_2/2\sqrt{(M + k_1)K}$. By selecting an appropriate value of k_2 any desired damping ratio could be achieved. The high frequency amplitude of the system was asymptotic to negative two due to the numerator of the transfer function being a constant. The active isolator allows the control of resonant amplitude without having to compromise high frequency performance. Crosby and Karnopp's theory showed that the active damper was an improvement upon the passive damper in all frequencies required for automotive purposes.

Hedrick and Wormley (1975) conducted a state of the art review of suspension systems. While primarily concerned with high speed train suspensions, the review does cover other ground vehicles. The authors noted that while the state of the art knowledge had increased there were still several areas of research that had to be researched further. These included;

– Conceptual design and optimisation.

– Hardware.

–System Cost.

As is demonstrated by the paucity of automobile models available with fully active suspensions, the areas of hardware and system cost have not been satisfactorily resolved. This is exacerbated by the availability of mature semi-active suspension systems that can achieve much of the benefit of a fully active system.

In Karnopp *et al.* (1974) the Skyhook damper was first proposed. While it has been adapted as the main damping strategy in commercial semi-active dampers, it was originally a fully active damping strategy. An 'ideal' algorithm for determining the force of an active damper in a one degree of freedom system was given determined to be 2.38

$$F_D = b\dot{x} \qquad (2.38)$$

where F_D was the force the damper supplies, b was a damping coefficient and $\dot{x}$ was the velocity of the sprung mass. Passive and semi-active dampers were unable to provide this damping at all times through a cycle. This approach will minimise the displacement within the limits of the speed of the system, but as has been noted, this approach does not include the wheel vibration and therefore will not stop 'wheel hop'. For damping the wheel motion another mechanism will be required to be utilised.
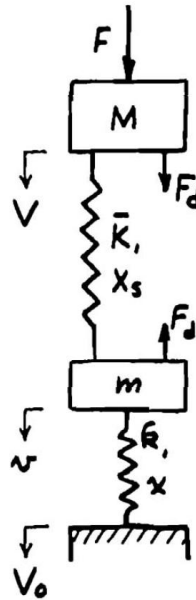
Figure 2.25: A two degree of freedom damper system. Fi s Force, M is the Sprung mass, V is the velocity of the sprung mass, F_d is the damper force, K_1 is the spring coefficient, X_s is the deflection, m is the unsprung mass, v is the velocity of the unsprung mass, k1 is the spring coefficient of the tyre, x is the absolute deflection of the surface and $V - 0$ is the velocity of the road surface.[Source:Karnopp (1983)]

The force of a damper for a two degree of freedom system representing a car body and wheel was given in Karnopp (1983). In this case the velocity of the car body, V and the tyre v needs to be determined and the car body and tyre each have their own linearised damping coefficient, B_1 and B_2 respectively. The damping force supplied was, in this case, given by 2.39.

$$F_D = -B_1 V + B_2 v \qquad (2.39)$$

Using 2.39, Karnopp then compared the theoretical effectiveness of passive dampers to this active damper by the use of their transfer functions. Karnopp concluded that for tracked vehicles which have a direct connection to the ground, such as bulldozers and armoured vehicles, a marked improvement over more conventional passive systems can be achieved through the use of an active suspension with body velocity feedback. However it was observed that for a vehicle with a typical pneumatic tyre, the necessity of providing wheel damping limited the isolation qualities of the main suspension. By combining a passive and an active damper better damping was achieved than through the use of a passive damper alone. While in certain cases the suspension was only marginally improved by the use of the active element, in other cases improved resonance control and isolation was achieved by the use of a simple feedback mechanism using the body velocity.

Karnopp (1986) carried on this research and pointed out that one could remove static deflection through the use of an active suspension. Also, this could reduce squat and dive when accelerating and steady state roll when cornering. The active suspension could also respond to preview information or adjust its dynamics in response to sensed aspects of the vehicle's motions and disturbances. Though, it was noted, that other schemes can achieve improvement over passive elements while using less power and simpler elements than an active suspension.

Karnopp concluded that even with complete state variable feedback, a reasonable ideal filtering behaviour can not be achieved by an active system. From his research a passive damper with adjustable parameters or a semi-active suspension could perform as well as an active system in filtering road way disturbances. It was noted that a relatively conventional suspension design was used and that only state variable feedback was studied. Though, if forces are supplied between a wheel and a suspended mass, then there will always be some limitations to what can be achieved by the system.

While work on optimal control theory of active suspensions had been conducted, previous prototype vehicles have not used much of this work. In the 1980s Peter Wright from Lotus and David Williams of the Cranfield Institute collaborated to together to create a broadband active suspension called "Modal Control". In this model the sprung mass motions were decomposed into three separate modes of motion: Heave, which is the vertical motion of the sprung mass. Roll, which is the angular displacement around the direction of travel and Pitch, which is the angular displacement fore and aft. Each sprung mass mode of motion was then controlled using second order dynamics. The aim of the Lotus Modal Control was to make the vehicle soft in the heave mode, yet rigid in the roll and pitch modes. The multi-input multi-output (MIMO) system was then structured so that the tunable parameters make sense. As such, this controller proved very successful and provoked much of the early industry interest in active suspensions, Williams and Haddad (1997) .

The modal control concept was derived for the single corner or a quarter car
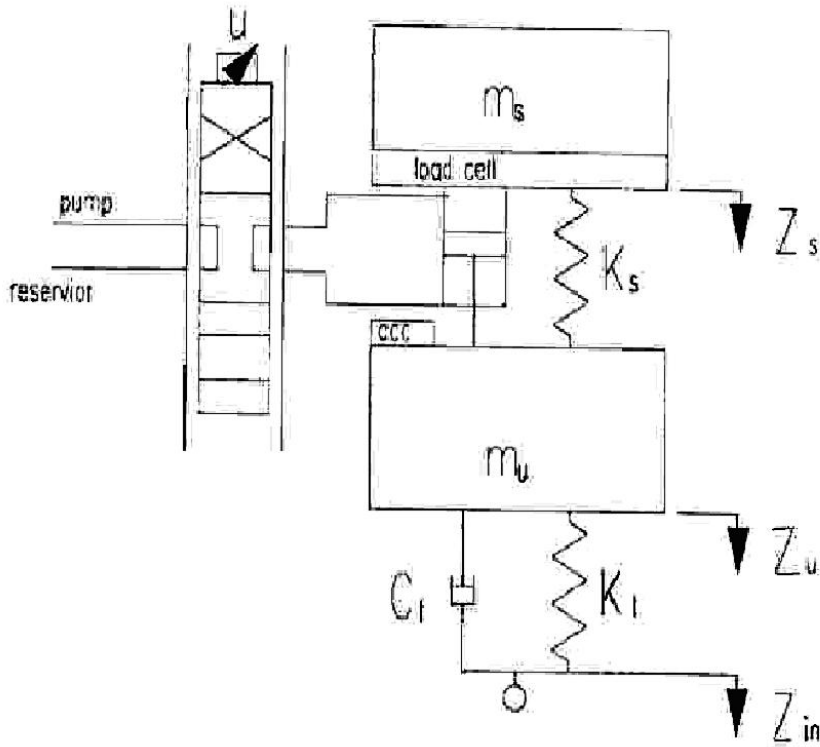
Figure 2.26: A quarter car model of a Lotus Modal Control System [Source:Williams and Haddad (1997)]

model as in figure 2.26. This can be considered analogous to a full vehicle in heave mode. The servo/actuator hardware in the suspension in part determined the form of the modal control system developed. The system used was hydraulic and the servo valve had a natural frequency on the order of 100 Hz. However the frequency could be increased to over 100 Hz if the system has no entrained air, does not use flexible tubing for piping and has small oil volumes. In the single mode model for a single degree of freedom on the sprung mass, the second order dynamics of the sprung mass was assumed and given as 2.40

$$m_s \ddot{z}_s + C_{des} \dot{z}_s + K_{des} z_s = 0 \qquad (2.40)$$

where m_s was the sprung mass, z_s, $\dot{z}_s$ and $\ddot{z}_s$ were the displacement, velocity and acceleration of the sprung mass, C_{des} was the desirable spring coefficient and K_{des} was the desirable spring constant. As z_s was inertially referenced, this will give the same value of C_{des} as Karnopp's Skyhook algorithm. Assuming that both the actuator and the load spring forces were transferred through the load cell, from a free body diagram the force at the load cell, F_{lc} was given by 2.41.

$$F_{lc} = -m_s \ddot{z}_s \qquad (2.41)$$

The velocity of the sprung mass could be expressed in terms of the velocities of the unsprung mass and the actuator, $\dot{z}_a$, as in 2.42.

$$\dot{Z}_s = \dot{z}_u - \dot{z}_a \tag{2.42}$$

Substituting 2.41 and 2.42 into 2.40 gave a term for the actuator velocity of 2.43.

$$\dot{Z}_a = \frac{-1}{C_{des}} F_{lc} + \dot{z}_u + \frac{K_{des}}{C_{des}}(z_u - z_a) \tag{2.43}$$

This gave the optimal velocity that the hydraulic actuator should be driven. In practice the displacement of the actuator was measured by a linear displacement transducer such as a LVDT. The velocity of the unsprung mass was obtained by integrating the acceleration of the unsprung mass. A key innovation of the Lotus algorithm was the addition of software implemented bump-stops. This reduced the open-loop actuator velocity demand as a non-linear function of the position of the actuator, Williams and Haddad (1997). In his research Williams uses the Lotus/Cranfield Modal Control model and changed this model from an open loop to a closed loop control system. It was then determined that the Modal Control model has comparable performance to independent Skyhook dampers on each corner of the car.

In 1990 a literature review into active and semi-active suspensions was conducted by Huisman (1990). The control algorithm was of crucial importance in the design of an active suspension. Seven different approaches of how to design the control system were given. These designs include the use of an equation for the activation of the damper, such as Karnopp's Skyhook damper. Another approach was to use the algorithms of an active damper and when the damper required power during a cycle, then it was turned off for that part of the cycle. Also suggested was an "optimal pole location" technique, a feedback and preview controller and "Optimal Control" controllers.

Huisman noted some practical problems with the use of active and semi-active dampers;
– determining the state of the system. He observed that it was very difficult to measure absolute velocities and displacements and this was probably the biggest practical problem in active dampers.
– A very fast switching damper was required. For a semi-active suspension the switching speed can be approximated by a first order time lag; i.e. with a "break"-frequency of 16.3 Hz. This was for a time constant of $9.76 \times 10^{-3}\ s$.
– For a closed loop control system the bandwidth should be kept down to $6 - 8$ Hz so as to reduce the power demands to a reasonable level.
– Lock up may occur in semi-active suspensions.
– For preview systems good results could be achieved, but the results from different authors could be difficult to compare.

Factors that Huisman noted, which were not previously discussed in this work, were that semi-active and active suspensions can experience difficulties when bumping into a pot-hole, due to the lack of speed of the actuators. This was published before magnetorheological dampers with much higher response speeds became available. One of the primary advantages of an electromagnetic damper was also the theoretical high actuation speeds. A result of interest was that when fast switching dampers were used, the stiffness of the spring can be decreased. By decreasing the spring stiffness, the passenger comfort was improved and may be of benefit in further research.
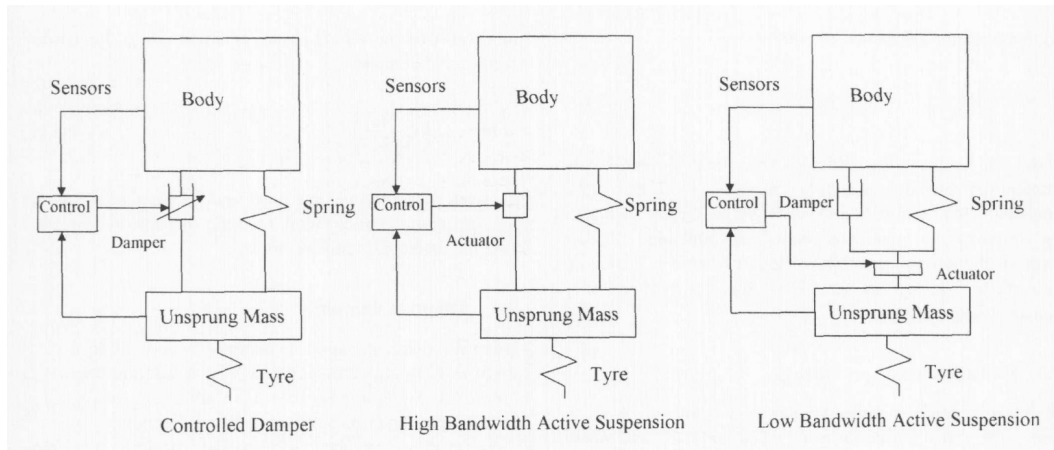
Figure 2.27: Three types of controlled dampers examined by Williams (1997). [Source: Williams (1997)]

Three different types of active suspensions were examined by Williams (1997) and are illustrated in figure 2.27. The first was the high bandwidth damper with controller bandwidths of over 20 Hz. In this system the actuator sits between the body and the unsprung mass and the actuator was dual acting. There was a passive spring to carry the static load which was placed in parallel. Two different types of low band pass active systems acting in the 3–4 Hz range and with the actuator being applied in one direction only, were explored. The first has the actuator in series with a spring. A separate passive damper was placed in parallel. In the second, the active element, the passive damper and the spring were all in series. A controller for a quarter car was used that utilises linear quadratic equations. The power consumption for each of the dampers was determined as if they were using a hydraulic system. For an ideal active suspension system the power consumed by the damper should be given by 2.44

$$W_i = F_a \cdot v_a \tag{2.44}$$

where W_i was the ideal work, F_a was the force of the actuator and v_a was the velocity of the actuator.

However, no system is ideal and there will be a system head loss in the pump and in the valves. It was calculated that the power required to be installed for hydraulic active dampers was 3,140 W for a High Bandwidth system and 3,950-4,040 for a Low Bandwidth system. The highest demand occurred in cornering through a slalom course. Power consumption while driving on a secondary/country road in a straight line were determined to be 1,800 W for the high bandwidth damper and 1,400-2,080 W for the low band-width damper. In Kim and Okade. (2002) it was reported that a typical active suspension of an automobile was said to consume about 5 HP (3.8 kW) of power. Taking into account energy losses in the system, these figures were comparable.

As in the case of active dampers there, were many control strategies given in the literature. In most cases these studies were purely theoretical and involve no construction of a physical damper to confirm the theoretical observations. Strategies published for active suspension systems in cars include Linear Optimal Control, Wilson *et al.* (1986), Sliding Mode Control, Yoshimura *et al.* (2001), Non-Linear Actuator Control using neural networks, Lauwerys *et al.* (2002), Linear parameter-Varying Gain-Scheduling, Fialho and Balas (2002), the use of time scale separation and an "input decoupling transformation" Campos *et al.* (1999), a Model Reference Adaptive Controller Esmailzadeh and Fahimi (1997) , a Fuzzy logic controller Ji *et al.* (2005) a factorisation approach to feedback stability Turkay and Akcay (2008) and Model Reference Adaptive Controller in a cascade controller, Maleki *et al.* (2003).

In the case of the fully active damper one of the limiting factors was the delay in time between an event occurring, such as wheel hop and the time for the correcting force to occur. While this should be able to be eliminated by a road preview, a component of random events will always leak through the damper system into the passenger cabin. With passive dampers this was an irresolvable problem. In the case of fully active dampers and to a lesser degree in semi-active dampers, a solution to this was through the use of road preview. In this strategy sensors are used to determine the road displacement in front of the wheel and to adjust the damping coefficient of the system at the same time the event occurs. By these means the damper can almost perfectly counter any road motions.

Preview Systems

The concept of preview was proposed in the Journal of Basic Engineering in 1968 by E. K. Bender. Since then there have been many papers on this subject. In Marzbanrad *et al.* (2002) an optimal active control system was developed for a full car model. The system incorporated a preview of the road surface and also an alternate controller was used where the displacement of the front wheels was used as a preview of the road surface for the rear wheel. The displacement information was sent to the rear wheels with an appropriate delay for the velocity of the vehicle.

Marzbanrad et al determined that the suspension that gave the least acceleration response was the active suspension with preview, followed by the active system with a delay and finally the independent active system. The improvement for the active system with preview was for all the types of road signal that they trialled. Even a short length of time for the preview produced an improvement. With further increases of preview time the improvement increased up to a critical value, after which their was no improvement with increase of preview time. It was further noted that the control power combined with the power dissipated by the active system with a preview was less than the combined power of the active system alone. It was noted that the combined power of both of these active systems was less than the power dissipated by the passive damper. Further, it was noted that for the active dampers the performance was not sensitive to the variations of sprung mass caused by a changing number of passengers or a changing load. This was consistent across all the road inputs trialled. It was also determined that for all the filtered white noise road irregularities the preview control improved the suspension performance.

A prototype vehicle was used to test the sensors and algorithms for the preview of an active system in Kim *et al.* (2002). A model for all four wheels and having a total of seven degrees of freedom was developed. It was noted that it was impossible to measure the height of the road surface directly from the vehicle as the body motions of the vehicle produce a contamination to the preview data. The solution presented was to have two sensors to measure the distance to the road surface mounted in tandem in the direction of travel. To validate the model of the sensor's response to the vehicle's motion, a series of runs were conducted with an automobile travelling a straight-line course over a variety of known and random road surfaces at various constant velocities ranging from 10–80 kph, depending upon the road conditions. The sampling rate of 1 kHz was used for each sensor. It was concluded the two sensor approach when applied to a road preview system did compensate for the signal contamination caused by the vehicle motions. Further, it showed that in all three main areas of interest, passenger acceleration, tyre deflection and rattle space, that there was an improvement of performance over an active system and when compared to a passive system there was a 60% reduction in the r.m.s. acceleration of the passenger compartment, a 40% reduction in r.m.s. tyre deflection and approximately a 45% reduction in r.m.s. suspension travel.

Marzbanrad *et al.* (2003) developed a three dimensional, seven degree of freedom car riding model which was subjected to two inputs. Contactless sensors were placed on the front bumper to measure the road irregularities and to thereby achieve an enhanced control scheme. A linear quadratic control scheme was implemented and the road signal was inputted into the controller a short time after the same signal being input into the model. This improved the body acceleration, tyre deflection, suspension working space and the control force required. The research showed that there was a minimum preview time required which depended upon the types of

components, the preferences and the components required to construct the system. It also confirmed that there was an optimal preview time after which any increase of preview time does not produce any improvements in the desired properties.

Conclusions

In the areas of ride comfort, tyre deflection and rattle space, significant improvements can be made through the use of an active element in the suspension system. With a preview of the road, this performance can be further improved. For a hydraulic system, the cost of this improvement was the use of 3–4 kW of power that has to be supplied to the active elements. For large vehicles using hydrocarbons this extra power demand was less significant. However, in the case of an electrical vehicle, a constant drain of 3–4 kW would have a major effect upon the range of the vehicle. This was further accentuated for a lightweight vehicle for which this constant power drain will have a larger proportional effect. This raised the possibility of alternate technologies other than hydraulic to supply the actuator force for an active element,

2.4.2   Active E.M. Suspensions

In the case of electromagnetic active suspension systems there were several advantages and disadvantages noted when compared to hydraulic systems. In Gysen *et al.* (2008a) advantages noted were that for the high band width with a frequency of over 10 Hz for an e.m. system, there was no need for continuous power to be supplied to the damper, the ease of control of an electronic system, the absence of fluids, there was improved dynamic behaviour, also stability improvement, that there was accurate force control and that the damper can be used in both directions of motion. The disadvantages noted were the increased volume of the suspension due to lower force density, the relatively high current for a 12 V system and that conventional designs need excitation to provide a continuous force. It should be noted that were such a system to be installed in an electric vehicle, then the available voltage was over 100 V and that circuitry already exists that can switch high currents.

In the production of active electromagnetic dampers there were two common approaches available from the literature. One option proposed was the use of a standard electric motor, the drive shaft of which was connected to a rack and pinion device or a screw that rotates the shaft. By operation of the motor the active damping was achieved. The second method proposed was the use of linear actuators.

In the work of Martins *et al.* (1999) a hybrid passive/active system was used to reduce the size of an electromagnetic damper for the required authority. The damper was constructed of ring shaped Neodymium permanent magnets as is shown in figure 2.28. The magnets were radially magnetised and alternate the direction of the magnetic field for each magnet. They were mounted on a magnetic steel driver rod which passes through the void in the centre of each magnet. The magnet

stack was surrounded by an armature and the assembly was contained inside a soft magnetic steel cylinder to improve the closed loop magnetic circuits. The entire assembly then acted like a permanent magnet brushless spin motor and could provide active damping when commanded by a control system. The space in the magnet assembly was then filled with a hydraulic fluid so it also acts as a conventional passive damper in parallel with the active e.m. damper. Running a series of simulations adding an active component to a passive damper demonstrated an improvement in performance over the passive damper alone. In a quarter car system the active damper provided approximately 20% of the force generated by the passive damper, however it reduced passenger acceleration by in excess of 65%. For a sprung mass of 290 kg meeting a 0.0254 m bump at a rate 1 Hz, the peak power consumed by the e.m. damper was of the order of 40 W and an r.m.s. value of 28 W. This compared to a power consumption of 3500 W r.m.s. for an equivalent active hydraulic damper, without a spring, in the same conditions. This demonstrated that effective active damping could be achieved in a vehicle with a much lower power consumption than an equivalent hydraulic system.
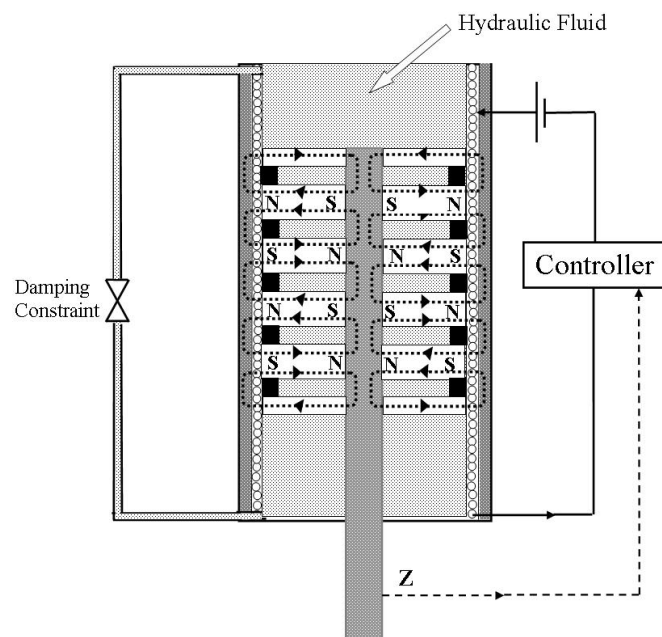
Figure 2.28: A hybrid active damper as proposed by Martins et al (1999). Key. Light grey is hyraulic fluid, dark grey is steel/iron and black is a non-magnetic material.

In Martins *et al.* (2006) a prototype active e.m. suspension system was constructed. This system took advantage of the then new magnet and electronic advances. The damper was designed to have a stroke of 160 mm,a peak velocity of 1.2 m/s, to be able to supply a maximum steady state force of 1,050 N and an r.m.s. power in normal operation of 615 W. The physical dimensions of the proposed damper were a

diameter of 110 mm and a length of 600 mm. The damper was essentially the same as proposed in Martins *et al.* (1999) and illustrated in figure 2.28. The non-moving parts weighed 19 kg and the moving parts weighed 9 kg for a total weight of 28 kg. The damper had an equivalent damping coefficient of 1350 N/m/s at 3.28 Hz and amplitude of 8 mm. The active element was a 7 pole actuator using twenty coils with two phases.

The controller was a sliding mode controller that was to achieve Skyhook damping. It was concluded that the force values produced were sufficient for use in an automobile, however the weight of the unit was larger than a comparable hydraulic damper. It was conjectured that by improving the coolant system, the weight of the entire system could be reduced. It should be noted that the e.m. damper had a mass of 28kg, compared to a nominal mass of 4 kg for a commercial hydraulic damper. This system has several times the mass of a comparable hydraulic system. It would be a specialist application where the advantages of the system would overcome the weight disadvantage.

In the work of Kim *et al.* (2001) an active electro magnetic damper was constructed and tested. The damper, as illustrated in figure 2.29, has several interesting features. The system consisted of a base plate that was displaced vertically. Attached to the base plate was a spring and damper in parallel. Little explanation was given of this damper, but it was probably a passive hydraulic damper. The spring damper was connected to the upper (moving) plate, to which a permanent Samarium-Cobalt magnet was attached. Above this was an electromagnet that was fixed to the supporting plate. There was an accelerometer attached to the upper (moving) plate, which from which the signal was input into a controller taht then drives the electromagnet. This whole system was mounted so that it was a single degree of freedom system.

Points to note were the use of both an active damper and a passive damper in the same system. Also of note was that the electromagnetic force will be very non-linear and acts over a very short distance. The maximum displacement of the magnets was 20 mm. An unusual aspect of this design was the use of a magnet and an electro-magnet which were directly opposed, rather than a coil-magnet or linear actuator. Designed for damping frequencies found in automotive applications the damper was tested between 0.1 Hz and 20 Hz. At 2 Hz the damper showed an improvement in displacement of the sprung mass of approximately 75%. At 10 Hz the improvement was approximately 67%. For a sprung mass of 10.4 kg, a force of 95 N was generated using 5 A of electricity. Unfortunately the power was not given, nor can it be computed from the data provided.

Chaves *et al.* (2003) constructed a physical quarter car prototype which used a double phase permanent magnet linear motor as an active element with a maximum force of 980 N. A spring was used to carry the weight of the vehicle. The parameters of the system were established so that the resonant frequencies of the system were
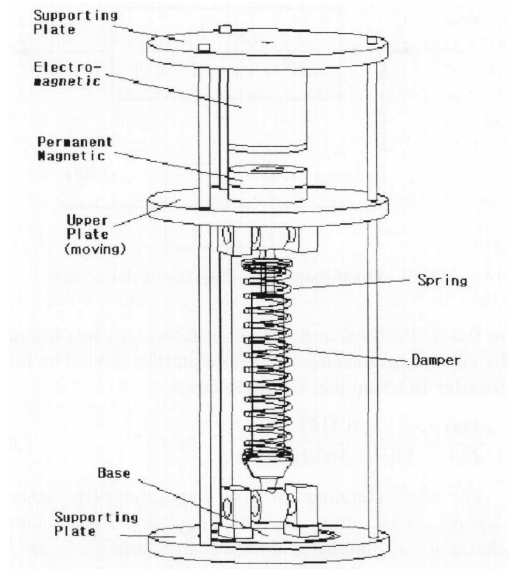
Figure 2.29: The model of an active electromagnetic damper as proposed by Kim *et al.* (2001) [Source:Kim *et al.* (2001)]

1.4 and 10 Hz. The quarter car model was built with a tyre running on an endless road. The sprung mass was 200 kg, the unsprung mass was 36.5 kg, the spring coefficients were 16,000 Nm^{-1} for the spring and 130,000 Nm^{-1} for the tyre. The theoretical performance for this system with passive, semi-active and fully active control laws are illustrated in figure 2.30. It was of interest to note that the two invariant points that exist for a two degree of freedom system. For the first of these two points the semi active damper shows an improvement over the passive damper and the active damper produced a significant improvement compared to the other two types. However for the second invariant point, there was no improvement for the semi-active system when compared to the passive system and the active system showed greater relative accelerations than the other systems. This second frequency was in the 60 Hz range and was above the frequency that most suspensions were concerned with.

The details of the construction of the active actuator were not given by Chaves et al in any further detail than has already been given. For this system Chaves et al concluded that the system can bring benefits to the passenger's comfort over passive and semi-active systems.

In the case of an ideal Skyhook damper as proposed by Karnopp, the majority of the damping cycle energy was being dissipated and approximately 25% of the cycle energy needed to be supplied to the damper. If the dissipated energy could be regenerated and stored until required, it was then possible to build an active damper that required no supply of external power. This would negate one of the disadvantages of an active system. In Nakano *et al.* (2003) the concept of a self powered e.m. damper was investigated. The mass was supported by a spring and
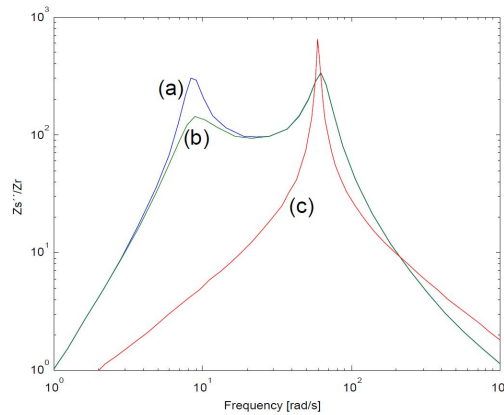
Figure 2.30: Theoretical frequency response of a) a Passive Damper, b) a Semi-Active Damper and c) an Active damper. [Source:Chaves *et al.* (2003)]

a linear electric actuator was proposed as the active element. The controller was based upon Karnopp's Skyhook. The regenerated energy was stored in a capacitor and relays were used to switch the direction of the current to the capacitor and the damper. The frequency response for the damper is given in figure 2.31. In this figure the value of 'n' was a non-dimensional feed back gain which was the ratio of the damping co-efficient of the Skyhook damper to the equivalent damping coefficient provided by the active element.
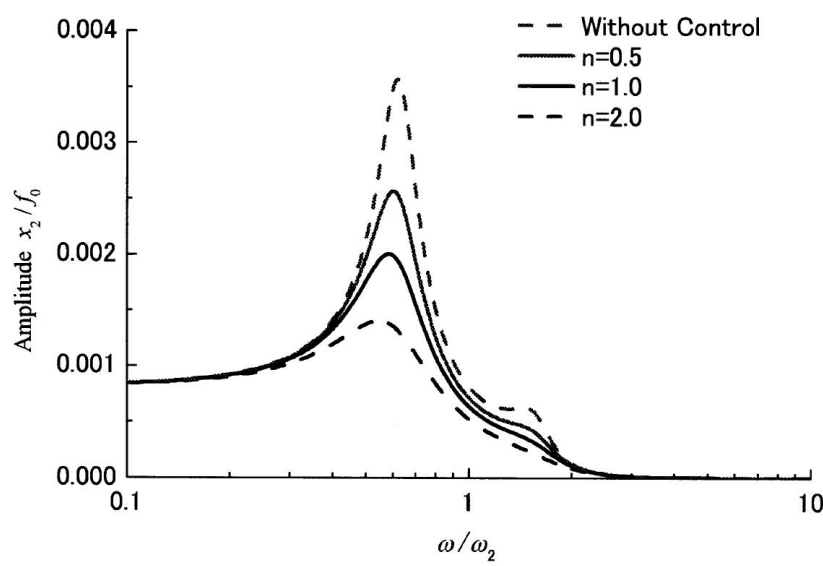
Figure 2.31: The frequency response of the displacement of the sprung mass in a two degree of freedom system. x_2/f_o is the displacement of the sprung mass relative to the surface, ω/ω_2 is the angular velocity of the surface to the sprung mass. [Source:Nakano *et al.* (2003)]

Experimental results showed that when n = 0.5 the power generated was greater than required. When n = 1.0 was the 'break-even' point where the power generation
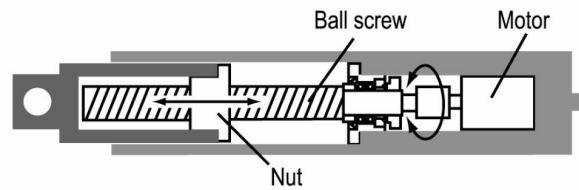
(a) The Active e.m. Damper.
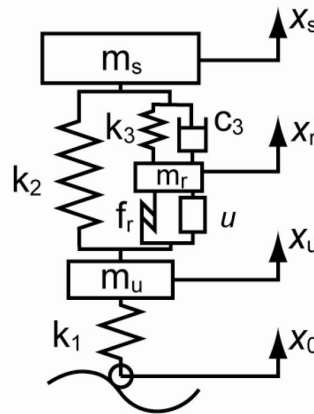
(b) The damper in a 3 degree of free-
dom system

Figure 2.32: Kawamoto's active e.m. damper. [Source: Kawamoto *et al.* (2007)]
Key: m_s, m_u, and m_r are the sprung mass, the unsprung mass and the mass of the
moving rod in the suspension system, I_d is the equivalent inertial inertia, k_1, k_2 and
k_3 are the spring constants of the tyre, suspension and mount, c_3 is the damping
coefficient of the mount, f_r is the Coefficient of dynamic friction and x_s, x_r, x_u, x_0
are the displacements of the sprung mass, rod, unsprung mass and road profile
respectively.

slightly exceeds power demand and when n = 2 the power demand was greater than
the power generation.

As Nakano et al were required to use relays, the switching speed of the circuit
was slower than would be desired. Further, relays provide a binary response, but
do not provide a continuously variable voltage/current. From figure 2.31 it can be
determined that when n= 1, which was when the energy break even occurs, there
was still a strong signal from the road surface being applied to the sprung mass.

Kawamoto *et al.* (2007) proposed a commercial screw and ball system to convert
rotary motion from an electrical motor into linear motion of an actuator. A model of
the damper and a three degree of freedom quarter car system were created. In this
model there were three masses that move, the sprung mass, the unsprung mass and
also the mass of components of the active element it itself. An experimental damper
was constructed which showed a good correlation with the model. For a frequency
of 2 Hz the peak power consumption was 15.3 W which was also regenerated by the
damper. No direct performance results were published. The primary results of this

research was that a model could be constructed which has a good correlation between theory and experiment. Also that vibration control and regeneration of energy for an active system can also be achieved. Even if no energy was regenerated, a power consumption of 15.3 W would be of interest for a light weight vehicle that requires low power damping.

In Gysen *et al.* (2008b), a brushless synchronous tubular permanent magnet actuator combined with a passive spring a system was designed that also provided for active roll and pitch control during cornering and braking. After research driving a vehicle around the Nürburgring in Germany, it was determined the maximum force required by the front actuators would be 4 kN. It was noted that the Nürburgring was a racetrack and did not represent normal driving conditions. It was therefore decided that the front actuators would require a mean force of around 700 N under normal conditions. An active e.m. damper was constructed, of which little detail was provided. The initial unit had a maximum continuous power consumption of 318W/wheel. A final design provided a continuous force of 755 N at a maximum speed of 1m/s and a maximum force of 4kN at 0.1m/s. While the peak power consumption was 2kW, it was determined that the r.m.s. power consumption for around town driving was 16 W. This would show a decrease of over 50 times less power consumption compared to a more conventional hydraulic active suspension system.

Further research by Gysen *et al.* (2008a) used a Halbach magnet array in the damper system. This arrangement of magnets is shown in figure 2.33 and augments the magnetic field on one side of the magnet and reduces the field on the other side to close to zero. For the Halbach effect to work with ring shaped magnets the magnetic fields of the magnets would be arranged so that the outside of the magnets have the following magnetic fields in order: up, into the ring, down, out of the ring, up. This pattern repeats as often as desired. In the case of the damper used by Gysen, which has a series of ring shaped magnets mounted on a central spindle of steel, the magnetic field was optimised on the outside of the stack so as to produce the maximum magnetic field through he three phase armature. The magnetic field was minimised on the side of the spindle. However no comparison was made between the damper using a Halbach magnetic array and the previous magnet arrangement.

Work was conducted by Zhang *et al.* (2009) into an active damper with regeneration of energy. The paper was too brief to ascertain much information. It was concluded that in passive mode, the larger the electrical resistance the greater the force, which was at odds with the results published in the work itself. While a full size damper was used and installed in a vehicle on a shaker rig little detail was given. Further, the only results given were that the suspension could generate voltage.

An active suspension using a ball screw to convert rotational motion into linear motion was explored theoretically in Amati *et al.* (2006). This proposed damper is illustrated in figure 2.34. The physical components of the damper were (1) the
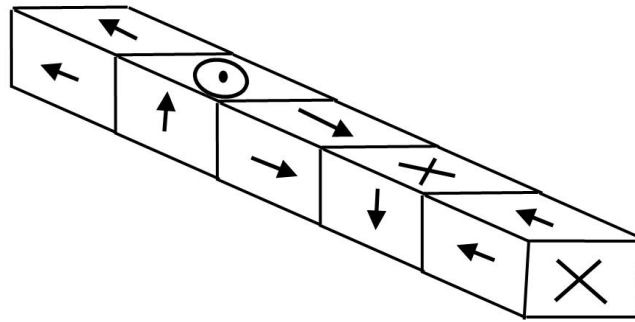
Figure 2.33: The Halbach magnet array. In this example the magnetic field on the top of the array is large and on the bottom surfaces is very much lower.

screw, which was rigidly connected to the moving piston (6). These were bolted upright to reduce secondary motions. The motor was constructed of (2) the stator, (4) the rotor and (5) the housing. The guiding tubes and the nut on the screw (11) were connected to the unsprung mass. The mechanical configuration was completed with a rubber bump stop (9), the coil spring support (10), ball bearings (3a and 3b) and bushings (7a and 7b).
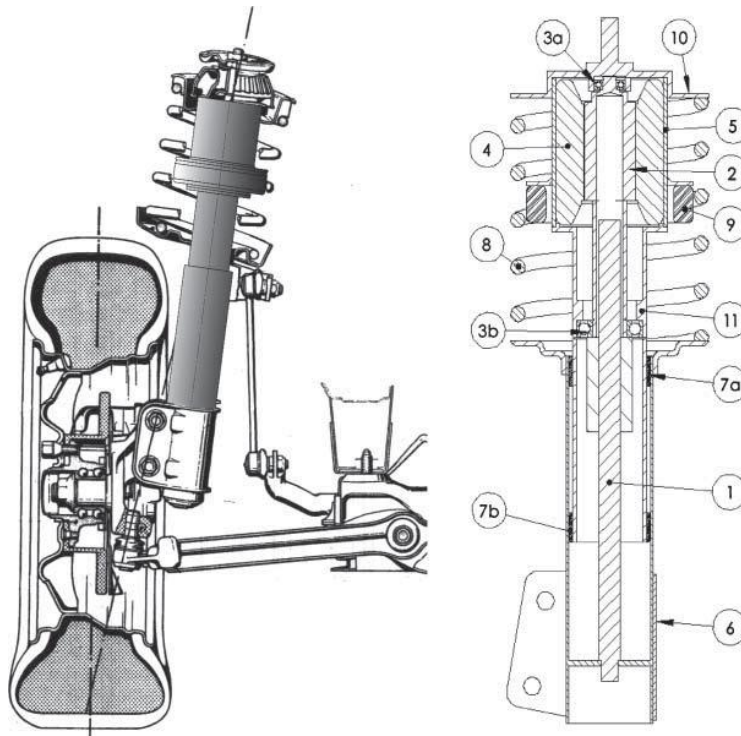
Figure 2.34: An electro-mechanical damper in a McPherson Strut Suspension and the cross section of the electro-mechanical damper. [Source:Amati *et al.* (2006)]

The total mass of the damper as designed was to be 5kg, as compared to 4.1 kg for a hydraulic damper with continuously variable damping. This was compared

to an e.m. passive damper of similar performance which weighed 15 kg. Research on this damper was continued in Amati *et al.* (2011). Amati achieved a maximum damping coefficient of greater than 12.1 kNs/m. Using the same damper it was calculated in Amati *et al.* (2011) that the damper was capable of achieving 2,000 Ns/m of damping per kg of damper weight. This compares to 2,440 N s/m/kg for a passive hydraulic damper, 580 Ns/m/kg for an eddy current damper such as proposed by Ebrahimi and 490 N s/m/ kg for a commercial linear motor used as a passive damper.

Conclusions

The active e.m. active damper has shown that it is possible to theoretically obtain good damping performance at a low energy cost. While few papers published give the power consumption of a damper, it has been stated in two papers that active damper for vehicle can be achieved with less than 20 W of power per wheel. This is of interest in the use of a light weight electric vehicle. Due to the light weight of the vehicle there is an expected reduction in ride comfort available from passive dampers. When compared to an active hydraulic system, the active damper requires much less power than the 3.5 kW of the hydraulic system. At 80 W for the whole active system, this represents approximately 1–2% of the typical power consumption of an electric vehicle such as the University of Waikato's Ultracommuter. While the e.m. damper may be heavier than a comparable hydraulic damper, the power supply and distribution networks already exist in an electric vehicle and does not require a separate power technology. This reduces the final complexity of the system.

This leaves opportunities for alternative technologies such as the active e.m. damper. Due to these benefits several automotive manufacturers are developing and introducing active suspensions. The research is often commercially sensitive and is not published in peer reviewed journals. However, active electromagnetic damping could be of particular interest in lightweight electric vehicles.

2.5   Modelling the Magnet

Overview

For the modelling of an e.m. damper it was required to provide a model of the magnetic fields that the damper will be experiencing. The magnets used in the proposed research were cylindrical rare earth permanent magnets. Whilst magnets have been known from antiquity, the modelling of magnets was much more recent. The two major methods available for modelling the magnet were the use of the Finite Element Method and the modelling of the magnet as a solenoid. The Finite Element Method has achieved wide spread popularity and was available in commercial software. The solenoid model of the magnet was less common. This may partially be

due to the inability to perform the calculations required at a sufficient speed until after the finite element method became popular.

2.5.1   The Finite Element Method

The Finite Element Method (FEM) was a method for determining the approximate solutions to boundary value problems of differential equations by the use of numerical means. By the use of the calculus of variations, the error function was minimised and a stable solution was obtained. The structure being examined was broken into a series of smaller sub-domains which connect simple element equations, named finite elements, to approximate a more complex equation over a larger domain. The fundamentals of the Finite Element method were established by Strang and Fix (1973), Zienkiewicz *et al.* (2005) and Bathe (2006). The Finite Element Method was applied to magnetic fields as' early as 1967, Zienkiewicz *et al.* (1967). The Finite Element Method was also applied to solid structures such as car frames from the 1960s onwards using the work of Zienkiewicz and Taylor (2000) among others.

The Finite Element Method of analysis typically determines the magnetostatic field using Maxwell's equations of electromagnetism. In typical applications a high degree of non-linearity of the field can exist. The solutions to this generally used an iterative approach in which a series of linearised problems were solved. Zienkiewicz *et al.* (2005)

The Finite Element Method is used extensively in industry and many commercial computer products were available. In the literature there were thousands of papers dealing with the issue of the Finite Method and magnetic fields. These include the design of magnets Liu and Liu (2006), two and three dimensional magnetic fields Fujiwara *et al.* (2002),Barton and Cendes (1987), determining the flux Nakata and Takahashi (1982) and for use in passive dampers Kanamori and Ishihara (1989).

However, for the purposes of the proposed research other methods were investigated. This would allow the development of a model from first principles and would allow a single integrated suite of computer programs to be constructed using a single software system. The use of a commercial finite element method package would have raised issues of transportability of data and would entail data conversion steps. The option of construction of a FEM package seemed more time intensive than was required. It was also one the aims of research to investigate less commonly used techniques in new applications. Further, it was felt that the solenoid method was not widely used due to the inability to compute analytically the magnetic field. However, since then the 1960s computing power has increased by over nine orders of magnitude and it was now possible to numerically solve the mathematics required. The use of a solenoid model could offer benefits of simplicity when compared to the FEM approach.

2.5.2   Other Magnet Models.

While the Finite Element method is commonly used in commercial applications, there were other approaches to determining the magnetic field. These approaches include the Coulombian approach and the Amperian approach.

The Coulumbian Approach

In the Coulombian model a cylindrical magnet that was axially magnetised can be charged by two charged planes which were located at the upper and lower surfaces of the surface Ravaud *et al.* (2010). The two planes were given a pole strength. A permanent magnet has been modelled as a dipole with a finite distance between the poles. Such a mathematical model was given by Jiles (1998) in 2.45

$$B = \frac{\mu_o P}{4\pi} \left(\frac{1}{(x - \frac{L}{2})^2} - \frac{1}{(x + \frac{L}{2})^2} \right) \tag{2.45}$$

where B was the magnetic field in T, μ_o was the permeability of free space, P was the magnetic pole strength in A·m, x was the distance from the pole in m, and L was the length of the dipole in m.

   While such an approach can give a reasonable approximation of the magnetic field at a distance from the magnet, it can be seen that as $l/2$ approaches the value of x, then the magnetic field approached infinity. This model produces a reasonable approximation of the field at a distance from the magnet larger than several lengths of the magnet. However, when examining the magnetic field near the poles and inside the magnet, then the utility of the model was reduced. For a a model of the magnet that requires these points, as in this research, then this model was not usable.

   In Ravaud *et al.* (2010) a more complete Coulombian model was derived analytically which gave the same result as the thin wall coil approach for the magnetic field of the magnet. He then extended this to determine the axial force, the stiffness and mutual induction between two permanent magnets using this approach. This final analytical model would still need to be modelled numerically due to the use of elliptical integrals. While this approach may offer an analytical solution using the Coulombian approach, it was published after the approach direction of this thesis was decided and a model had already been constructed. While a good comparison between the Coulombian method with a filamentary model was achieved, neither were tested against a prototype.

The Filamentary Model

One method to determine the effect of a magnet on a passive damper was by determining the mutual inductance between the magnet and the coil as in the work of Akyel *et al.* (2002). This used the concept of filament coils (Maxwell's coils). In this

approach the conductor was divided into meshes of thin circular filamentary coils. For two parallel coils on a common axis with radius r_1 and r_2 the mutual inductance between the coils is given in 2.46 and 2.47

$$M_{MAXWELL} = \frac{2\mu_0\sqrt{R_1 R_2}}{k}\left[\left(1 - \frac{k^2}{2}\right)K(k) - E(k)\right] \qquad (2.46)$$

$$k^2 = \frac{4R_1 R_2}{(R_1 + R2)^2} \qquad (2.47)$$

To determine the inductive link between two coils with inclined axes and in air, Babic and Akyel (2008) uses the filament method. In this work it was assumed that the wires have a square cross section or a negligible cross section. The work of Akyel *et al.* (2009) extends the work of Babic and Akyel (2008). This allows for the use of use of coils with a rectangular cross section, thin disk coils (pancakes) and circular filamentary coils..

In Babic and Akyel (2012) extended upon the work in Babic and Akyel (2008) and Akyel *et al.* (2009). The general case for the magnetic force between two inclined circular filaments were presented. This paper allows for the circular elements to be non-axial and in any orientation. An analytical solution was developed and then verified by comparison of examples with accepted models and would produce the force in an active damper. This approach would yield the force on an active damper. But would not produce the force produced in a passive damper. This would not produce a full model of the damper.

The Amperian Model

In the Amperian model of a permanent magnet, the magnet was modelled as a thin walled cylindrical coil. A current passing through the solenoid produces the magnetic field. This approach was to model the solenoid as a series of loops with a filamentary current. At a point the magnetic field from each point was summed for each loop in the solenoid.

The work of Kuns (2007) derives a general solution for determining the magnetic field produced by a loop of current carrying wire by using Maxwell's equations. The model takes the magnetic vector potential and determines its divergence. To determine the off axis magnetic field, the use of elliptical integrals was required. This approach gave a solution that could be readily numerically modelled and which could be developed in a general computing package. For these reasons it was chosen for further research.

Conclusions about Magnets

While there were several methods of determining a magnetic field at a point, the Amperian model as derived in the work of Kuns (2007) was deemed the most suitable

for use in determining the magnetic fields to be used in an e.m. damper. The Finite Element Method, while commonly used, requires its own specialist program to determine the field. Using the Amperian model, this requirement for specialist programming resources could be reduced and the Amperian model could be adapted for determining the the magnetic field and the flux inside a coil.

2.6 Discussion

This review has examined several main areas of vibration damping with an emphasis on their application to lightweight electric vehicles such as the University of Waikato currently owns and operates.

While the hydraulic passive damper was the predominant damper in operation by private automobiles, it was not the only available technology. In the field of electromagnetic passive dampers there were three common technologies: eddy current damping, linear induction damping and rotary generator damping. The linear induction damper produced a simple mechanical element which could be modelled. A major consideration in the choice of an e.m. passive damper instead of a hydraulic damper, would be the mass of the damper to achieve the same damping.

The use of a linear induction damper allows the use of alternative control strategies with little power input. Of these the semi-active system was already in commercial production. When compared with electrorheological dampers the e.m. damper offers potential advantages in the use of a low level of control power, the reduction in system complexity and a possible reduction in mass.

A major proposed use of the e.m. damper has been as a regenerative damper to produce electrical power. This was of particular interest for use in electric vehicles to extend the range of the vehicle. However the maximum potential total power regenerated by the dampers would be less than 5% of the vehicles propulsive power, assuming a 100% conversion of the mechanical energy into electrical energy. The potential benefit of the e.m. damper in regenerative mode was offset by the amount of extra mass that was required when compared to a commercial passive damper and whether the energy regenerated by damper exceeded the energy required to propel the extra mass of the damper. Due to the low power regenerated there was no requirement to examine this strategy any further.

In damping the active suspension system is the aim of many organisations. There were few few full active systems available in commercially available cars. This was due to their complexity, cost and power consumption. An e.m. damper offers the potential of all the benefits of the hydraulic system with much reduced cost and power consumption. While there were many potential active control strategies, the Skyhook control algorithm proposed by Karnopp in 1974 was considered the simplest for practical implementation in testing. Active dampers were constructed with or without a spring element. An active damper without a spring element offers a more

faithful reproduction of the required damping forces. However, the energy demands were greater as the damper must also provide forces to hold the car body off the ground. A system with a spring offered a reduced power consumption in return for less authority on high force demands.

2.7 Research Questions

In the area of e.m. dampers there were several areas that appear to be less researched than was required for constructing practical dampers for real world applications. In the area of simple systems involving a coil and a magnet the research as published in the literature is sparse. This poses several questions that this work aims to answer.

It is proposed to build a model of a linear e.m. passive damper which consisted of one or more cylindrical magnets and one or more cylindrical coils. This would be constructed as an integrated suite of programs. This would then be used to determine the practicality of passive e.m. dampers with a particular focus on lightweight electric vehicles.

It is also proposed to build a model of a linear e.m. active damper which consists of one or more cylindrical permanent magnets and one or more cylindrical coils. This would be an integrated suite of programs. This would then be used to determine the practicality of an active e.m. damper for use in a light weight electric vehicle.

The contributions of this research are perceived to be

(i) An integrated model of a simple passive linear e.m. damper consisting of cylindrical coils and cylindrical magnets for use in light weight electric vehicles. The non-linear nature of such a system requires the use of such a model in the construction and design of e.m. dampers. The use of non-Finite Element Methods would make this research novel in the literature.

(ii) Determination of the effectiveness of the linear passive e.m. damper for use in lightweight electric vehicles. The benefits must be two fold in that the damper must be shown to be as effective as current commercial dampers and that the weight of the damper was not a significant impediment to the implementation. This use of the model would be novel.

(iii) An integrated model of a simple active passive linear e.m. damper consisting of cylindrical coils and cylindrical magnets for use in lightweight electric vehicles. The non-linear nature of the magnetic fields requires a model rather than an approximation. The construction of such a model for automotive applications without the use of the Finite Element Method would be novel.

(iv) Determination of the effectiveness of the linear active e.m. damper for use in lightweight electric vehicles. This involves the weight of the damper and the power consumption of the e.m damper. The use of this model would be novel.

The use of these methods will enable the design of dampers for use in the University of Waikato electric vehicle fleet.

Chapter 3

Methodology

Introduction

Several stages were required to determine if it is possible for an electromagnetic suspension to have enough authority to damp the motion of a light weight electric vehicle, yet have a power consumption low enough so as to no affect the overall performance of the vehicle.

As the damper model proposed consisted of a single magnet moving through one or more solenoids, a way of modelling the permanent magnet was required. This was required to produce the magnetic field at any point, including inside the magnet itself. Due to the nature of the damper the magnetic field would be non-uniform. Using this model it was also be required to determine the magnetic flux over an area. This would be required for the passive damper model. For the active damper the magnetic forces at a point was be required. For use in the damper models these fluxes and forces were provided to the damper models in the form of a look up table.

A model of the passive damper was required as this is the most common form of damping in current automotive use. Also a model of the active damper was needed. Experimentation was used to determine if there is a relationship between the models and an actual prototype.

Once the relationship between the model and experimental data was determined, then the model could be scaled up to determine the proposed dampers in automotive applications.

The magnet, passive damper and active damper   The research was divided into three units, each of import. The magnetic field was modelled so that it could be used in the models of the passive and active dampers. The passive damper was modelled as this is the simplest functional damper and it can also be used to model semi-active dampers. The active damper was also modelled as this was the basis of the research.

The Magnet A model of the permanent magnet was constructed from Maxwell's equations. Numerical methods were used to emulate the magnet rather than using the Finite Element Method. The reasons for this were explained in Chapter 2. Once a theoretical model ws developed this was implemented numerically using Matlab Simulink software. This model of the permanent magnet was then verified by placing a prototype magnet on a stand and measuring the magnet field over a grid. A comparison was then be made between the Simulink model and the experimental data to validate the model.

For use in the passive damper the total flux of a coil needed to be determined as the coil moved in the system. By numerically integrating over the area of a single loop of the coil and then summing the fluxes of the loops of the coil the total flux of the coil was determined. By passing the magnet through a coil the change in voltage could be measured. By integrating the flux over time the total flux of the system could be calculated and compared to that produced by the model By comparison of these data sets the accuracy of the flux model could be calculated.

In the case of the active damper the magnetic field was required to determine the Lorentz force acting upon the solenoid. Firstly, the force generated by one loop of the solenoid was determined. This was then summed over the number of loops in the solenoid. A look up table could then be generated for the field. As validation of the magnet has been performed previously, the validation of the force would be performed by measuring the maximum generated force experimentally and comparing this value to the value generated by the model. Further validation would occur when validating the active damper.

The Passive Damper A model of the passive damper was developed from the equations of motion for a single degree of freedom system. The damping force would be determined by the use of Faraday's Law. This equation would then be used to determine the force generated by the passive damper. This force would be used in the equation of motion. This equation was used in Matlab Simulink to model the motion of the system using numerical modelling. A prototype damper would be constructed, a model of which which would also be produced in Simulink, using the lookup table mentioned previously, to determine the flux at any point in the dampers motion.

A series of data runs would then conducted in the time domain using a step input signal and using different masses as the unsprung mass. A further series of data runs would be conducted with a fixed weight as the sprung mass, but a pseudo-sine wave input of varying frequency to obtain a frequency domain graph. The experimental data would then compared to the model response to determine the validity of the model.

The Active Damper Using the equation of motion for a dingle degree of freedom system a theoretical model would be developed in a computer program. In the case of the active damper a practical prototype could be constructed using VISSIM as a control package in preference to Matlab due to resource constraints. The input to the control system was an accelerometer which is fed into VISSIM using the REALTIME package. A control response would be generated and a current amplifier would produce the requested magnetic field. Experimental runs were to be conducted to determine both the time domain response and the frequency domain response. The theoretical and experimental results could then be compared to determine the validity and accuracy of the model.

Scaling of results After the models for the passive and active damper were developed, then they would be used to model passive and active dampers of sufficient authority to provide reasonable damping of a full scale lightweight electric vehicle. Of particular note was the accelerations felt by the passengers. The physical weight of the damper and the power requirements of the damper.

Conclusion Using this methodology it was possible to investigate the research question

Chapter 4

Modelling a Magnet

4.1 Introduction

For the construction of an e.m. damper, both passive and active, a solenoid and permanent magnet were utilised. The permanent magnet was cylindrical and the solenoid was a cylinder that the permanent magnet could be translated through. The poles of the magnet were oriented in the direction of travel. This was constructed physically and as a computer model to predict the behaviour and performance of the passive and active dampers.

In both the passive e.m. and active e.m. dampers the forces generated and the damping achieved were caused by the interaction between the permanent magnet and the solenoid. For both cases it was required to construct a mathematical and computer model of the permanent magnet.

The two predominant forms of modelling the magnet available, were using the Finite Element Method or by numerically modelling the magnet as a solenoid. The latter approach was chosen for a variety of reasons as given in Chapter 2. This led to easier integration of the data and the use of less individual computer programs and other computer resources. After the magnet was modelled it was compared with experimental data to confirm the computer model.

4.2 Numerically Modelling a Magnet as a Solenoid

It is well known that a permanent magnet can be modelled as a solenoid. This approach enabled the modelling from Maxwell's equations and also enabled a much more "hands on" construction and control of the final model. For the simplest magnet model the solenoid could be represented by two loops, one at each pole. This gave an approximation similar to 2.45. A closer approximation of the magnetic field was obtained by increasing the number of coils in the solenoid. At a point in space the magnetic field for each loop was summed to provide the final magnetic field at that point. For a single loop of current carrying wire as illustrated in figure 4.1

the on axis magnetic field along the z axis can be determined using the Biot-Savart law for steady, filamentary currents in free space given in 4.1,
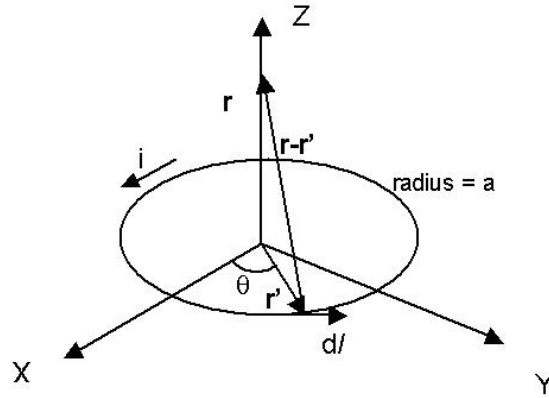
Figure 4.1: The magnetic field for a single loop of wire.

$$B = \left(\mu_0 \, \frac{I}{4\pi} \right) \int d\mathbf{l} \, \mathbf{x} \, \frac{(\mathbf{r} - \mathbf{r}')}{\mid \mathbf{r} - \mathbf{r}' \mid^{\mathbf{3}}} \tag{4.1}$$

where B was the magnetic field measured in Tesla, μ_o was the permeability of free space, r was the distance from the centre of the coil on the z axis to the point in space being measured in m, r' was the distance the wire was from the axis in meters and **dl** was the length to be integrated.

The integration length could be determined by 4.2

$$\mathbf{dl} = -a \, d\theta \, sin\theta \, \mathbf{a_x} \, + \, a \, d\theta \, cos\theta \, \mathbf{a_y} \tag{4.2}$$

where a was the radius of the circular loop of wire in m. Also, $\mathbf{dlx}(\mathbf{r} - \mathbf{r}')$ can be determined by 4.3,

$$\mathbf{dl} \, \mathbf{x} \, (\mathbf{r} - \mathbf{r}') = (az \, cos\theta \, \mathbf{a_x} + az \, sin\theta \, \mathbf{a_y} \, + \, a^2 \, \mathbf{a_z}) \, d\theta \tag{4.3}$$

By substituting 4.2 and 4.3 into 4.1, the Biot-Savart law now becomes 4.4

$$B = \left(\mu_0 \, \frac{I}{4\pi} \right) \int_0^{2\pi} \frac{\left(az \, cos\theta \, \mathbf{a_x} \, + az \, sin\theta \, \mathbf{a_y} \, + \, a^2 \, \mathbf{a_z} \right)}{\left(z^2 + a^2 \right)^{3/2}} d\theta \tag{4.4}$$

Integrating 4.4 gives 4.5 for the on axis magnetic field.

$$B \, = \, \frac{\mu_0 a^2 I}{2(z^2 + a^2)^{3/2} \mathbf{a_z}} \tag{4.5}$$

A general solution for the determination of the magnetic field at any point was required. For a current carrying loop as illustrated in figure 4.2 the far magnetic field can be approximated using 4.6.
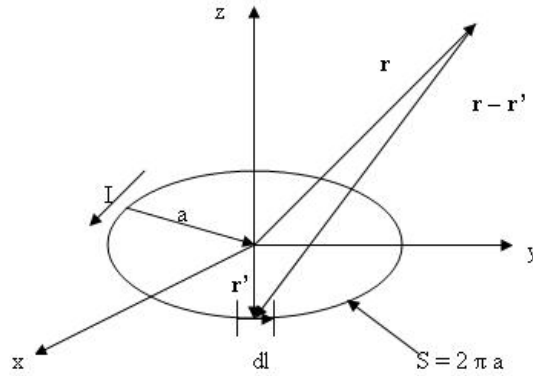
Figure 4.2: The off axis magnetic field for a single loop of wire.

$$B = \frac{\mu_0 SI}{4\pi r^3}(2cos\theta\hat{a}_r + sin\theta\hat{a}_\theta) \qquad r >> a \tag{4.6}$$
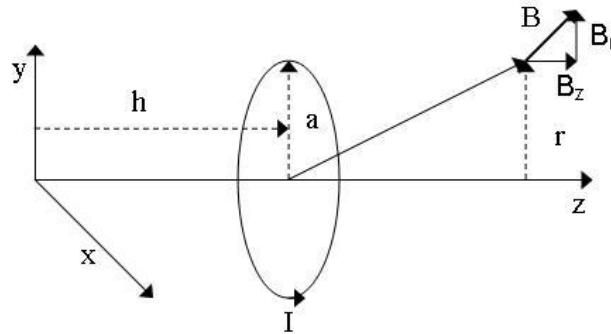
Figure 4.3: Biot Savart Law for off axis magnetic field for a current loop

However, the general solution for the magnetic field was more problematic. Using the Biot Savart law on a loop as shown in figure 4.3 requires the use of elliptical integrals to sum the values around the loop. For a loop that was centred on the z axis and was a distance away from the origin, Kuns (2007) derives from Maxwell's equations the general solution for the magnetic field of a single loop as 4.7

$$B_{(r,z)} = \frac{\mu_0 Ik}{4\pi\sqrt{ar^3}}\left[-(z-h)\left(K - \frac{2-k^2}{2(1-k^2)}E\right)\hat{\mathbf{r}} + r\left(K + \frac{k^2(r+a)-2r}{2r(1-k^2)}E\right)\hat{\mathbf{z}}\right]$$
$$\tag{4.7}$$

Polar coordinates were used where the loop was centred on the z axis, with the loop parallel to the x and y axis, a was the radius of the loop, r was the distance from the z axis from the origin, h was the distance from the origin in the z axis, K was the complete elliptical integral of the first kind with regards to k^2, E was the complete elliptical integral of the second kind with regards to k^2 and k was a constant that was determined by 4.8.

$$k = \sqrt{\frac{4ar}{(r+a)^2 + (z-h)^2}} \tag{4.8}$$

In Kuns (2007) it was demonstrated that due to symmetry the on-axis magnetic field was given at a point where r = 0 and that the equation 4.7 simplified to equation 4.9.

$$B = \frac{\mu_0 I a^2}{2[a^2 + (z-h)^2]^{\frac{3}{2}}} \hat{\mathbf{z}} \tag{4.9}$$

which was the Biot-Savart law for the on-axis magnetic field of a current carrying loop. As there is currently no analytical solution to elliptical integrals, equation 4.7 must be modelled numerically.

4.3   Constructing the model

The magnets being modelled in the damper were cylindrical Neodymium permanent magnets. The solenoid model was used to determine the magnetic field as in figure 4.4. The magnet was modelled as a cylinder of 1,000 current carrying loops evenly spaced along the length of the magnet. The magnetic field from each loop was summed at a point to obtain the total magnetic field. The magnetic field was returned as the components along the z axis and the r axis. Equation 4.7 was used to determine the magnetic field at the point. The major variables that defined the magnet were the length, the radius and the current in the loops. The current was constant for all loops and was proportional to the strength of the magnetic field.

The magnet was modelled in MATLAB as a function that can be called by the programs that required to know the field at a point. The model magnet function had four main inputs. The magnet was modelled as a solenoid made up of a series of loops. The magnetic field was modelled for each loop of the solenoid and then summed over the total number of loops. This was then created as a function that could be called by the MATLAB programs that were trying too map the flux or force.

The inputs   There were three main attributes required as inputs for the model. The model was designed to model a cylindrical magnet so there were the physical size in the form of the length and the radius of the cylinder. The third property was
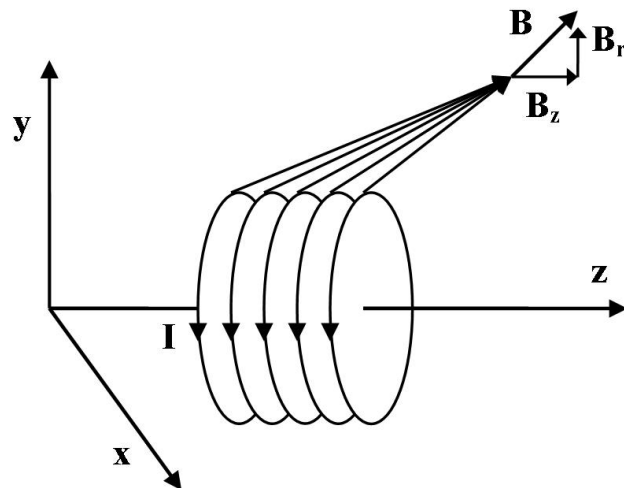
Figure 4.4: Determining the magnetic field generated a solenoid.

the current that was applied to the solenoid. A fourth input was the position that the measurement was taken in relation to the centre of the coil.

The solenoid   The solenoid was made up of a series of loops rather than a helix. The size and spacing of the loops were determined by the inputs. This allowed for simplicity of construction. The difference between the field generated by the helix and the loops reduced as the number of turns in the solenoid increased. The number of turns determined the 'smoothness' of the modelled data and the accuracy with which the model described the magnet. For this research a coil of 1000 loops was used. This provided a good compromise between the accuracy of the model and the computing power that was available.

The single loop   The single loop was modelled as a MATLAB function. The inputs to this function were the radius of the loop, the loop current and the z and radial distance from the loop to the measurement point. When modelling the field produced by the loop there were three solutions which were dependant upon the location of the point being measured. If the measurement point was on axis then equation 4.5 was used. If the point to be measured was on a plane that was within the space encircled by the loop then the magnetic field was returned as zero. This was because there was no field in the radial direction or along the z axis. rather the magnetic field travels in either a clockwise or anticlockwise direction inside the loop itself. In the final case equations 4.7 and 4.8 were used to determine the field. The MATLAB language had a function that numerically solved the elliptical integrals and was used for the modelling.

The completed functions   The solenoid model returned the z and radial components of the magnetic field at a point. The magnet size, the current and measurement point were entered into the MATLAB function. The model of the solenoid was 1000 loops and for each of these loops the distance between the loop and the measurement point were calculated. These were input into the Single Loop function which was described above. The input to the function was the radius of the loop, the current and the measurement point. It returned the z and radial component of the magnetic field. For the applications that were to be used, only the z component was used. But both were returned in case, at a later point, it was decided that the radial component was also required. The magnetic field from each loop was summed and the z and radial components to the magnetic field were returned.

4.4   Verifying the Magnetic Field of the Model

To verify the magnetic field a model was created to map the magnetic field at a specific point from the magnet. This model would also return the magnetic field inside the magnet itself. The magnet chosen to model was a cylindrical Neodymium magnet with a length of 28 mm and a diameter of 19 mm with axially located poles. The magnet had a strength rating of N35. This produces a nominal magnetic field of 0.5733 T at the surface of the magnet. As the magnet was axially magnetised there was rotational symmetry around the axis of the length of the magnet. A two dimensional model was therefore sufficient for use in the damper models.
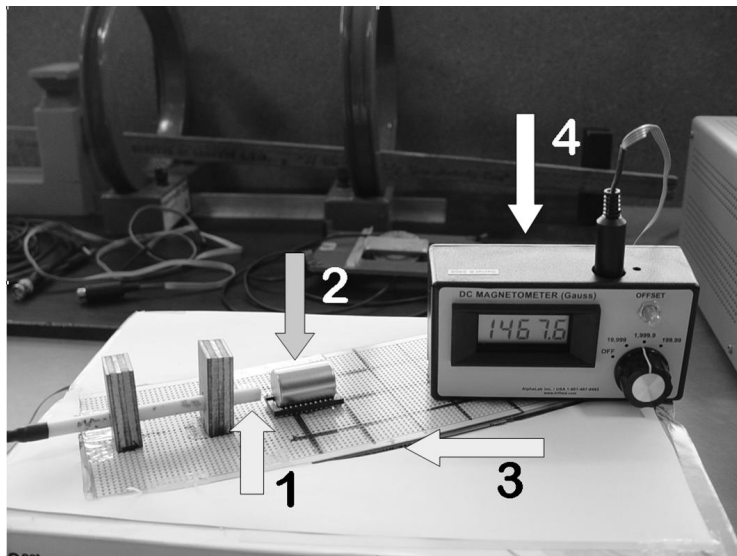
Figure 4.5: The magnet test apparatus. The Key. 1) the magnetic probe, 2) the magnet and holder, 3) the mounting board, 4) the magnetometer

A physical test apparatus was constructed as illustrated in figure 4.5. A perforated construction board with a hole spacing of 2.5 mm was used to achieve a consistent displacement. The magnet was mounted on a carrier that had pins spaced

for the perforated board. An Alphalab Model 1 DC Magnetometer measured the magnetic field in Gauss. The probe was fixed in a non-ferrous holder and the magnet was translated both along the axis and at a radius from the axis. The maximum distance translated along the axis was 62.5 mm in 26 measurements. In the radial axis there were 11 measurements from the axis to a radius of 25 mm.
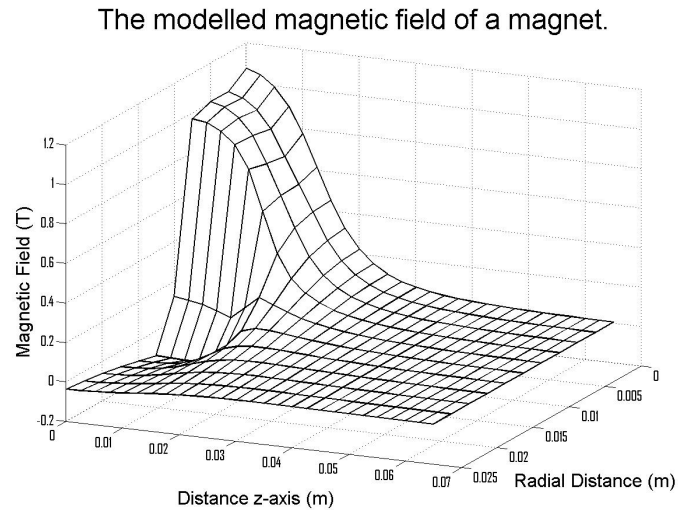
Figure 4.6: The magnetic field of a cylindrical magnet when modelled witha current of 27 A

After the probe was zeroed the magnetic field was recorded at these locations and are shown in figure 4.6. The magnetic field inside the magnet was also modelled but was unable to be verified directly. The modelled magnetic field was then subtracted from the measured magnetic field in figure 4.7 to determine the accuracy of the model. It was observed that the largest variations occurred where the magnetic field was the greatest and where the most rapid changes in the magnetic field occurred.

One major cause in the variation was the size of the magnetic probe used to measure the field. The magnetic detector physically measured in the order of 4.2 mm by 3.5 mm by 1.0 mm thick. The construction of the detector also allowed for a small but indeterminable offset. While the model returned the field at a single point, the detector returns a value from the sensor that has a a value that was some unknown function of magnetic field over the volume of the sensor. This physical size can in the most extreme case produce a severe gradient across the volume. In the end-pole measurements, the model returned a magnetic field of 0.5744 T at the front of the sensor and a field of 0.5415 T 1 mm from the face. This was a difference of 6 % between the front and back faces of a 1 mm thick sensor on the axial line of the magnet. For the sensor on the centre line, the magnetic field at the edge of the face of the sensor was modelled as 0.5132 T, which was a reduction of field strength of 11 % from the centre line measurement.

Of interest was the magnetic field parallel to the z axis. This would be the

location of the coils of the solenoid. For a sensor placed at the centre of length of the magnet and at a radius of 12.5 mm from the z axis. The field at the inner edge of the sensor was -0.1375 T and at the outer edge of the sensor the field was -0.0956 T. This was a drop of 30 % over the length of the sensor. While modelling a larger magnet would reduce this gradient effect, it would still be large in the areas of interest due to the short range nature of strong magnetic fields.

The absolute difference in measured and absolute magnetic fields
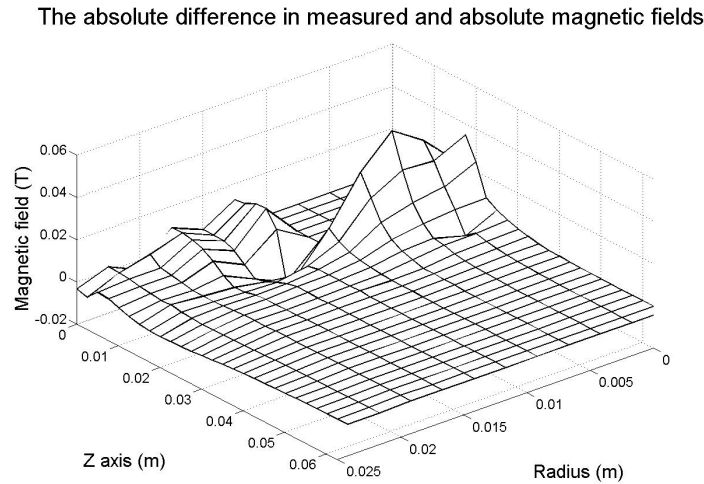
Figure 4.7: The measured difference in magnetic field between the modelled and measured magnetic field.

The absolute percentage difference between the modelled and measured field is given in figure 4.7. In this case it was noted that the greatest variations in the magnetic field occurred when the values of the field were the lowest and also when the field changes from negative to positive values. At these points the field was much lower than typical nearby values. In figure 4.7 the outermost radial values were not included as these small values and where the magnetic field changes direction produce large percentage variations even when the difference between the absolute values of the measured and modelled fields were very small.

Comparing the modelled to measured values.

Modelling the permanent magnet as a solenoid with 1000 turns the average field strength for a grid of 26 by 10 measurements was used to determine the accuracy of the model. As the magnetic field of the magnet was also dependent upon the current being applied to the solenoid model of the magnet, a means of determining the solenoid current was required. The magnetic field at the centre of the poles of the magnet was measured and averaged. The model was then used to determine the current required in the solenoid that represented the magnet that would produce that field. A solenoid current of 27 Amps was determined to be a close approximation of the magnet strength at the end of the magnet.

Figure 4.8: The absolute percentage difference between the measured and modelled magnetic fields

Table 4.1: Agreement between the measured and modelled magnetic fields

	Modelled (T)	Experimental (T)	% Agreement
Average Field Strength	0.02628	0.02794	94
Average Absolute Field Strength	0.04150	0.04238	98

In table 4.1 are given the comparison between the measured and experimental magnetic fields. These were the average magnetic fields of the entire area, less the field inside the magnet. In the case of the values of the fields the agreement was 94 %. As many of the readings have a negative field the absolute values of the field were also compared. In both cases there was an over 90% agreement between the measured and experimental values. This was within the experimental limits imposed by the measuring equipment.

To determine the accuracy of the magnet two methods were explored. In the first method the absolute field strength was summed over all of the points measured. The modelled absolute field strength was calculated and also summed for the same points. This gave an agreement of 93% between the total values of the modelled and measured fields. A major problem with this approach was that for several measurements at the ends of the magnet, there was a large discrepancy between the modelled and measured field strength, in part due to difficulty of measurement due to the physical size of the probe previously mentioned. The second technique used was to use the relative difference between the measured and the modelled values. Taking the absolute percentage differences returned an agreement of 91.4%. This however had regions where the absolute difference between the measured and absolute field were small yet the percentage difference was over 100 %. This particularly occurred where the magnetic field would reverse direction. Removing the most excessive measurements around where the field changes from negative to positive gave a 93.7

% agreement between the measured and experimental values for the magnet. Again these values were within the limitations of the experimental apparatus.

4.5   Conclusions

A numerical model of a cylindrical permanent magnet was constructed using the model of the magnet as a solenoid. This model produced the magnetic field for a single loop of current at any point. This was used in a MATLAB function to determine the magnetic field produced by a solenoid of 1000 turns. This model produced the magnetic field of the far field, the near field and inside the magnet. A map of the magnetic field around the magnet was then measured experimentally and compared to a map of the modelled magnetic field was also produced. The magnetic field generated by the magnet as a solenoid agreed with the experimentally measured values to within 91%. These comparisons between the modelled data and the measured data had several differences that had an unreasonable effect upon the comparisons. Excluding these readings the solenoid model of the magnet produced a close approximation of the observed magnetic field and should be capable of producing look up tables for the magnetic field that an em damper experiences and the flux within an e.m. damper.

Chapter 5

The Passive, Semi-Active and Regenerative E.M. Damper

5.1 Introduction

The hydraulic passive damper is the most common type of damper that is commercially available. The hydraulic damper is also the design which semi-active and regenerative dampers are based upon. However, this research focuses on passive e.m. dampers, which can be divided into linear and rotational types. The passive linear e.m. damper, as proposed in this research, uses the change of magnetic flux in the coil to change the kinetic energy of the motion into electrical energy which is then turned into heat energy by the resistance of the coil. Due to the non-linear magnetic field produced by a single permanent magnet and coil the damper, the field is modelled numerically.

The modelled damper was used to predict the behaviour of the passively damped system to a step input. This was then compared to experimental results. The performance of the damper was then tested in the frequency domain using a series of experimental runs at various frequencies. The results from the theoretical model using the same frequencies were then compared with the experimental results to validate the model.

To determine the suitability of the passive e.m. damper for lightweight electric vehicles, the model was then scaled up to the values for a known electric vehicle.

5.2 Basic principles of the passive e.m damper

The vast majority of vehicles on the public roads use passive hydraulic dampers. These a reliable and well established. A passive e.m. damper offers potential advantages of system simplicity, low wear and possible long term reliability. For a passive e.m. damper the fundamental principle used is magnetic induction. For a solenoid and a permanent magnet, movement of the magnet produces a change in

the magnetic flux within the solenoid. The change of magnetic flux in the solenoid induces a current in the solenoid. This current in turn creates a magnetic field. By Lenz's Law this created magnetic field opposes the original magnetic field. The larger the current is, then the larger the force that is induced. This requires the lowest reasonable resistance in the solenoid to generate the greatest possible forces. The kinetic energy of the sprung mass is turned into heat energy in the solenoid by the electrical resistance of the solenoid.

For a single coil within a magnetic field, the magnetic flux through that coil is given by 5.1

$$\Phi_B = \int \mathbf{B} \cdot d\mathbf{A} \tag{5.1}$$

where Φ_B is the magnetic flux in Webers, $\mathbf{B}$ is the magnetic field in Tesla and $\mathbf{A}$ is the area in square meters. If the loop was perpendicular to a uniform magnetic field then this simplified to 5.2

$$\Phi_B = \mathbf{BA} \tag{5.2}$$

When there was a change in the magnetic field, then an Electromotive Force (EMF) was created in the loop of wire. The size of this EMF is given by Faradays Law in 5.3,

$$\mathcal{E} = -\frac{d\Phi_B}{dt} \tag{5.3}$$

where a change in magnetic flux over a period of time produced an EMF. When the loop was continuous and conducting, then a current would be generated. Due to Lenzs Law this current was generated so as to create a magnetic field that opposed original field. Thus, the EMF produced opposed the flux change.

For multiple loops in the uniform magnetic field the EMF changed to 5.4

$$\mathcal{E} = -N\frac{d\Phi_B}{dt} \tag{5.4}$$

where N is the number of loops in the magnetic field. Using the equation for Power, 5.5

$$P = VI \tag{5.5}$$

where P is power was in Watts, V was voltage in Volts and I was current in Amps and substituting Ohms Law, 5.6

$$I = \frac{V}{R} \tag{5.6}$$

where R was the electrical resistance in Ohms, the power was given by 5.7

$$P = \frac{V^2}{R} \tag{5.7}$$

The resistance of the wire in the solenoid was determined by 5.8

$$R = \frac{\sigma L}{a} \tag{5.8}$$

where ρ was the resistivity of the conductor in ωm, L was the length of the conductor in metres and a was the cross sectional area of the wire in square meters. This resistance was for a given temperature as the resistance would change with a change in temperature. Substituting 5.8 into 5.7 gave 5.9

$$P = \frac{V^2 a}{\sigma L} \tag{5.9}$$

By taking $\mathcal{E}$ as equivalent to V; Faraday's Law, equation 5.3, was substituted in to 5.9 to yield 5.10

$$P = \left(\frac{N d\Phi_B}{dt}\right)^2 \frac{a}{\sigma L} \tag{5.10}$$

where A was the area of the loop and L was the total length of the wire. Because the flux $\Phi = BA$ and A were being held constant, then

$$P = \frac{a N^2 A^2}{\sigma L}\left(\frac{dB}{dt}\right)^2 \tag{5.11}$$

The mass of the conductor in the damper could be determined from 5.12

$$M = \rho L a \tag{5.12}$$

Rearranging for the cross sectional area of the wire a, gave 5.13

$$a = \frac{M}{\rho L} \tag{5.13}$$

and substituting 5.13 into the power equation 5.11 gave 5.14

$$P = \frac{M N^2 A^2}{\sigma \rho L^2}\left(\frac{dB}{dt}\right)^2 \tag{5.14}$$

From basic geometry; $A = \pi r^2$ and $L = N \cdot 2\pi r$ where r was the radius of a loop in the solenoid. Substituting these into 5.14 yielded 5.15

$$P = -\frac{M N^2 (\pi r^2)^2}{\sigma \rho (N 2\pi r)^2}\left(\frac{dB}{dt}\right)^2 \tag{5.15}$$

Which simplified to 5.16

$$P = -\frac{Mr^2}{4\sigma\rho}\left(\frac{dB}{dt}\right)^2 \tag{5.16}$$

From 5.16 it could be determined that the power was not dependant upon the number of windings in the solenoid, rather the mass of the conducting material and the size of the solenoid wire loop in the uniform magnetic field.

The force generated by the damper is related to the power by 5.17

$$P = Fv \tag{5.17}$$

where F was the force in Newtons and v was the velocity in m/s.

From the research of Browne and Hamburb (1986) it was shown that power dissipated by a damper in a production passenger automobile was between 3–57 W, depending upon the surface and speed. Typical values for highway driving were in the range of 10–15 W per damper. Rearranging 5.16 for the mass of copper yielded 5.18

$$M = \frac{4P\sigma\rho}{r^2}\left(\frac{dB}{dt}\right)^{-2} \tag{5.18}$$

With rare earth magnets it is possible to achieve magnetic fields of up to 0.6 Tesla over a large pole area. Using such a field, the maximum change of magnetic field would be twice this amount as the magnet travels from a North Pole to a South Pole of the magnet. At higher frequencies the displacement is usually much less than at lower frequencies, therefore the change in flux is usually much reduced. In a private automobile two frequencies of interest were the resonant frequency of the sprung mass, typically between 1–2 Hz, and the wheel hop frequency which is typically around 10 Hz. Optimising the damper for a sprung mass frequency of 1.5 Hz and with the radius of the damping solenoid as 0.025 m, the amount of copper required would be 0.296 kg per W of damping. For the 10–15 Watts of damping required for general use this would equate to 2.96–4.44 kg of copper per damper. This damper mass did not include the magnet end pieces, the mass of the magnet or the mechanical elements to connect the damper to the automobile. It is probable that the damper would weigh at least twice the weight of the copper. In actual road way applications the higher frequency vibrations have a smaller magnitude of the vibration than low frequency vibrations. In a physical damper these smaller vibrations would cause a much smaller change in flux and therefore power generated, than larger vibrations. To compensate for this decreased power and damping an increase of copper in the solenoid would be required. This could create a potential increase of damper mass of up to five factors or more.

For a non-uniform magnetic field.

The above calculations were for a uniform magnetic field, however a permanent magnet does not generate a uniform magnetic field. The field strength changes, with distance from the poles. Therefore calculations of the magnetic field at popint in space relative to the magnet were needed. Numerical methods described in Chapter 4 were used to model the magnet

5.3 Modelling the suspension system

In the simulation of the passive damper there were two components that were required to be modelled: the magnet and the suspension system. The general suspension system was modelled mathematically as a one degree of freedom system. To this was added any natural Coulombic and viscous damping in the system. Finally the damping provided by the passive damper was added.

The damper was modelled using Faraday's Law. The flux of the entire solenoid was determined at fixed distances from a permanent magnet to create a look-up table. This was then used in the model of the suspension system to provide the damping of the passive element.

Modelling a passive damper

Faraday's Law was used to model the force generated by the solenoid. To determine the force, the flux of the coil needed to be determined. The damper was modelled to be a representation of a real world prototype. In this prototype the permanent magnet was cylindrical as was the solenoid. The solenoid was hollow and large enough to allow the passage of the magnet through it. The permanent magnet was modelled in the manner described in Chapter 4.
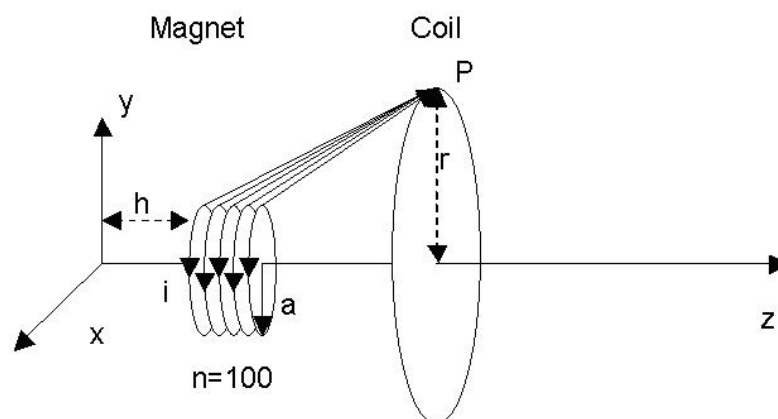
Figure 5.1: A model of the magnet

A representation of the magnet and a single loop of wire in the model represented

in figure 5.1. At point P the magnetic field was the sum of all the magnet fields produced by each loop.

For the damper Faradays Law is used as mentioned earlier in 5.3

$$\mathcal{E} = -\frac{d\Phi_B}{dt} \tag{5.19}$$

with the flux being the area multiplied by the magnetic field.
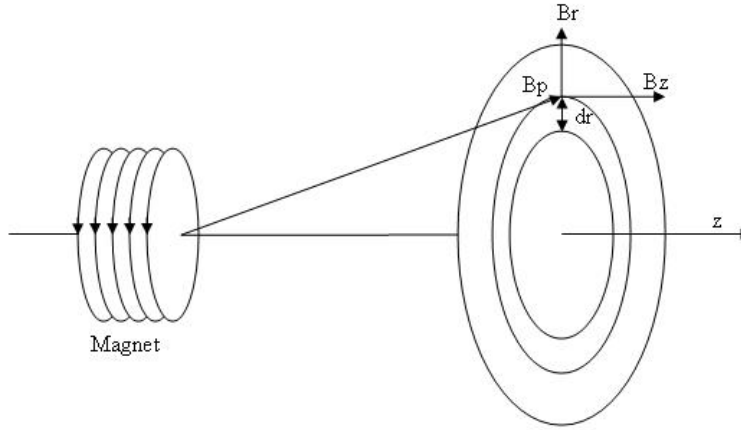
Figure 5.2: The flux of a given area

For a single loop in a coil the flux can be approximated as a series of small concentric rings centred on the z axis, of a known thickness, dr, and area, $dA = \pi r^2\, dr$ and by determining the magnetic field at that point in the ring, as illustrated in figure 5.2. By symmetry the magnetic field at any point on that ring will be constant and the total magnetic field at point P is $\mathbf{B_P} = \mathbf{B_r} + \mathbf{B_z}$. An integration of area for the magnetic field was performed using numerical means. The total flux for a single loop was therefore given by 5.20

$$\Phi_B = \sum \mathbf{B_p}\, dA \tag{5.20}$$

Usually a solenoid is made up of more than one loop, each being a different size and/or being at a different position on the z axis, so for each loop the flux must be determined individually. The total flux of the coil being given by 5.21

$$\Phi_{Total} = \sum \Phi_B \tag{5.21}$$

As Faradays Law is dependant upon both time and the flux, movement of the coil and the magnet relative to each other must be taken into account where the E.M.F. is the change in flux caused by the relative motion divided by the time over which the motion occurred.

For the actual implementation of the model on a computer for a specific mag-

Table 5.1: Properties of the magnet and coil

	Magnet	Coil
Length (mm)	28.0	63.4
Radius (mm)	9.5	19.1

net(s) and coils(s) a look up table was constructed. On initialisation of the program the magnetic fluxes of the whole coil were calculated at various distances relative to the magnet, up to the maximum possible amplitude of motion. The symmetry of the system was used to reduce the calculation time. Two approaches were examined for use of the lookup table. The first involved a temporal look up where the time was taken as the changing variable. Due to the force generated by the solenoid it was determined the time interval required to travel from one loop to another i.e. for the magnet to travel from 103 mm to 104 mm takes 13.2 ms; from 104 mm to 105 mm the time is 15.4 ms. This allows the precise values the flux to be used, however at low velocities the time intervals became large. Also the implementation of this scheme in VSISSIM was not directly supported. Therefore interpolation was used to determine the values of inter-loop values of the coil.

A lookup table of the flux of the damper was constructed using MATLAB. The properties of the magnet and coil are given in table 5.1. The coil was composed of 120 windings in 3 layers of 40 windings each. The radius of the coil was the average diameter of the three layers. The wire was 1.4 mm diameter copper enamelled winding wire. The total resistance of the coil was 0.22Ω.

Using the MATLAB model of the flux, the flux of the 120 turn solenoid and the 28mm magnet are shown in figure 5.3.
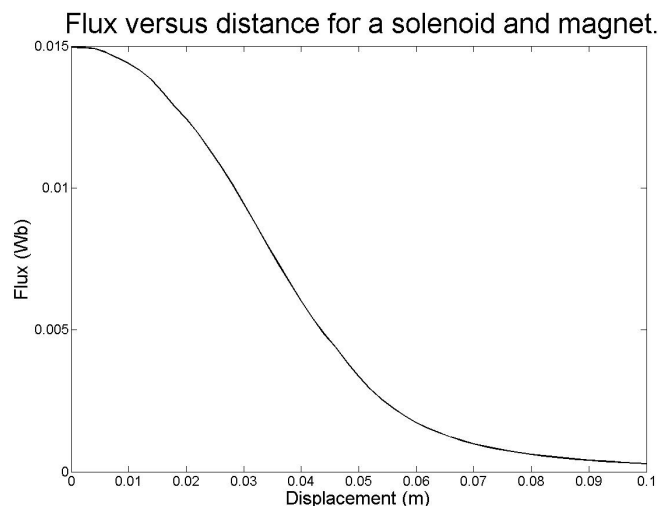
Figure 5.3: The flux of a solenoid vs the displacement of the coil from the centre of the magnet.

The maximum flux occurred when the magnet was in the centre of the coil. To

verify the modelled flux the magnet was translated through the coil and the voltage versus the time was recorded. As the magnet passes through the solenoid a voltage is produced due to the varying flux. The results of the experimental data run are illustrated in figure 5.4
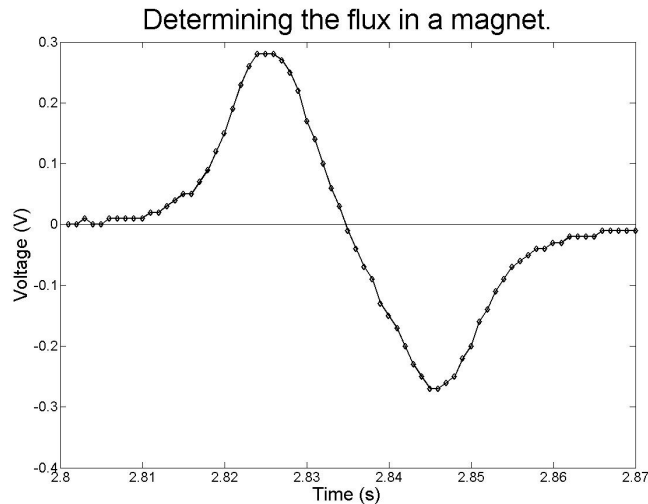
Figure 5.4: The voltage produced by the magnet in the solenoid as it translated through the solenoid.

The flux of the magnet in the centre of the coil was obtained by summing the E.M.F. and multiplying by the time increment. The coil was in a circuit with a wire acting a load resistor. In the circuit there were two separate resistances; the resistance of the coil and the resistance of the wire. Combined, these acted as a voltage divider. To compensate, the raw voltage figure was multiplied by a correction factor of the ratio of the coil voltage to the wire voltage. In this case $0.220\Omega : 0.051\Omega$. Summing the positive portion of the graph and the negative portion and then taking the average of the absolute values yielded a flux of 0.0154 Wb. The Modelled value was 0.01485 Wb, which was 96.6% of the measured value. This was then used to determine a correction factor for use in the passive damper.

5.4   Optimising the damping

In the solenoid-damper system, the region where the greatest damping occurred was in the region where the magnetic flux was changing most rapidly. By differentiating the slope of the line given in figure 5.3, the rate of change was determined. This is displayed in figure 5.5. The change in the magnetic flux was not a simple curve and was the result of the interactions of the flux changing between North Pole, South Pole and the coil.

The maximum change in flux occurred when the centre of the magnet was a distance of 0.033 m ±0.001 m from the centre of the coil. This distance corresponds
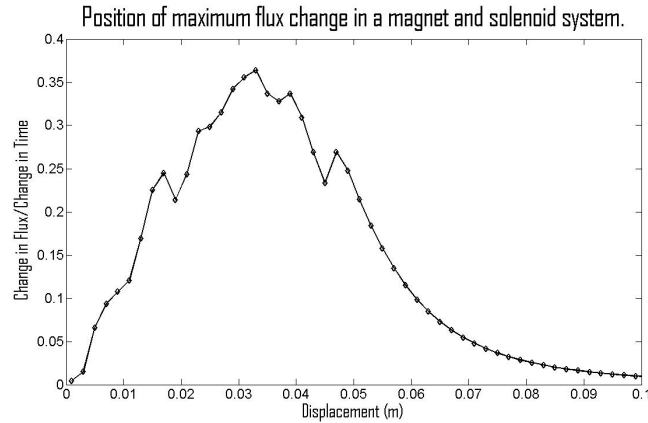
Figure 5.5: The change in flux vs. the distance of the magnet from the solenoid. The magnet length = 0.033 m.

with the distance at which the centre of the magnet exited the coil. It was also noted that the greatest damping occurred between displacements of 0.015 m and 0.050 m. The jagged zigzags that occur on the graph correspond with the distance when the first portion of the magnet leaves the coil and when the final portion of the magnet leaves the coil. For the greatest passive damping in experimental runs the default position of the magnet was with the centre of the magnet at the edge of the coil.

5.5 Testing in the time domain

To determine the behaviour of the passive damper a rig was built to obtain experimental data. A model of the damper was also constructed in MATLAB. The experimental results were then compared with the modelled results.

The experimental apparatus that was constructed to test the validity of the model is shown in figure 5.6. Special care was taken in the construction of the equipment so that no ferromagnetic materials were used. The magnet was mounted on the end of a spring and allowed to travel freely in the vertical direction. The spring was able to be moved in all three dimensions to ensure that there was minimal interference caused by contact of the magnet with the solenoid and to ensure that the magnet started from the optimal position for passive damping.

Test runs were conducted with various weights attached to the magnet as sprung masses. Before these runs were performed the natural damping of the system had to be determined without the passive damper being operational. As the passive electromagnetic damper consisted of a shorted solenoid, the deactivation of the damper was achieved by breaking the circuit. This natural damping was caused by, amongst other things, the hysteresis in the spring and air resistance. The natural damping of the system had components of both Coulombic damping and viscous damping.

To determine the extent of the natural damping a data run was conducted for
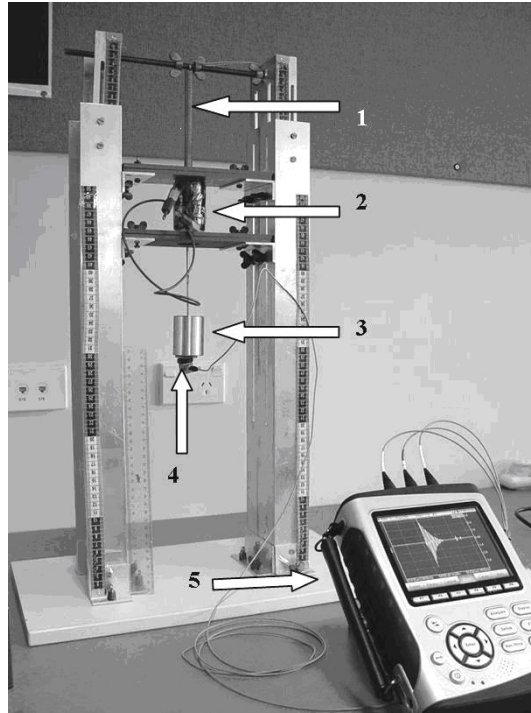
Figure 5.6: The experimental apparatus for a passive damper. 1) Is the spring, 2) the solenoid with the magnet inside it, 3) the sprung mass, 4) the accelerometer and 5) the COCO80 signal analyser. The damper assembly consists of elements 1,2, and 3. The measurement apparatus consists of elements 4 and 5.

each sprung mass that was to be used for data collection. The time domain vibration was then modelled in MATLAB SIMULINK. The sprung mass was raised a height of $1.5 - 2$ cm and then released as a step input. To prevent Nyquist Aliasing, the input sample fequency was set at 1,000 Hz or greater, this frequency being at least two manitudes of order larger than the undamped natural frequency.

Figure 5.7 represents a typical natural vibration run. In this run a 700 g weight was used for the sprung mass. When the mass of the accelerometer, magnet and the weight carrier was added, the sprung weight was 797 g and the step input was 0.020 m. Included in this figure are both the modelled and the experimental results, the two data sets having been superimposed upon each other. It was discovered that there was a difference of 6% in the amplitude of the experimental measurements and the modelled data. The modelled data was then increased by 6%. Without the calibration the natural damping curves would remain be the same, however the calibration was performed for easier analysis of the data.

A series of modelled runs were performed in which the natural damping coefficient and Coulombic damping were trialled until a good match was achieved between the modelled and the actual data sets. This was determined by visual inspection of the superimposed data sets. The natural damping of the masses used in the passive damping experiments were determined to be as in table 5.2.
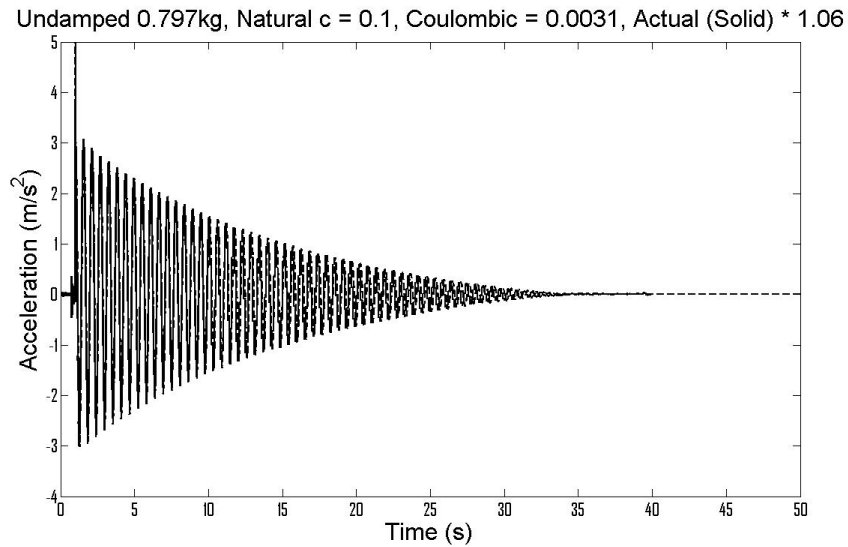
(a) From 0–50 s
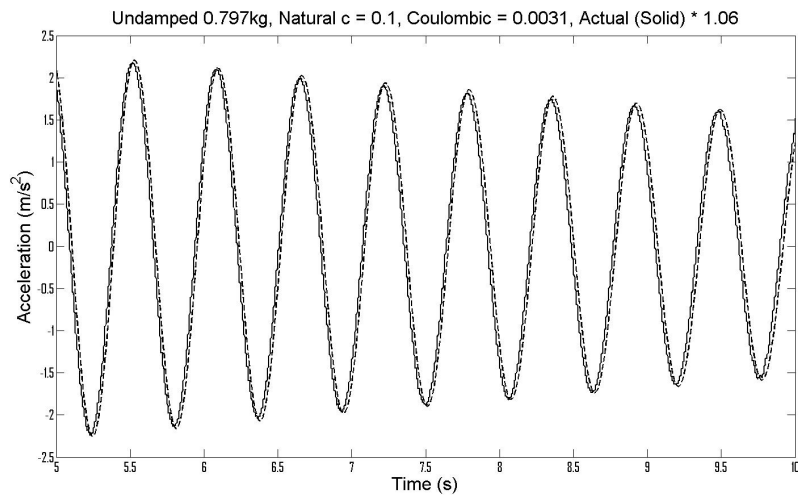
(b) Detail of 5–10 s

Figure 5.7: The natural damping for a sprung 797g mass. The Solid line is the actual measurement at 1,000 Hz and the dashed line is the modelled value.

These damping figures were then used in the MATLAB model of the passive e.m. damper.

The model of the passive damper

The passive e.m. damper suspension model was made in three parts. There was the equations of motion of the damper which are well known used to model the undamped motion of the sprung mass. There was also he natural damping of the system which is caused by friction and hysteresis effects, among other factors. This had components of both viscous and Coulombic damping. The third factor that was added to this model was the damping produced by the passive e.m. element.

Table 5.2: The Coulombic and Viscous damping of various naturally damped masses.

Mass (kg)	Coulombic (N)	Viscous (Ns/m)
0.397	0.005	0.210
0.497	0.0019	0.125
0.597	0.0041	0.120
0.697	0.0031	0.110
0.797	0.0031	0.100
0.897	0.0042	0.085
0.997	0.0022	0.090
1.097	0.0023	0.100

Equations of motion.   The basic equation for a single of degree damped system for a step input is given in 5.22.

$$k(z_1 - z_0) + c(\dot{z}_1 - \dot{z}_0) + m\ddot{z} = 0 \qquad (5.22)$$

where k is the spring constant, z_1 is the displacement of the sprung mass, z_0 is the displacement of the unsprung mass, $\dot{z}$ is the velocity of the unsprung mass, c is the damping coefficient of the system, m is the sprung mass and $\ddot{z}$ is the acceleration of the sprung mass. The velocity of the system was determined by integrating the acceleration. The displacement ot the sprung mass was determined by the integration of the velocity.

The natural damping.   For the equation of motion, the term c could be used as the natural damping coefficient of the viscous damping and given the term c_{nat}. An addition term was required to account for the Coulombic damping. This could be included in 5.22 as the term F_c. This yielded 5.23.

$$k(z_1 - z_0) + c_{nat}(\dot{z}_1 - \dot{z}_0) + m\ddot{z} + F_c = 0 \qquad (5.23)$$

The values of c_{nat} and F for each mass were determined experimentally and are given in table 5.2 where the term for the Viscous damping was c_{nat} .

The e.m. damper.   For the equation of motion, a term needed to be introduced for the damping produced by the e.m. element. This was the passive damper and supplied a force F_{damper}. This was added to 5.23 to give 5.24

$$k(z_1 - z_0) + c_{nat}(\dot{z}_1 - \dot{z}_0) + m\ddot{z} + F_c + F_{damper} = 0 \qquad (5.24)$$

To determine the damping provided by the passive electro-magnetic element, the relative position of the sprung and unsprung masses were added to the damper offset. This offset allowed for the magnet to be placed at positions other than the centre of the coil. The final displacement was then used to reference the magnetic

flux look up table to obtain the flux in the coil. For this purpose linear interpolation was used. The flux was then differentiated to obtain the voltage generated. This was divided by the resistance of the damper solenoid to obtain the power generated by the e.m. damping solenoid. The power generated was divided by the relative velocity of the masses to determine the force provided by the damper.

5.5.1 Results

A series of experimental test runs were conducted using the base weight of 97 g and added weights in the range of 300-1,000 g. The mass was released with a step height of between 2-1.5 cm. The variation in height was prescribed by limitations in the test equipment when larger masses were used. In figure 5.8a is the modelled and experimental performance of the electromagnetic damper acting on a total sprung mass of 497 g in the time domain. This was obtained using the test apparatus previously described. The mass experienced a vertical downward step of 0.02 m. In figure 5.8b the step size was 0.015 m. In all cases the magnet was modelled as a solenoid with a current of 30.4 Amps.

These two cases represented the extremes of mass that returned reasonable values. As observed from figures 5.8a and 5.8b, there was a close agreement between the predicted displacement of the modelled and experimental displacements.

The damping coefficient of the damper could be measured from the recorded data using 5.25

$$c = 2\xi\omega_0 m \tag{5.25}$$

where ξ is the damping ratio, ω_0 is the natural frequency and m is the mass. To determine ξ equation 5.26 was used.

$$\xi = \frac{d}{\sqrt{4\pi^2 + d^2}} \tag{5.26}$$

In 5.26 and 5.27 the quantity d was determined by taking the displacement of two peaks of the signal and recording the number of complete oscillations between the peaks. This was then calculated using 5.27

$$d = ln\frac{d_1 + d_2}{n} \tag{5.27}$$

where d_1 was the amplitude of the first peak chosen, d_2 was the amplitude of the second peak and n was the number of oscillations. The natural frequency was given by 5.28.

$$\omega_0 = \sqrt{km} \tag{5.28}$$

where k was the spring constant and m was the sprung mass.
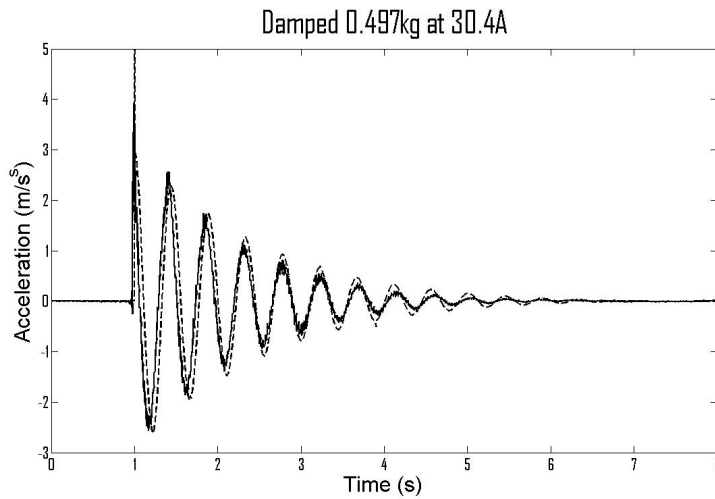
(a) The modelled and experimental damping of a 497g mass. Step size = 0.02m. Magnet current = 30.4A. Natural damping = 0.1 Ns/m. Coulombic Damping = 0.0024N "—-" = experimental. "- - - -" = modelled.
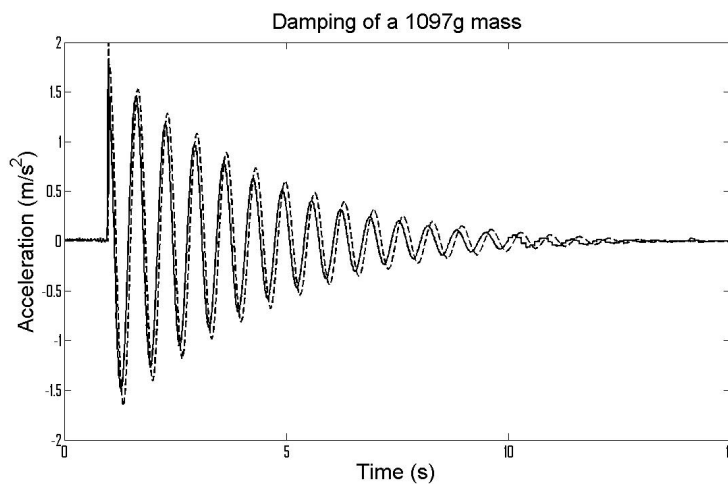
(b) The modelled and experimental damping of a 1,097g mass. Step size = 0.015m. Magnet current = 30.4A. Natural damping = 0.125 NS/m. Coulombic damping = 0.0019N."—-" = experimental. "- - - -" = modelled.

Figure 5.8: Modelled and experimental natural damping of the e.m. damper.

Table 5.3: Total damping coefficient of a passive e.m. suspension system - Modelled and experimental

Mass (g)	Total Modelled (N s/m)	Total Actual (N s/m)	Total Percentage
1097	0.6786	0.7416	91.5
997	0.6123	0.5733	93.6
897	0.6823	0.7733	88.2
797	0.6672	0.8047	82.9
697	0.6993	0.8872	78.8
597	0.7523	0.9976	75.4
497	0.7313	0.9413	77.7
397	0.9433	0.8697	108.5

The measured and modelled damping coefficients of the total damper system for various sprung masses are given in table 5.3. The total damping was the damping provided by both the natural damping of the undamped system and the damping provided by the passive e.m. damper. The percentage was the percentage of the modelled data compared to the experimental data. In all cases, except 397 g, the model under reported the value of the system. The value of 497 g was considered the limit of the model to return valid data.

Table 5.4: The damping damping coefficient of the passive e.m. damper only - Modelled and experimental

Mass (g)	Damper Modelled (N s/m)	Damper Actual (N s/m)	Damper Percentage
1097	0.5786	0.6416	90.2
997	0.5223	0.4833	92.5
897	0.5973	0.6884	86.8
797	0.5672	0.7047	80.0
697	0.5993	0.7872	76.1
597	0.6327	0.8776	72.1
497	0.6083	0.8183	74.3
397	0.7333	0.6597	111.2

The damping coefficients of only the e.m. damper component, for various sprung masses, are given in table 5.4. In the case of the damping of the total system and the case of the damping provided only by the passive e.m. damper, the accuracy of the model increased as the mass increased. This indicated a systematic uncertainty in the model. The two probable causes of this uncertainty were that the Coulombic damping was not fully accounted for and that the model of the damping was under reporting the value of the magnetic field and hence under reporting the flux used in the damper calculations. As the mass of the damper increased the damping of the system decreased and approached the value of the modelled system. Other sources of discrepancy resulted from the coil being wound onto a PVC core, which was paramagnetic. This was not included in the modelling of the damper. A further

assumption was the axisymetric nature of the field within the magnet; this was observed to be not fully accurate. The resistance of the coil is important in the final force generated. The resistance of the coil was accounted for, but the reactance of the coil for an alternating current caused by the magnet was not modelled. An analysis of the reactance of the coil produced a difference of less than 0.1% for the impedance of the coil. From testing, the system showed sensitivity to the initial conditions and the measurement with the total mass of 1000 g showed some of this sensitivity in the result. Resolution issues due the scale of this experiment were apparent during testing. Any disparity between the model and measured results would cascade as the dynamic model was modelled using the solutions produced by the static model. Excluding the 397 g mass, the model of the total damper system demonstrated an 84% agreement between the modelled data and the experimental data. For the model of the damper alone there was a 82% agreement between the modelled data and the experimental data. Except for the case of the 397 g mass the model underestimated the damping. As the mass increased the accuracy of the model also increased.

These runs demonstrated that damping occurred, but the magnitude of the damping was very low compared to the size and mass of the damper. The step input confirmed that the model was a simulation of the real life damping, but in real life it is rare to have a single step input. Instead there is a continuous road signal input. To determine the effectiveness of the passive e.m. damper, this continuous input was required to be modelled.

5.6   Testing in the frequency domain

To determine the effectiveness of the passive e.m. damper and to verify the accuracy of the modelled passive damper with a psuedo-sinusoidal input, the passive damper was tested at a variety of frequencies from below the resonant frequency of the system to approximately 9 Hz. The upper frequency limit was determined by experimental apparatus. A series of experimental runs were conducted over the frequency range and compared to the theoretical model. The magnet used was the same 29 mm long neodymium magnet that was previously modelled. The coil was the single coil as described previously. The frequency of the VISSIM model was set at 1,000 Hz.

A comparison was conducted between the measured non-damped motion of the system and the modelled non-damped motion of the system. The results are given in figure 5.9a. The values displayed are the absolute r.m.s. velocity of the damper at the various frequencies for experimental runs of over 30 seconds. At the near resonant frequency of 1.58 Hz the modelled displacement and velocity increased by several factors. The physical model does not allow this much movement and therefore is much more limited in both displacement and velocity. At frequencies over 4–5 Hz the accelerometer drift of the measuring accelerometer when integrated
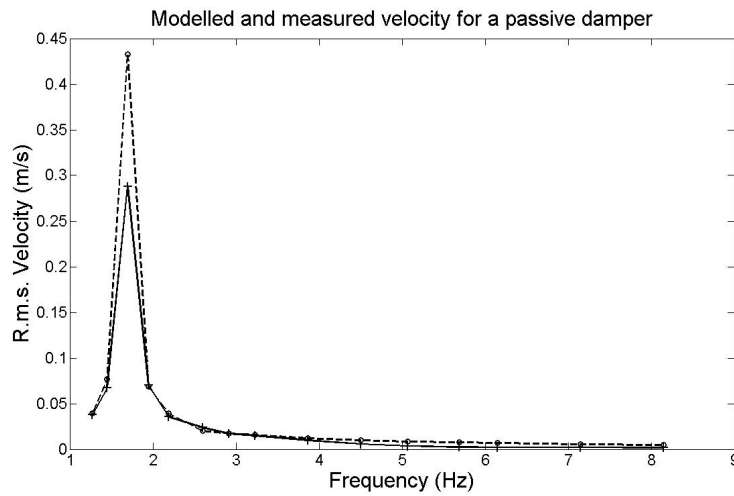
(a) Comparison of the modelled and actual passively damped motion in the frequency domain. "——" actual measurements and "- - - -" are the modelled values.
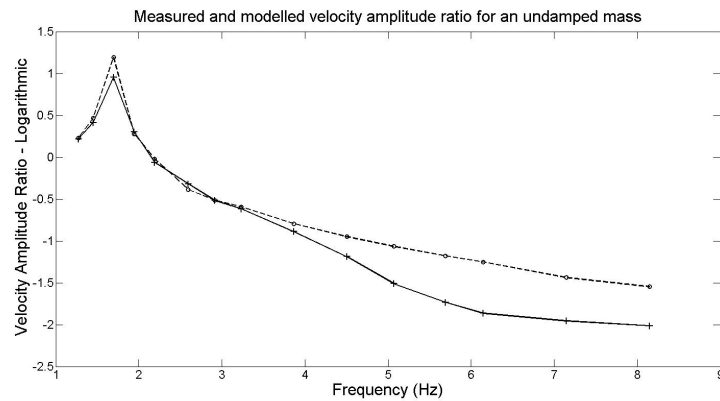
(b) A comparison of the modelled and actual damped velocity amplitude ratio of the undamped mass in the frequency domain. "——" actual measurements and "- - - -" are the modelled values.
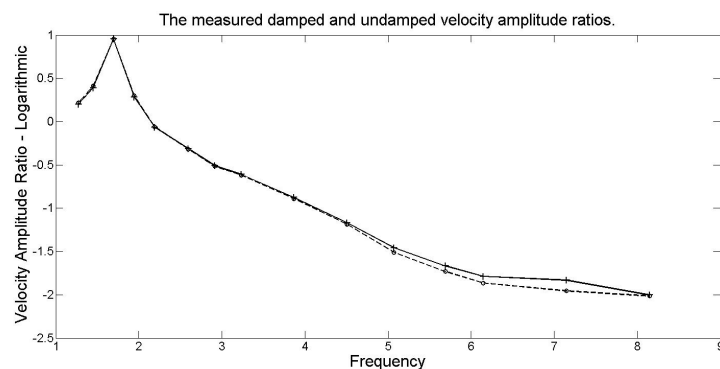
(c) A comparison of the measured damped and undamped velocity amplitude ratios. "——" damped and "- - - -" are the undamped values.

Figure 5.9: Modelled and experimental damping of the e.m. damper for a psuedo-sine wave at various frequencies

can become larger than the actual velocity measurements. In the range of 1–4 Hz there is a better than 93 % agreement between the measured and modelled values. However for frequencies above 4 Hz the agreement drops rapidly to 38%. This rapid drop is caused by accelerometer drift and secondary motions of the mass. These effects were noted for both the damped and undamped motion. In the case of higher frequencies the relative performance of the damped and undamped systems are compared, rather than the absolute values.

The velocity amplitude ratio is a standard measurement of damper performance and is determined by dividing the velocity of the sprung mass by the vertical velocity of the input motion. The results are given in figure 5.9b. Due to the large range of values a logarithmic scale allowed for better interpretation of the results.

To determine the performance of the damped system compared to the undamped system, a series of 30 second runs were conducted. These experimental data runs used a series of varying masses and measurements were taken when the sprung mass was damped and another when it was undamped. The results are displayed in figure 5.9c. The damper used did not exhibit a large authority over the sprung mass and consequently the damping effect was very small. The average reduction in r.m.s. velocity below 2.5 Hz was less than 3 %. The damping observed had very little effect on the sprung mass. It was noted, though it was hard to observe directly from this figure, that the damper reduced the velocity of the sprung mass at frequencies below 2.5 Hz. At frequencies above 2.5 Hz the damped mass experienced higher velocities than the undamped mass.

While the passive damper was sufficient to produce observable damping effects, the size of this damping was very small. To determine if this is of any practical a larger scale model is required to be constructed.

5.7   Scaling up the passive e.m. damper

To determine the feasibility of the passive electromagnetic damper as a component for full size automobiles a two degree of freedom model of a car suspension system was created. A model of the magnetic fields of the two larger magnets was then constructed using the techniques in Chapter 4. This was then used to model the fluxes in the coils and to make a look up table of the force generated by the magnet and coil at various displacements, as described earlier in this chapter.

For a quarter car, the masses could be modelled as a two degree of freedom as in figure 5.10, where m_1 was the unsprung mass/tyre, m_2 was the sprung mass/car body, z_0 was the displacement of the road surface, z_1 was the displacement of the unsprung mass, z_2 was the displacement to the sprung mass, k_1 was the tyre stiffness, k_2 was the shock absorber spring stiffness, c was the damping coefficient of the tyre and F_D was the damper force. For a two degree of freedom system the equations of the displacement of the unsprung and sprung masses were given by 5.29 and 5.30
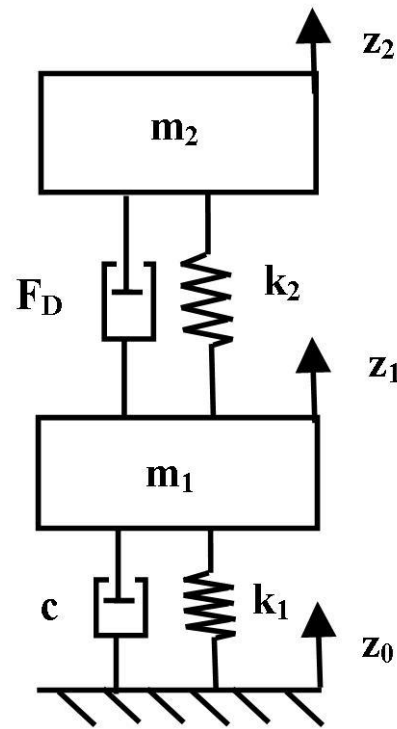
Figure 5.10: A two degree of freedom suspension system.

$$m_1\ddot{z}_1 + k_1(z_1 - z_0) - c(\dot{z}_1 - \dot{z}_0) + k_2(Z_2 - z_1) + F_d = 0 \tag{5.29}$$

$$m_2\ddot{z}_2 + k_2(z_2 - z_1) - F_d = 0 \tag{5.30}$$

As the damping from tyres are usually considered negligible the equations simplified to 5.31 and 5.30.

$$m_1\ddot{z}_1 + k_1(z_1 - z_0) + k_2(z_2 - z_1) + F_d = 0 \tag{5.31}$$

$$m_2\ddot{z}_2 + k_2(z_2 - z_1) - F_d = 0$$

This was modelled in VISSIM for a light weight electric vehicle similar to the University of Waikato BEV or Ultracommuter electric vehicles. For such a vehicle typical values would be as in table 5.5. The natural frequency of the sprung mass is set at 1.25 Hz.

Table 5.5: Values for a two degree of freedom quarter car system for the University of Waikato Ultracommuter automobile.

Properties	Value
Sprung Mass	200 kg
Unsprung mass	25 kg
Spring Stiffness	12,500 N/m
Tyre Stiffness	100,000 N/m

The values in table 5.5 were used in the VISSIM model to determine the dominant frequencies. These were determined by use of a fast Fourier transform and the results are illustrated in figure 5.11. The resonant frequency of the sprung mass is 1.322 Hz and the frequency of the tyre 'hop' is 10.41 Hz. These were both realistic values so these were used as the base values for the rest of the modelling.
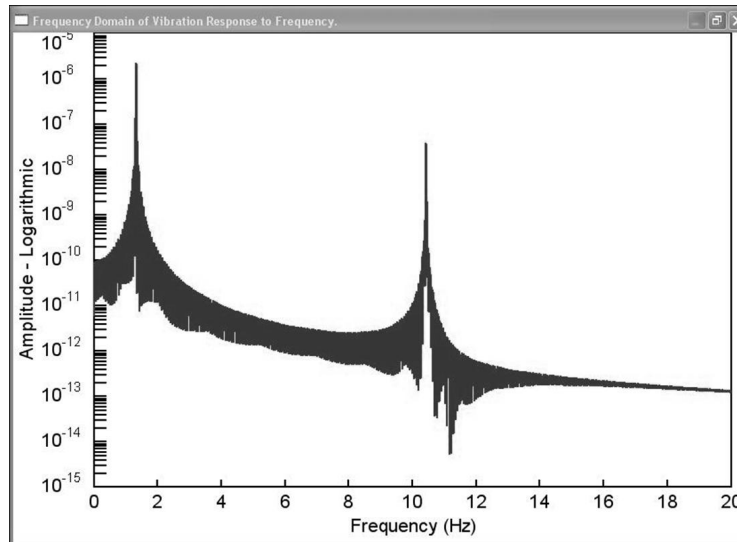
Figure 5.11: Fast Fourier Transform of the undamped two degree of freedom model.

A pair of larger magnets were modelled for suitability for use in a more powerful damper. Both were cylindrical and axially magnetised. The first of these was model number N3522, which was a Neodymium magnet with a diameter of 35 mm and a length of 22 mm. This is a medium sized commercially available magnet with good strength and which would allow a high packing density of magnets into the smallest column. The other magnet chosen was model N5550, which was 55 mm long and 50 mm in diameter. This was chosen as it was the largest Neodymium magnet that was readily available in New Zealand. Each of these magnets were matched with an appropriate coil. In each case the coil length was set as the same as the magnet length and each of the coils consisted of a single layer of wire. The properties of the magnets and their responding coils are given in table 5.6.

For the damper to be effective, a damping ratio of 0.5 should be the minimum achievable figure. For the Ultracommuter vehicle, this gave a damping coefficient of 1,600 Ns/m. For a single coil and magnet the maximum damping coefficient achieved for the ND3522 magnet was 4.60 Ns/m and for the ND5550 the maximum achieved was 20.9 Ns/m. The weight of the magnet-coil system was 0.0934 kg for the ND3522 and 0.5106 kg for the ND5550. With the masses and spring stiffnesses involved a single magnet and coil of the types in table 5.6 achieved only a small percentage of the required damping coefficient.

There are several means that could be used to increase the performance of the damper. The first explored was by increasing the number of layers of windings on

Table 5.6: Values for two magnets and two coils.

Property - Magnet	ND3522	ND5550
Diameter (mm)	35	55
Length (mm)	22	50
Mass (kg)	0.0740	0.4153
Field Strength at Pole (T)	0.5791	0.5783
Property - Coil		
Length (mm)	22	60
Radius (mm)	20	30
Turns	22	50
Wire diameter (mm)	1.0	1.2
Mass Coil (kg)	0.0194	0.0953
Resistance Coil (Ω)	0.0563	0.14

the coil. For each additional layer the area of flux changed as the radius of the layer also changed and therefore the damping force by that layer would also change. So for most accurate results the flux for each layer should be added separately and then combined in the final model. For the sake of simplicity of the model and to aid in rapid modelling the flux from the look up table was multiplied by the number of layers. In the modelling it was assumed that the layers being modelled were added equally to the inside of the coil and the outside of the coil, reducing the size of any differences. Further, the number of layers was limited to stop these differences becoming larger that 10%. It should be noted that the larger the numbers above 5 layers, the larger any discrepancy would become. By increasing the number of layers to 5, this also increased the damping effect by a constant multiplier and the achieved damping for the ND3522 was increased to 23.5 Ns//m and for the larger ND5550, 106.3 Ns/m and the masses were 0.171kg and 0.892 kg respectively. These damping coefficients remained insufficient to give the suspension system the required damping ratio of 0.6

A further way of increasing the damping force is by using a second coil with an opposing direction as illustrated in figure 5.12a. This second coil is wound in the opposite direction to the first coil and has a reversed polarity. This provides approximately twice the damping of the single magnet coil system, but without the requirement of adding a second magnet, only a second coil. So this increased the damping ratio to mass constant. For a single magnet and two matched coils, each of five layers, the damping increased to 47.6 Ns/m and 211.8 Ns/m. Due to the non-linear nature of the magnetic fields, the increase in the damping force and damping constant are also not of a linear nature. The mass of the damping systems are 0.268kg for the ND3522 and 1.368 kg for the ND5550 magnets. For the smaller magnet this is an increase of the damping coefficient of 103 % for an increase of weight of 57 %. For the larger magnet the increase in damping coefficient was 99% with a corresponding increase of weight of 53%.
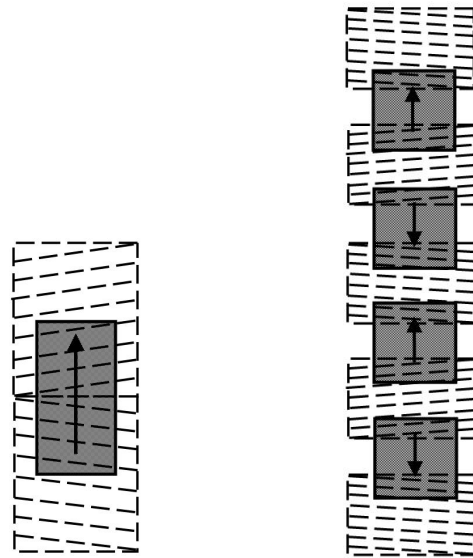
(a) A magnet and two coil damper system.

(b) A multi-magnet and multi-coil damper

Figure 5.12: Two dampers with multiple magnets and coils

It was possible to obtain greater damping coefficients through the use of a stack of magnets and coils of opposing magnetic fields and polarities as illustrated in figure 5.12b. The magnetic/coil stack acted as a two phase linear electromagnetic generator. The increase in magnets and coils increased the magnetic force generated compared to the mass of the system. Modelling was done to determine combinations of magnets and coils that would produce a damping coefficient of 1,600 Ns/m. An arrangement was determined for each magnet and is given in table 5.7.

Table 5.7: Passive e.m. damper properties to achieve a damping coefficient of 1,600 Ns/m.

Magnet	ND3522	ND5550
Number of magnets	17	8
Number of coils	18	9
Number of layers	10	5
Damping coefficient (Ns/m)	1,581	1,638
Mass (kg)	4.75	7.61
Length (m)	0.583	0.433

For installation of the damper into an automobile the most important considerations are the mass of the damper and the physical size of the unit. The later issue can be addressed by having two half length stacks in parallel. The damper mass given in table 5.7 is the mass of the magnets and the coils only. The mass does not include the connectors between the tyre and the magnet, not the magnet and the car. Nor does it include structural element so that the weight of the vehicle did not

crush the coils and damper. These elements would add to the final weight of the damper element. A complete commercial hydraulic damper, without a spring, for a typical vehicle with a similar weight to the University of Waikato Ultracommuter vehicle, was weighed at 3.8kg. Both of the e.m. dampers exceeded this weight before the mass of any connectors or other structure was included.

Discussion.

The e.m. damper described could be used either in a pure passive mode or by the addition of a low resistance, high power switch and a controller it could also be used as a semi-active damper. By a change of position of the magnets in relation to the coils, the passive damper could also be used as a dead band damper. With appropriate power handling circuits the passive e.m. damper could also be used in a regenerative mode.

Passive e.m. damper. As a purely passive damper the e.m. damper offers little, if any, advantage over a commercially available hydraulic damper. The weight of the e.m. damper would be in excess of three kilograms higher than already available dampers. The extra mass of the passive e.m. damper compared to hydraulic damper would also result in reduced fuel efficiency and additional running costs to the owner. While there may be benefits of reliability and simplicity of construction, these would be theoretical until further research is conducted. The design of the coils and their position relative to the magnets may improve the performance of the damper. Any increase would be expected to be small, but would be outside the scope of this work and would be the subject of further research.

Additional applications of a passive e.m. damper. The e.m. damper described could be used either in a purely passive mode or by the addition of a low resistance, high power switch and a controller the passive e.m. damper can be used as a semi-active damper. By a change of geometry of the magnets in relation to the coils, the passive damper could also be used as a dead band damper. With appropriate power handling circuits the passive e.m. damper could also be used in a regenerative mode to provide both damping for the vehicle and electrical power generation to increase fuel efficiency.

Dead-band damping. By a change in the position of the magnets relative to the coils and by changing the coil geometry dead band damping could be implemented easily using the passive e.m. damper. As the implementation of the dead-band damping is achieved purely through passive means the system complexity would be reduced compared to test rigs that have already been constructed. Whether the benefits of dead-band damping would exceed the weight penalties is again outside the scope of this work.

Semi-active damper. In the semi-active mode the passive e.m. damper may be competitive with commercially available magnetorheological dampers. Both dampers have additional requirements in the weight of the controllers. However magnetorheological dampers also require a power source to supply power to drive a set of coils. This extra mass on the magnetorheological damper may make the passive e.m. damper competitive when used in semi-active mode. In this case there is also further simplicity of the circuit design as a magnetorheological damper uses an electromagnet and a hydraulic damper as compared to the passive e.m. damper that only uses only an electromagnet and dispenses with the hydraulic component entirely. This is an area for further research.

Regenerative damping. By the addition of a power regulation system and a device to step up the voltage of the generated electricity, it would be possible to produce electricity for use in the vehicle. It has been explained earlier that power generated by an ideal damper would be in the range of 10–15 watts for a standard road surface. The power produced by a lightweight vehicle would likely be less than a heavier vehicle. It is unlikely that this generated power would exceed the extra engine power that would be required to propel the extra mass of the vehicle required for regenerative damping. This means that the passive e.m. damper is unviable for use in lightweight electric vehicles.

Combined damping strategies. When used as a dead band damper or a semi-active damper, the e.m. damper may offer little or no improvement of performance when compared to already existing technologies. While it is questionable that the power generated by a regenerative damper, when compared to a standard hydraulic damper, would exceed the power required to transport the extra mass of the damper; a regenerative e.m. damper may offer advantages over a purely passive hydraulic damper when used in combination with dead band damping or semi-active damping. The use of the e.m. damper technology would allow the combination of strategies with little additional hardware or complexity when compared to hydraulic technologies. This would be an area for further study and is beyond the scope of this research.

5.8   Conclusions

To determine whether a passive e.m. damper could provide sufficient damping for use in a practical electric vehicle, the theoretical model created in Chapter 4 was extended to determine the flux within a loop of wire created by a magnet. This model was tested and the experimental flux inside the coil was found to be 96.6 % of the predicted value. This was then used in a VISSIM model of Faraday's Law to determine the forces generated by the passive damper.

A single degree of freedom test rig was constructed and a variety of weights were used as a sprung mass. The modelled and experimental values of the behaviours of the sprung mass were compared. There was a greater than 80 % agreement between the results.

The passive e.m. damper was also tested with a psuedo-sine wave input at a variety of frequencies. For frequencies between 1-4 Hz there was a close relationship between the modelled and experimental data. At over 4 Hz, secondary effects would dominate and qualitative results were achieved rather than quantitative results.

A good measure of agreement was reached between the modelled and experimental results in the time domain and the frequency domain. The model was then used to construct two theoretical dampers to determine if the e.m. damper could be adapted for use on practical automobiles. These models were tested using a two degree of freedom model and the damping coefficient produced be the passive e.m. damper was determined and compared to the damping coefficient that would be required to give a damping ratio of 0.6. This damping coefficient was determined to be possible by the use of multiple magnets and multiple coils, of which each coil had multiple layers. The mass of magnets and copper required for the ND3522 magnet was 4.75 kg and for the ND5550 magnet the mass was 7.61 kg. This was a greater weight than a measured typical commercial hydraulic damper, before taking into account any fittings required for the structural integrity of the e.m. damper. While the damper may have secondary uses and applications, these were not the main thrust of this study and it could not determined that the passive e.m. damper offered any significant advantages over commercially available hydraulic passive dampers.

Chapter 6

The Active E.M. Damper

6.1 Introduction

Active suspension systems offer many advantages over passive systems. The costs and complexity of existing active hydraulic systems mean that not many fully active dampers are available on production automobiles. However, an active e.m. damper offers a potential to produce a very positive damping effect with reduced complexity compared to hydraulic active dampers. By having a spring in the suspension system the energy demand of the active e.m.damper is reduced as it does not have to supply energy to suspend the vehicle.

While it was possible to use both linear or rotary motors to provide the active e.m. damping, this research investigated a linear damper that was composed of one or more cylindrical magnets that travelled axially through one or more coils. These coils and magnets acted as a two phase linear electric motor. For most construction purposes this damper was identical to the passive e.m. damper examined in Chapter 5, with the exception of the addition of a power supply. This active e.m. damper was modelled numerically using much of the model previously developed for the passive e.m. damper.

Numerical modelling and simulation was used to predict the behaviour of the actively damped system to a step input. This was then compared to experimental results. The performance of the damper was then tested in the frequency domain using a series of experimental runs at various frequencies. The results from the theoretical model, using the same frequencies, were then compared with the experimental results to validate the model.

To determine the suitability of the active EM damper for lightweight electric vehicles, the model was then scaled up to the values for a known electric vehicle. Particular attention was paid to the power demands as this will affect the suitability for use in a lightweight electric vehicle.

6.2 Basic principles

With a coil and magnet system, if a current is applied to the coil then a magnet field is generated in coil. The magnetic field of the coil then will interact with the magnetic filed of the permanent magnet. This interaction produces a force. The force generated on the coil, was derived from the Lorentz Force Law.
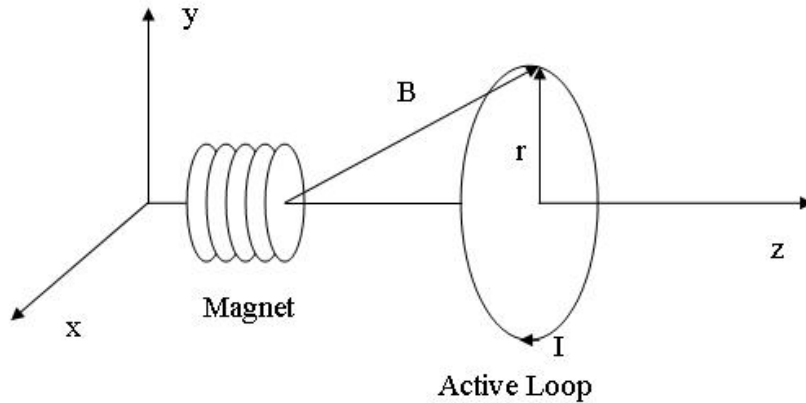
Figure 6.1: The force on a loop

For a permanent magnet and a single of current carrying wire, as illustrated in figure 6.1, the force on the wire is given by 6.1

$$F = BILsin\theta \tag{6.1}$$

where F is the force in Newtons, B is the magnetic field in Tesla, I is the current in Amperes, L is the length of the wire in meters and θ is the angle between the loop and the z axis. As the loop is on the x-y plane it is therefore normal to the z axis and the value of $sin\theta$ is equal to one. As the loop and magnet are both centred on the z axis and by symmetry the value of B is constant around the loop, then the length of the wire is the circumference of the loop, so $L = 2\pi r$ and the force equation simplifies to 6.2

$$F = 2\pi BIr \tag{6.2}$$

For a solenoid with multiple coils as illustrated in figure 6.2, the magnetic field $B\,sin\theta = B_z$, is the z component of the field of the permanent magnet. The force generated by the coil is the sum of all of the loops of the solenoid and was given by 6.3

$$F = \sum_{i=1}^{i=n} 2\pi r I B_z \tag{6.3}$$
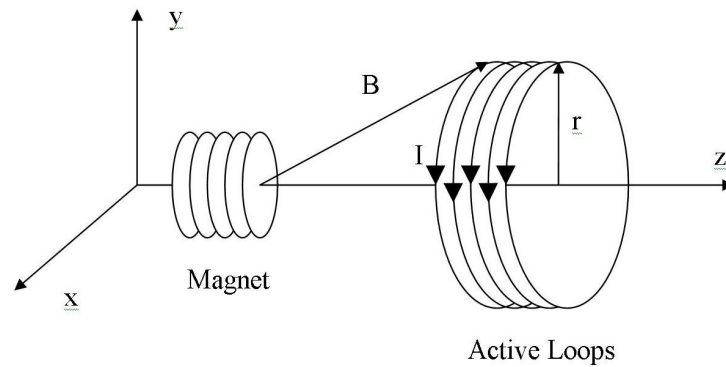
Figure 6.2: Modelling a magnet and a solenoid.

where r was the radius of the coil, I was the current and B was the z component of the magnetic field. If the geometry of the coil was constant, the Force was proportional to the distance the coil was from the permanent magnet and the current through the coil. As the current had a linear relationship to the force, this allowed the force of the damper to be modelled as a 'look up table'.

The power consumption of an active damper

A major consideration in an electric vehicle is the electrical power consumption. Any subsystem placed into such a vehicle must have a known power consumption. One of the potential benefits of an e.m. active damper system when compared with a conventional hydraulic active suspension is the much reduced power consumption. Using the developed models it is of interest to determine the power consumption of an active suspension for a light weight electric vehicle.

For an automotive system, the current used was determined by the maximum amount of power to be used in each damper and by the voltage the cars electrical system supplies to the coil. As stated above in 5.5

$$P = VI \tag{6.4}$$

by rearranging Ohm's Law for voltage, 6.5 was obtained

$$P = I^2 R \tag{6.5}$$

where R was the electrical resistance of the wire. The current required for a given force was determined by rearranging 6.5 to get 6.6

$$I = \sqrt{\frac{P}{R}} \tag{6.6}$$

where R was given by 6.7

$$R = \frac{\sigma L}{A} \tag{6.7}$$

and A was the cross sectional area of the wire, σ was the resistivity of the conducting material in the wire and L was the length of the wire in the coil. Substituting 6.7 into 6.6 yielded 6.8.

$$I = \sqrt{\frac{PA}{\sigma L}} \tag{6.8}$$

For a uniform field

For a uniform magnetic field the relationship between the force generated, the power consumed and the mass of the copper required could be determined by substituting equation 6.8 into 6.1. The force over the length of the solenoid for a uniform magnetic field was given by 6.9 using n as the number of turns in the solenoid.

$$F = n\, 2\pi r\, B \sqrt{\frac{P\,A}{\sigma n 2\pi r}} \tag{6.9}$$

In 6.9, it can be seen that the term $n2\pi r$ is the length L and the variables within the radical are equal to $I\,sin\theta$. This simplifies to 6.10

$$F = B \sqrt{\frac{2n\pi r P A}{\sigma}} \tag{6.10}$$

as A was equal to πR^2 where R was the radius of the wire. An important consideration was the weight of copper used in the damper. This can be determined from 6.11

$$M = V\rho \tag{6.11}$$

With a wire, the volume approximated to that of a cylinder, $V = L\,\pi\,R^2$, and so the mass of a single loop was given by 6.12

$$M = \rho L \pi R^2 \tag{6.12}$$

and the mass for the entire solenoid was given by 6.13, where L was $2\,n\,\pi\,r$ and the cross sectional area of the wire was $\pi\,R^2$.

$$M = 2\rho n r \pi^2 R^2 \tag{6.13}$$

Substituting 6.13 into 6.10 gave 6.14.

$$F = B \sqrt{\frac{MP}{\rho\sigma}} \tag{6.14}$$

where the force was now in terms of B, the magnetic field, M the mass of the coil, P the power used, ρ the density of the coil and σ the resistivity of the coil.

This demonstrated that for a uniform magnetic coil that the force generated was independent of the thickness of the wire or the number of turns of wire in the coil, rather it was dependant upon the total mass of conductor in the circuit. The weight of copper was the dependent factor in both passive and active dampers.

Using the values given in Gysen *et al.* (2008b) for a sedan driving around the Nürburgring in Germany, the vehicle dampers had a maximum force of 4,000 N and a continuous force of 700 N. Using the equation given in 6.14 and rearranging for the power, the required power for various masses of copper are given in table 6.1.

Table 6.1: Power consumption by weight, for a an active e.m. damper supplying of damping force of 4,000N and 700N

Mass of Copper	4,000N	700 N
1 kg	6,640 W	203 W
2 kg	3,320 W	102 W
3 kg	2,213 W	68 W
4 kg	1,660	51 W
5 kg	1,328 W	41 W

For a light-weight electric vehicle there were several factors that would reduce the power consumption compared to the test vehicle used. Firstly, the vehicle was not designed for use on a race track. Race vehicles traditionally use much more power and more powerful suspension systems than road cars. Secondly, the speeds of an electric vehicle designed for urban driving would be much less than required for highway or race track use. This would reduce the forces that needs to be generated and the power consumed. Third, the electric vehicles that were being investigated typically have less weight than most automobiles. This again reduced the force. As the power required was proportional to the square of the force, even small reductions in the force can have significant reductions in the power consumption. A reduction in force by 50% equates to a reduction in power of 75%. In a lightweight car the lighter the mass of copper the more efficient the car is, so it was desirable that the dampers will have less than say, 2 kg of copper.

For a non-uniform field

In the case of the uniform magnetic field it was possible to determine the magnetic field and use this as a constant in equation 6.3. However, the active e.m. damper being modelled did not produce a uniform magnetic field. This required equation 6.3 to be modelled numerically. The power consumption was also modelled numerically.

6.3   Mapping the force

Due to the non-linear nature of an active e.m. damper of the design proposed, a map of the force generated by the damper was required. As the damper was modelled with only a single degree of freedom then the field and forces only required to be mapped as a single dimensional model. This could then be converted into a lookup table that then can be used in the MATLAB and VISSIM models as required.

The look up table returned the force generated by the magnet on the coil by distance, when there was a one Amp current passing through the coil. When implemented into the damper model the only inputs required to determine the damper force were the position of the damper in regards to the permanent magnet and the current in the coil.

MATLAB was used to generate the look up table. To determine the magnetic field the magnet was modelled as in Chapter 4. The magnetic field was then used in equation 6.3 to generate the force experienced. The coil was 120 turns in three layers of 40 windings each. This was approximated as a single coil of 120 using the mean radius of the three layers. This was the same coil as was used in Chapter 5. The magnet was also the same magnet as was used in Chapter 5.

Experimentation was conducted to determine the force generated by the prototype coil as used previously. This the modelled forced and measured forces were determined and are given in table 6.2. There was a good agreement between the modelled and measured values.

Table 6.2: The maximum modelled and measured forces generated by a prototype coil.

Current (A)	Modelled (N)	Measured (N)	Agreement (%)
1	0.6061	0.64	94.7
2	0.9922	1.04	95.4
3	1.3783	1.42	97.1

The force generated by the magnet over a distance of ± 100 mm is given in figure 6.3. The displacement of the magnet and coil was measured from the centre of the magnet to to the centre of the coil. Points to note were that when the magnet was centred in the coil that no force was generated. The maximum force of 0.3686 N was produced when the magnet has been displaced 34 mm from the central position. This was when the centre of the magnet was at the edge of the coil. The region between 0.021 m and 0.050 m generates a force of 0.3 N or more for 1 Amp of current.
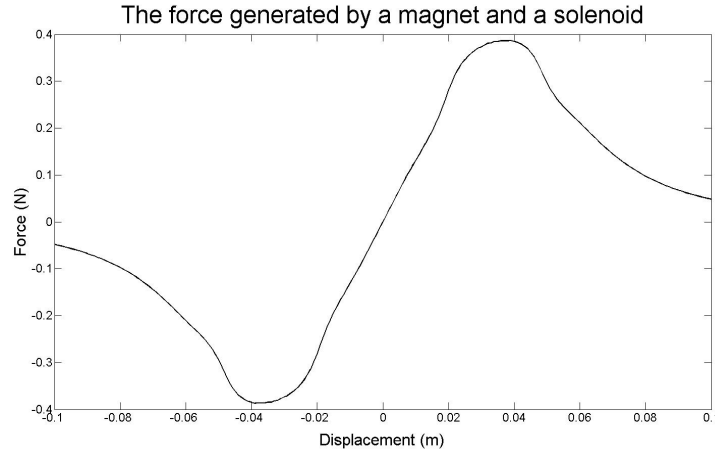
The force generated by a magnet and a solenoid

Figure 6.3: A look up table for the force generated by a magnet and coil. The force was measured for the displacement of the 29mm magnet from the centre position of a 66mm long, 120 turn, coil.

6.4 Modelling the active e.m. damper

The model of the damper shared several components with the model of the passive damper. The equation of motion was given by 6.15

$$a = \frac{k(z_0 - z_1) + F_{Active} + F_{Natural}}{m} \qquad (6.15)$$

where k was the spring constant, z_0 was the input displacement, z_1 was the displacement of the sprung mass, F_{Active} was the force generated by the active damper and $F_{natural}$ was the force generated by natural damping. From the acceleration of the sprung mass, a, the velocity was determined using 6.16 and the displacement was determined using 6.17.

$$\dot{z} = \int a \, dt \qquad (6.16)$$

$$z = \int \int a \, dt \qquad (6.17)$$

The natural damping force was produced in exactly the same way as detailed in Chapter 5. It comprised of both a Coulombic damping component and a viscous damping component. The same values were used as were determined in Chapter 5 for the masses being used.

To determine the active damping force, the inputs were the displacement of the ground, z_0, the displacement of the tyre z_1, the magnet offset, the velocity of the sprung mass and the desired damping coefficient value. This was the zero position that the permanent magnet sits in relation to the coil. The relative position of z_0 and z_1 were added to the magnet offset to give the magnets position. This value was used by the look up table to determine the force generated by the coil at a value of

one Amp. A correction factor was applied to compensate for the slight discrepancy between the modelled magnetic field and the measured magnetic field. The current to be supplied was determined by multiplying the chosen damping coefficient and the absolute velocity of the sprung mass. This value was then multiplied by the force from the look up table to give the damper force.

6.5　Implementing an active e.m. damper
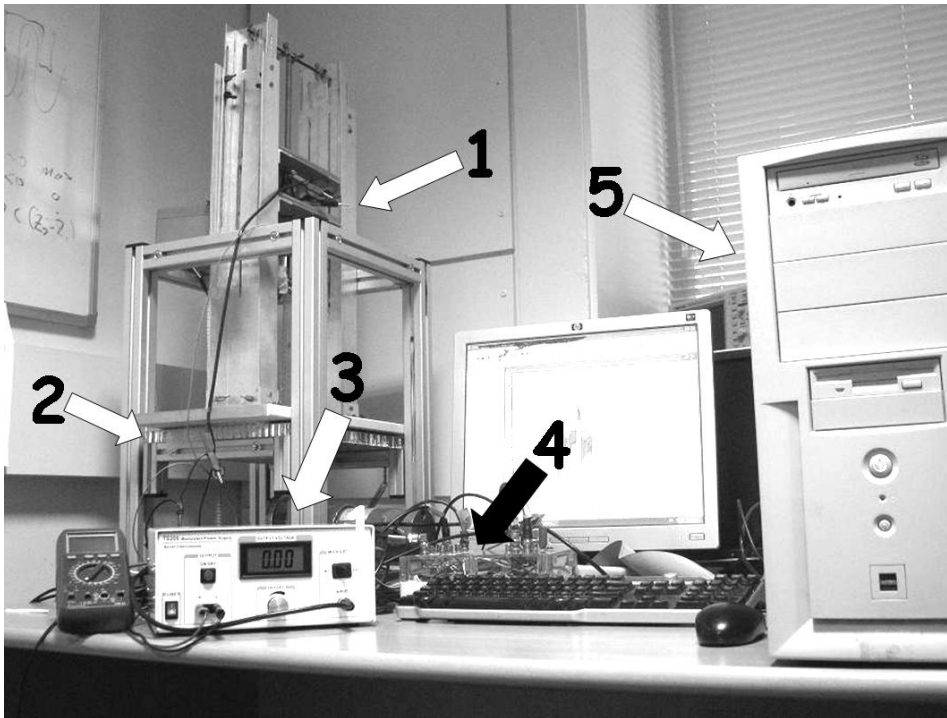
(a) The physical prototype. (1) - the spring, damper, sprung mass and accelerometer, (2) The vibration surface. (3) The current amplifier. (4) The data input/output ports. (5) The computer with VISSIM REALTIME.
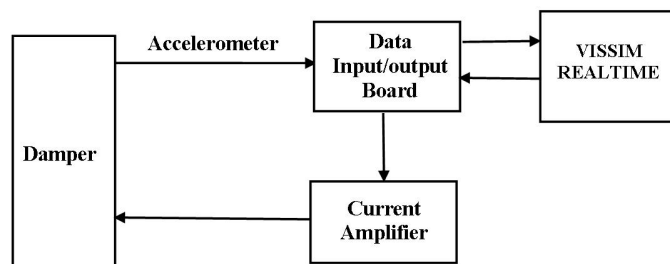
(b) The system diagram of the active suspension.

Figure 6.4: The experimental apparatus for an active damper.

The experimental rig that was used in Chapter 5 was modified by mounting the apparatus on a surface that could be displaced in a single degree of freedom. The

experimental apparatus is pictured in figure 6.4. The vibration input signal was provided by an electric motor that drove a circular offset cam which provided a pseudo-sine wave input.

For the implementation of an active damper, several components were required: an input signal, a controller, an output signal and the physical damper.

The input For the active damper at least one input was required. For a pure Skyhook damper the input should be the absolute velocity of the sprung mass. As it was difficult to obtain this directly it is more common to measure the acceleration of the mass using an accelerometer and integrate this to determine the velocity or to measure the displacement using a device such as an LVDT and differentiate this to determine velocity. It should be noted that in the real world a LVDT only produces the relative velocity between the sprung mass and the ground surface, it cannot deliver an absolute velocity in normal usage. For some control algorithms examined in Chapter 2 an LVDT would produce sufficient information. However, for a full Skyhook implementation the absolute velocity of the sprung mass compared to a fixed point in space was required. In a one degree of freedom system with a known input this could be determined using the LVDT. However, this would not be effective in a two degree of freedom system or with random inputs. As the system being examined was a single degree of freedom system a LVDT was tested and it was found that it created a resistive force of 2 Newtons. Because of the size of the mass involved, this was considered excessive so an accelerometer was used due to the small effect it has upon the damper performance.

The controller As this was not a study on optimisation of control dampers, it was decided to use the full Skyhook damper first proposed by Dean Karnopp. The control for this controller was given by $F = c\dot{z}$ where c was the damping coefficient and $\dot{z}$ was the velocity of the unsprung mass. The controller was written using VISSIM in the REALTIME package. The data input/output was through a Measuring Computing PCI-DAS6014 data acquisition board which was installed in an IBM based computer. The PCI-DAS6104 was chosen because it also had analogue output capacity. As the input frequency from the damper is in the range of 1–10 Hz. To prevent Nyquist Aliasing, the input sample fequency is set at 1,000 Hz or greater.

The output The analogue output signal was delivered from the DAQ board to an Accel Instruments TS200 Modulated Power Supply. This was used as a current amplifier which could produce a ±6 Amp signal. A load resistor was added to provide a total circuit resistance of 1Ω. This provided sufficient resistance to prevent the power supply overheating and the resistance created a direct relationship of $1\,V = 1\,A$ for the current output used to drive the damping coil(s).

The prototype active e.m. damper The damper was the same coil as used in the passive e.m. damper. This was mounted on the same vibration rig as used for the passive e.m. damper. The only significant change to the damper was that instead of a short circuit to provide damping, the leads of the damper were connected to the power supply which was under control of the VISSIM REALTIME controller.

6.5.1   The accelerometer and accelerometer drift

In an active suspension system a control law is required which is usually implemented through a controller. In the full Skyhook controller, the primary input is the absolute velocity of the sprung mass. This was and is difficult to measure directly, however the velocity could be determined by integrating the acceleration or differentiating the displacement. Due to the mass of the unsprung element, the measuring technique available with the lowest effect on the measurement was an accelerometer. Two accelerometers were used. The first was used by the VISSIM REALTIME package for the controller. The second accelerometer was required to record the results of the tests on a COCO80 Signal Analyser. The model chosen for the VISSIM REALTIME controller was the Analogue Devices ADXL325 model. This was mounted onto an evaluation board so that it could input data directly into the VISSIM REALTIME package. This was a three axis accelerometer which has a range of ± 5 g in all three axis. This package included an on board signal conditioner and was supplied with an external reference voltage for determining the acceleration. The accelerometer was designed for development and evaluation purposes and was uncalibrated.

The raw signal from the accelerometer

As VISSIM REALTIME was the controller of the active damper, an examination of the accelerations being read was conducted. In figure 6.5 it could be observed that there was an off-set of the signal. If this was integrated directly then the velocity output was as is illustrated in figure 6.6. This offset was the result of the accelerometer using a reference voltage. A separate voltage was supplied to the accelerometer and the accelerometer then returned a voltage between 0 V and the reference voltage. The value returned for zero acceleration was half the reference voltage. This offset could vary from run to run and was not always consistent. This removed the ability to determine a constant value and to subtract that from all future accelerometer readings.

It was decided that a computer software element was required that could determine the offset and could remove it during each run. This aim was achieved in a computer subroutine which measured the average value of the accelerometer for a period of greater than the period of one cycle of the wave being measured and then subtracted this from the current value. For most runs the value chosen was between 1 to 5 seconds. If the value was less than the period of the input signal then this
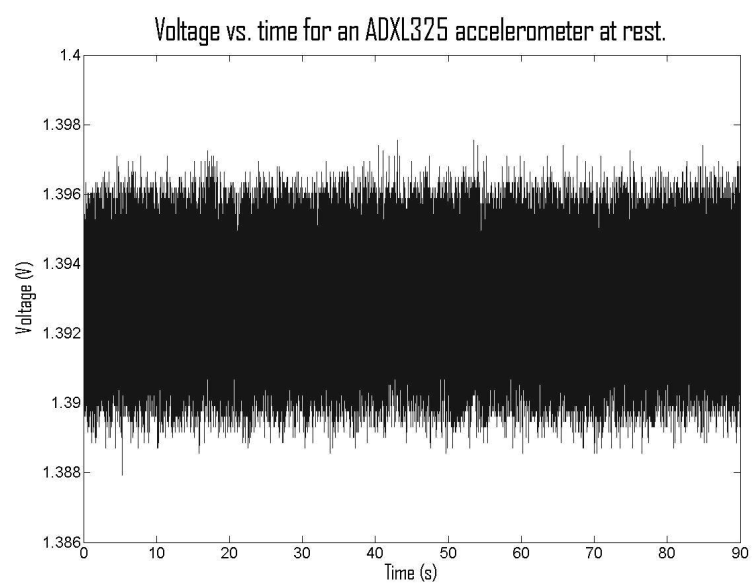
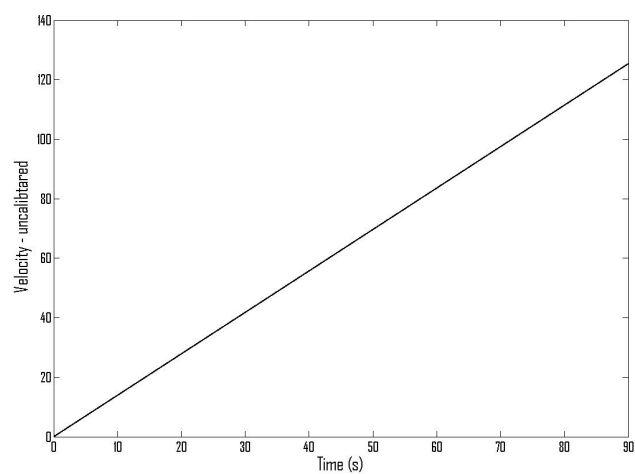Figure 6.5: The unprocessed signal from the accelerometer on a stationary object.

Figure 6.6: The velocity from the integration of the raw acceleration signal

could interfere with the measurement being taken and if the figure was greater than 5 seconds then the controller could not respond fast enough to counter drift events. The adjusted signal is given in figure 6.7.
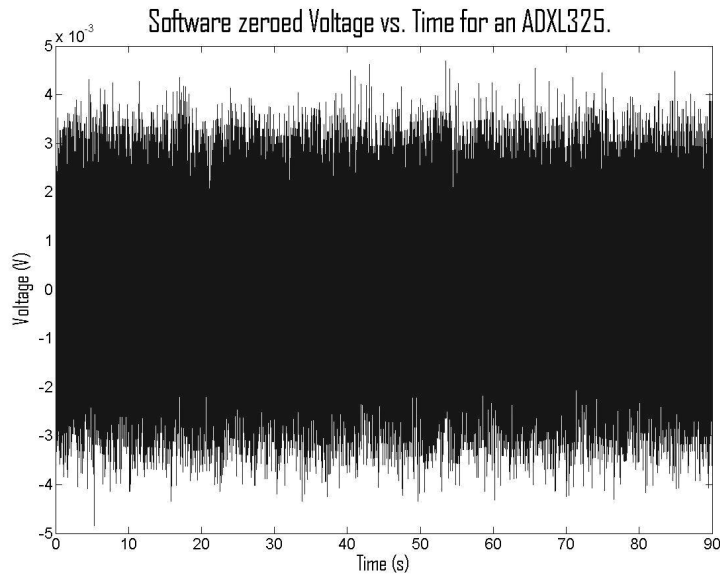

Figure 6.7: The accelerometer signal after being adjusted for the offset.

A comparison was then conducted between the adjusted signal and the raw signal. This comparison was performed for the two cases of the signal when there was no acceleration inputs showing only accelerometer noise and for the case where there was an acceleration signal from the weight oscillating.

To determine the accelerometer drift two signals were generated. The first was the instantaneous acceleration subtracting the mean acceleration of the entire data run. While this was an easy and practical technique that can be performed after the data run was complete, it could not be performed over such large periods during real time simulation. The second signal was run in real time as mentioned above. The real time offset signal maintains in excess of 97% agreement with the magnitude of the variation of the original signal. This approach produced a fast and quite accurate result that can be used in the real time processes. The residual accelerometer drift was obtained by subtracting the second signal from the first signal. The result is illustrated in figure 6.8.

It should be noted that in figure 6.8 that the resultant line was non-linear and was assumed to be a 'random walk'. As such there was no predictive algorithm that can determine the acceleration variations. The discrepancy between the average signal and instantaneous signal was a changing bias that would produce significant effects when integrated for the velocity measurement.
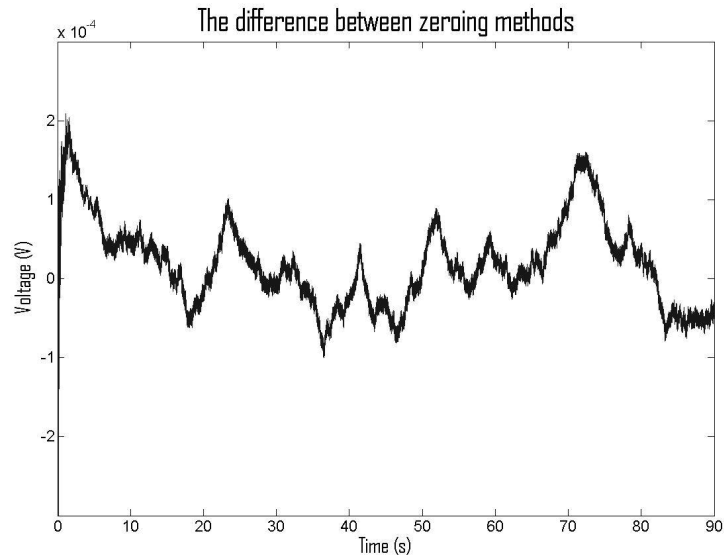
Figure 6.8: Comparison of original signal (offset) with the adjusted signal for no acceleration.

Calibration of the accelerometer

To calibrate the accelerometer a run was conducted on the vibration apparatus with both the ADXL325 accelerometer and the pre-calibrated PCB356A02 accelerometer. The output from the ADXL325 accelerometer was recorded directly to VISSIM REALTIME while the output from the PCB356A02 was recorded with a COCO80 Signal Analyser. This data was then imported into VISSIM REALTIME. Both data sets were then displayed superimposed. As both accelerometers had been measuring the same input signal, the phase of the ADXL325 signal was then adjusted so that both signals were synchronised. The signal of the ADXL325 accelerometer was then amplified until both of the waveforms recorded were a good visual match. It was determined that the ADXL325 signal had to be magnified 81 times to produce the same signal as the PCB356A02. The calibration was accordingly set as 1 V = 81 m/s^2.

With the calibration of the accelerometer, the velocity of the accelerometer could then be determined by integrating the acceleration output signal. A custom integrator was constructed so as to reduce the processor time required. No interpolation was included so as to also reduce the processor time. This was considered unnecessary as self correction software was included in the acceleration signal. Using the same accelerometer test data as for the previous examples, a comparison was performed between the custom integrator and the VISSIM integrator using a 4th order Runge-Kutte algorithm to perform interpolation. In figure 6.9 a comparison was performed between the two signals. Due to the nature of integrated signals to drift after a period, the comparison shown is between 89.9 and 90 s. As is observed the two signals have a very close relationship, the major difference being a phase
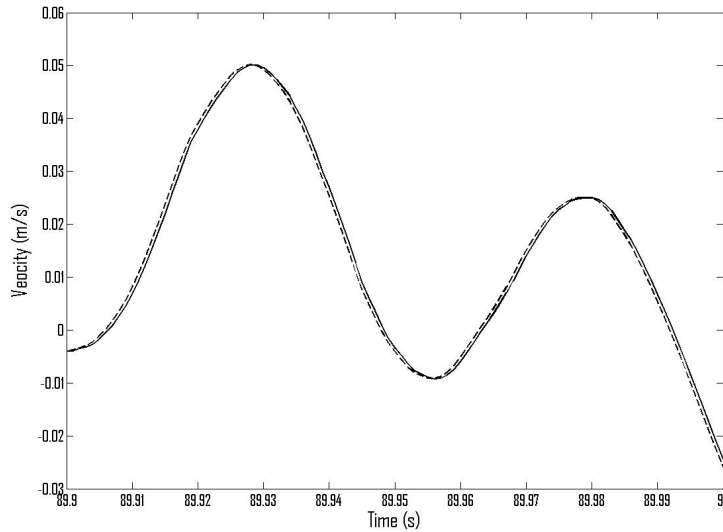
shift of 0.5 ms.

Figure 6.9: Comparison between velocities between the custom and VISSIM integrators. The VISSIM integrator with 4th order Runge-Kutte interpolation is represented by the solid line. The dashed line is the velocity from the custom integrator.

The accelerometer signal. An examination was made of the input accelerometer signal. While the signal had a component of noise it could be observed from figure 6.10 that there was a 50 Hz signal in the noise. This was combined with the accelerometer drift. The source of the 50 Hz signal was traced to the computer and/or Data Acquisition Board. Beyond that the source of this signal could not be determined. The r.m.s. value of the signal was 0.001778 V. This gave a calibrated acceleration of 0.1427 m/s^2 r.m.s. In the case of an acceleration signal as illustrated in figure 6.11 resulting from a 1 cm drop in the sprung mass, the noise represents 21% of the maximum input signal. Between time 15 and 25 s the signal was superimposed upon the 50 Hz signal.

The use of a low pass filter was investigated to remove the 50 Hz signal, however this introduced a time delay into the signal. For the filters available in the VISSIM system being used, the delay times were determined to be be as given in table 6.3. Any delay in signal could have a large effect on the performance of the damping system. For the system controlling a 10 Hz input signal, a 33 ms delay represents 1/3 of a complete cycle. This would have greatly reduced the effectiveness of any damping algorithm.

The 50 Hz input was a very close approximation to a sine wave and as such over a longer period of time the signal would cancel out or reduce its effect on the signal. This would show in an integration as a reduction in the noise in the signal. The signal was then integrated to verify the effect of the 50 Hz on the velocity signal.
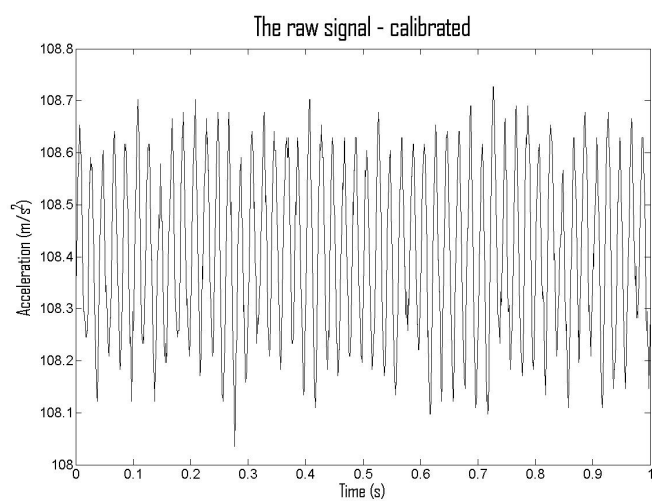
Figure 6.10: The raw signal which acceleration has been calibrated. Short time scale.
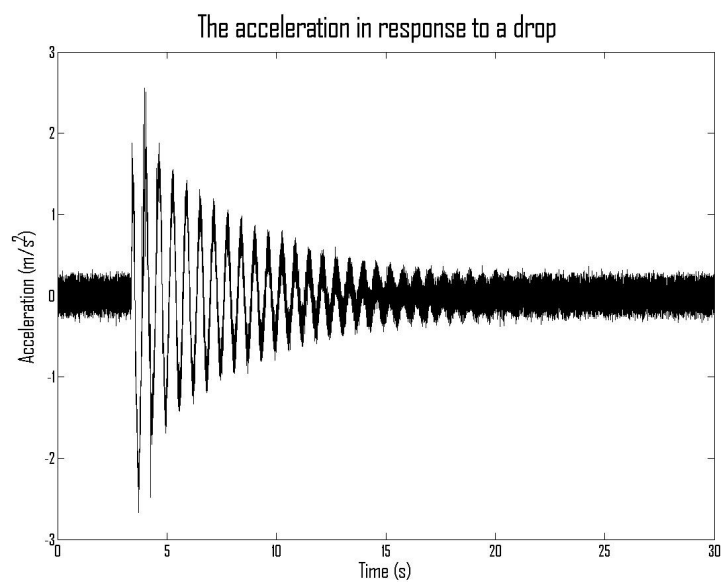
Figure 6.11: Comparison of signal to noise for acceleration.

This presented a mean r.m.s. value of 4×10^{-5} m/s. When compared to the velocity obtained from the drop signal used in 6.11, the maximum velocity obtained was 0.29 m/s. This represents a variation of 0.014 % of the velocity signal. It was therefore decided that for velocity measurements the use of a low pass filter was not required for a useful velocity signal.

Table 6.3: The signal delay due to the use of signal filters

Filter	Delay (ms)
Buttersworth , 5th order	110
Bessel, 2nd order	57
Chebyslev, 2nd order	33
Inverse Chebyslev, 4th order	44
Differentiator	393
Hilbert Transform	57

Determining the velocity from the accelerometer.   The acceleration measurement was the input for the custom integrator used to determine the velocity. The velocity for the same nominal run is illustrated in figure 6.12. This variation of velocity was due to the accelerometer drift as illustrated in 6.8. In the case of the active damper using a Skyhook algorithm, the accelerometer was the only data input into the system. Discrepancies of 0.6 m/s, as illustrated, could be larger than the data measurements required. Therefore a way of removing this random drift was developed.
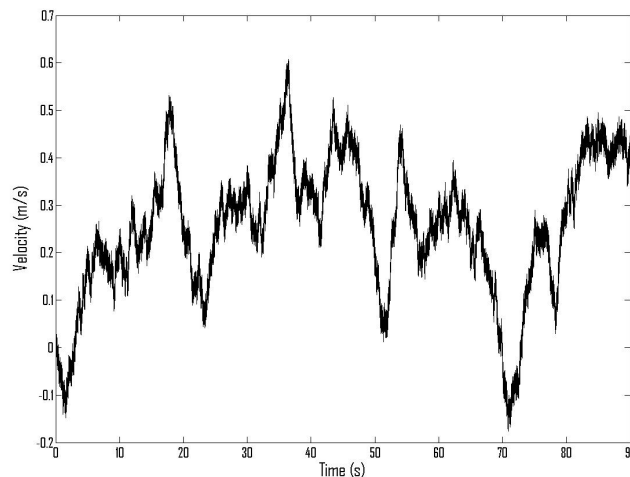
Figure 6.12: The velocity drift of the integrated acceleration signal.

Due to the requirement to run in real time with the minimum delay between the input and the output, the same levelling function as was used on the acceleration signal as was used on the velocity signal. The running average measurement for a fixed period was subtracted from the measurement thus acting as a self levelling

unit. The data run used for figure 6.12 was used as the input for the smoothing algorithm and the period of time that the signal was averaged for were 5, 2, 1, 0.5 and 0.1 seconds. The results are given in figure 6.13
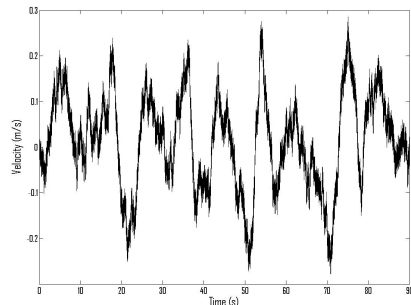
(a) The integrated velocity with a 5 second running mean
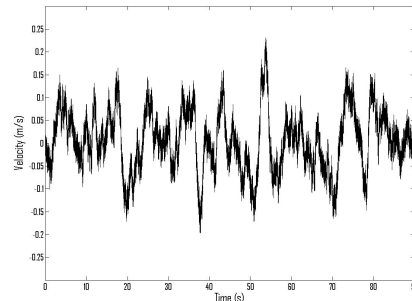
(b) The integrated velocity with a 2 second running mean
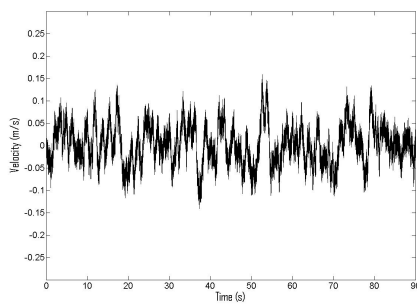
(c) The integrated velocity with a 1 second running mean
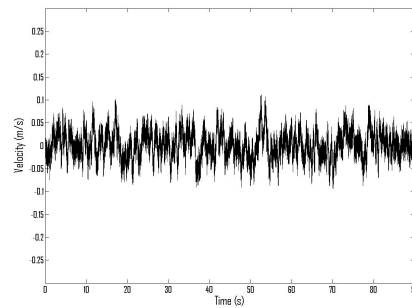
(d) The integrated velocity with a 0.5 second running mean
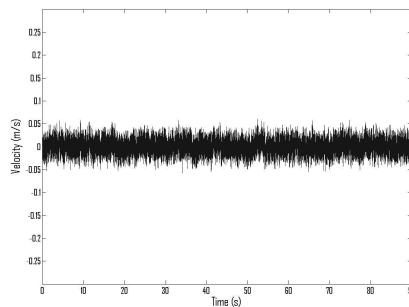
(e) The integrated velocity with a 0.1 second running mean

Figure 6.13: The integrated velocity after self levelling was applied for various time periods.

It was observed as the time period over which the running mean was measured was reduced, the self levelling effect was improved. With a five second sample, self levelling was achieved, but the variation in signal could still exceed ±0.2 m/s. At a time period of 0.1 seconds the deviation from the zero velocity was a maximum of ±0.05 m/s. While this was desirable there are two areas of caution to note. In the first, the self levelling effect also affected any signal that was processed. For

periods much longer than the period of the signal the effect of this approaches zero. As the period of the running average approaches zero, then the signal reduction approaches 100%. It was decided that the optimum period for the running average was determined to be between one and five times the length of the longest time period of the signal to be measured. While the lower figure produced a maximum reduction of signal strength of 24%, it also produces the fastest response. At twice the period of the signal the reduction was 14.2% and at five times the signal frequency the worst signal reduction was 6.5%.

For the research into the damper the typical frequencies examined were in the range of 1 Hz to 10 Hz. With a running mean set at one second the largest reduction in signal occurs at 1.5 seconds. This was near the resonant frequency of 1.65 Hz. At this frequency the reduction in signal would be reduced by 18 %. As the frequency increases the reduction in signal will decrease. At higher frequencies the maximum reduction decreases. It should be noted that the self levelling element introduces a 'memory' effect into the control system. As the self levelling element contains the mean measurement over a period of time, that will affect the displacement that the damper will try and maintain.
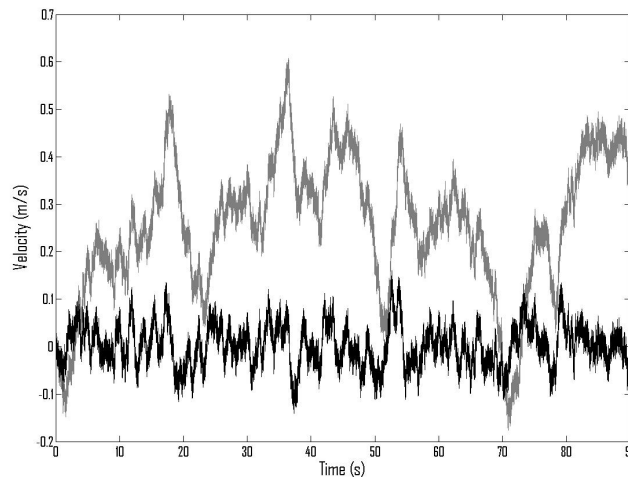
Figure 6.14: The random drift signal with no self levelling and 1 s self levelling. The light grey signal was without smoothing and the black signal was with self levelling of a 1 second running mean.

As was observed in figure 6.14, the original signal was in the positive velocity regime for most of the 90 second data run. The actual velocity for this run was 0 m/s. By using the 1 second running average as a self levelling algorithm, the absolute mean velocity was reduced from 0.2645 m/s to 0.0368 m/s. In table 6.4 the length of the running mean was compared with the mean velocity and the absolute mean velocity. In this case the mean velocity represented the discrepancy of the total run from the zero. If the mean was low then it indicated that the positive and negative velocities cancelled out. If a further integration was to be performed

upon the data, the lower these discrepancies were, then the smaller the drift that was transmitted into the transformed data. The absolute mean data represents the magnitude of the difference between the data run and actual observed velocity. This showed the magnitude of the error in data being used for the velocity measurements.

Table 6.4: The self levelling of the system dependant upon the time of the running mean.

Self Levelling Time (s)	Mean velocity (m/s)	Absolute Mean Velocity (m/s)
None	0.2550	0.2645
5.0	0.0127	0.0860
2.0	0.0048	0.0536
1.0	0.0022	0.0368
0.5	0.0011	0.0256
0.1	0.0002	0.0175

For the case of a running mean of one second the reduction in the mean velocity was 91% and for the absolute mean velocity it was 86%. For most data runs the value of one second was used for the running mean. This was a good compromise between the signal that was transmitted and the amount of noise that was suppressed.

Determining the displacement from integration of the velocity signal.
Integrating the velocity signal the displacement of the sprung mass could be determined. This would be of use in the active damper to compensate for the non-linear damping characteristics. In figure 6.16a the signal from the self levelled velocity was integrated. All measurements were well in excess of the $\approx \pm 5\,cm$ displacement achievable in the physical model. A displacement of 1,200 m from the start position was obviously nonsensical. A self levelling element also using a one second running mean was introduced and the results are shown in figure 6.16b. Again the modelled displacements were much larger than are actually available. This technique was therefore not suitable for determining the displacement in a real time manner.

6.5.2 The implementation

The active control system was made of several units: the active e.m. damper, an accelerometer that was attached to the sprung mass, a data input/output board, a computer running VISSIM REALTIME and a current amplifier. These are represented in figure 6.4b.

In the final implementation of the Skyhook damper the accelerometer signal was the input for the VISSIM REALTIME controller. The signal was amplified by the calibration factor. The signal was processed by the self levelling unit. The signal was then integrated to obtain the velocity of the sprung mass. This was multiplied by a damping coefficient which was fixed by the user. This processed signal was then exported to a current amplifier. This current amplifier had a load resistor so
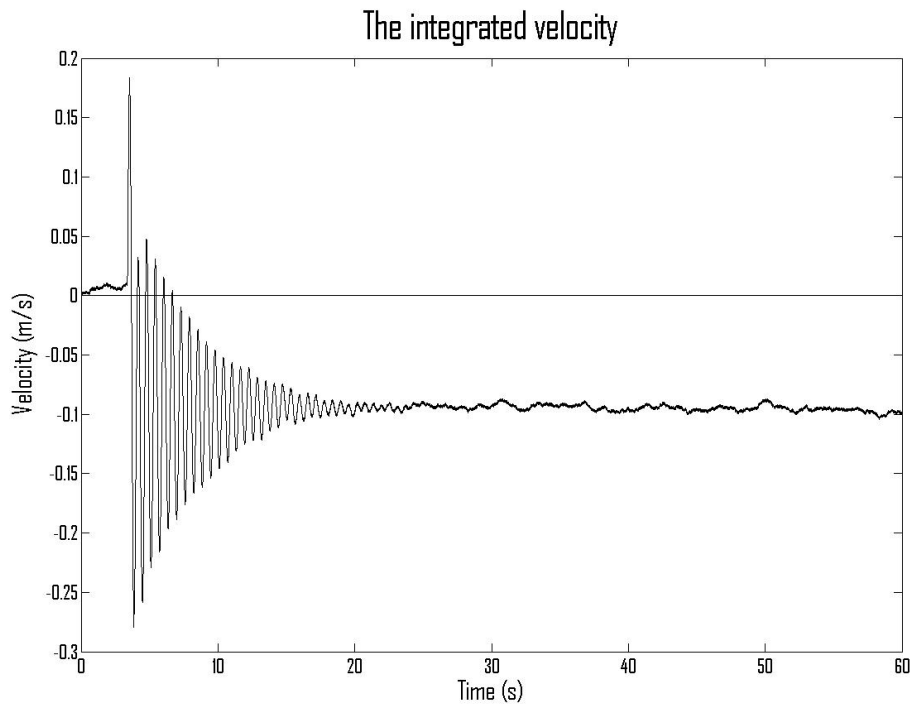
(a) Integrating the acceleration to obtain the velocity
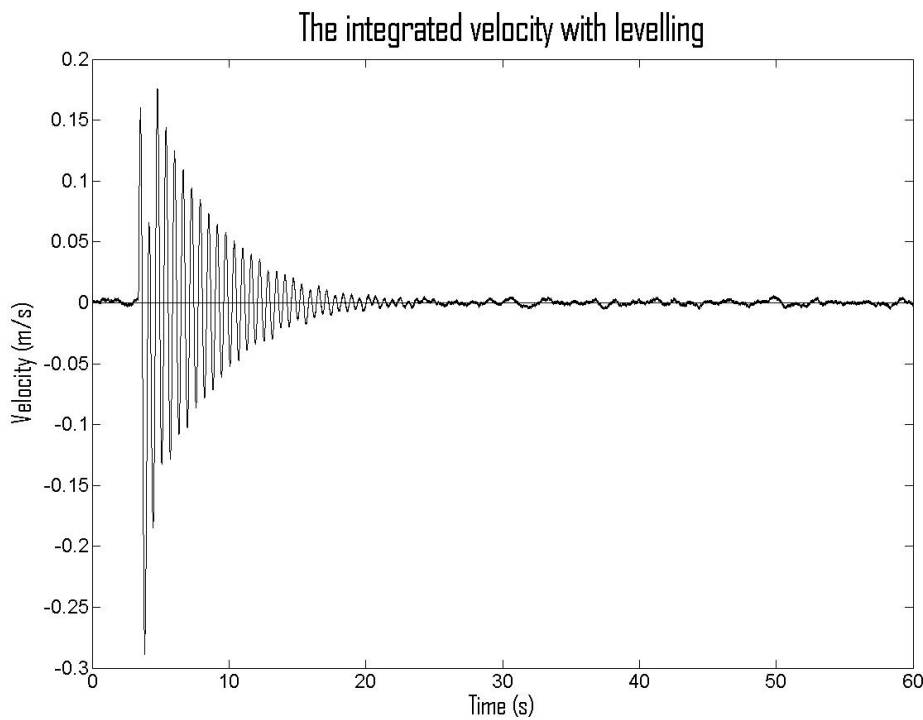
(b) Integrating the acceleration to obtain the velocity using a self levelling element.

Figure 6.15: Integrating the acceleration to obtain the velocity using a self levelling element.
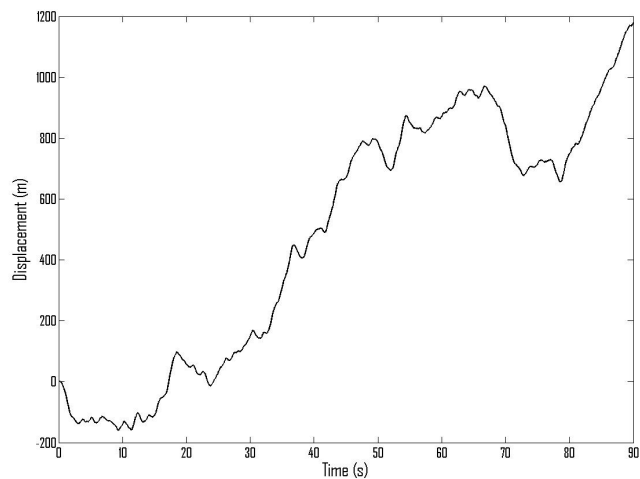
(a) Integrating velocity to obtain displacement
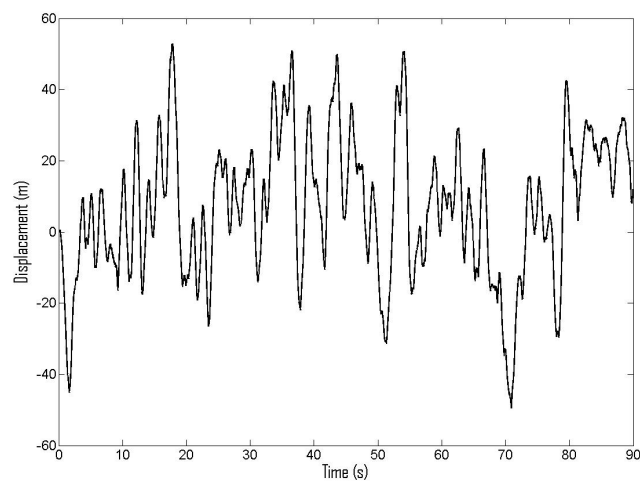
(b) Integrating velocity to obtain displacement using a self levelling element.

Figure 6.16: Integrating velocity to obtain displacement using a self levelling element.

that the external load on the current amplifier was 1 Ω. With this load the current amplifier would produce a current of 1 Amp for every Volt that was on the input side. This current was then passed through the coil to produce the damping force.

6.6   Time domain

To determine the effectiveness of the model of the active e.m. damper the experimental damper apparatus as used in Chapter Five was modified. The sprung mass had a second accelerometer added to provide state information for the VISSIM REALTIME controller. The controller was Karnopp's ideal Skyhook, $F = -c\dot{z}$.

When the damping coefficient of c was set to values of 200 Ns/m or above the system would be considered grossly overdamped if it were a passive damper. The damping between the model and the experimental damper was compared when the damping was set at 200 N s/m and 20 N s/m. The lower damping coefficient allowed a closer inspection of the behaviour of the damper. The two damper runs are presented in figure 6.17

As noted in the figures 6.17, the measured input signal has a large noise component. This accelerometer was separate and less noisy than the accelerometer that supplied the control signal to the damper. In both cases the modelled data demonstrated a good relationship with the measured data.

6.7   Frequency domain

The damper was tested with a pseudo-sine wave input at a variety of frequencies from below the resonant frequency of the system to approximately 9 Hz. The upper frequency limit was determined by the experimental apparatus. A series of experimental data runs were conducted over the frequency range and compared to the theoretical model. The magnet was the same 29mm long neodymium magnet as used in previous experiments. The coil was the single coil as described previously. The damper value was set at 100 Ns/m and the time step for the VISSIM simulator was set at 0.001 seconds.

A comparison was conducted between the measured non-damped motion of the system and the modelled non-damped motion of the system. The results are given in figure 6.18. The velocity amplitude ratio is a standard measurement of damper performance and is determined by dividing the absolute velocity of the sprung mass by the absolute vertical velocity of the road surface.

It was observed that the maximum velocity was larger than the maximum modelled velocity. This was in part due to the narrow range of the resonant frequency. The exact resonant frequency was not one of the measured frequencies included in this data run. Also of note was that at higher frequencies the actual damping was less than the modelled damping. This was due in part due to secondary motions
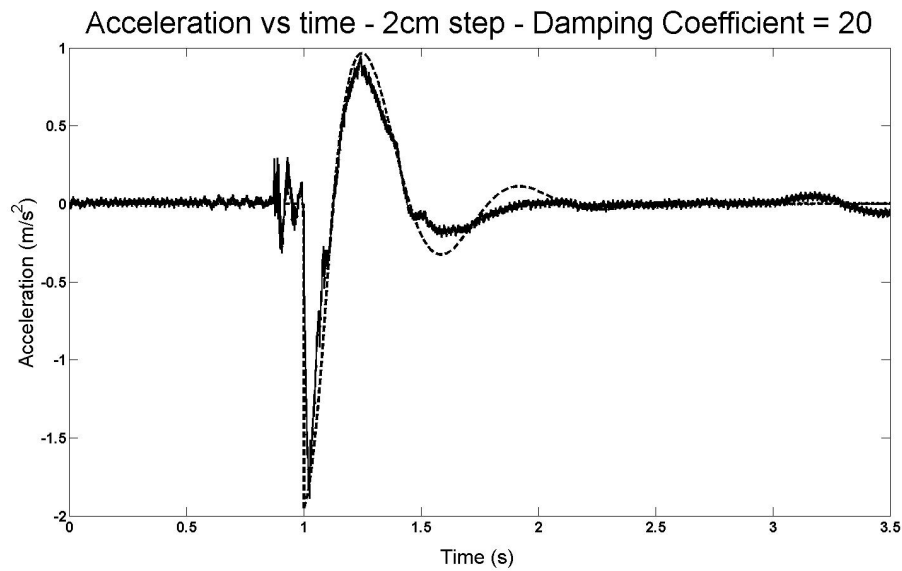
(a) Acceleration vs time for a 2 cm bump with an active damping coefficient of 20 N m/s.
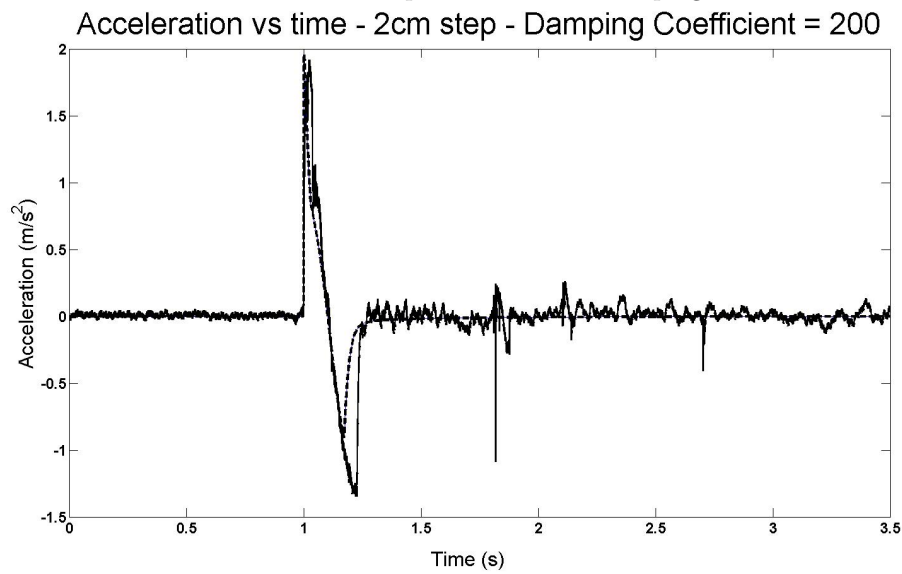
(b) Acceleration vs time for a 2 cm bump with an active damping coefficient of 20 N m/s.

Figure 6.17: Acceleration vs time for a 2 cm bump with different active damping coefficients. "——" measured. "- - - -" modelled.
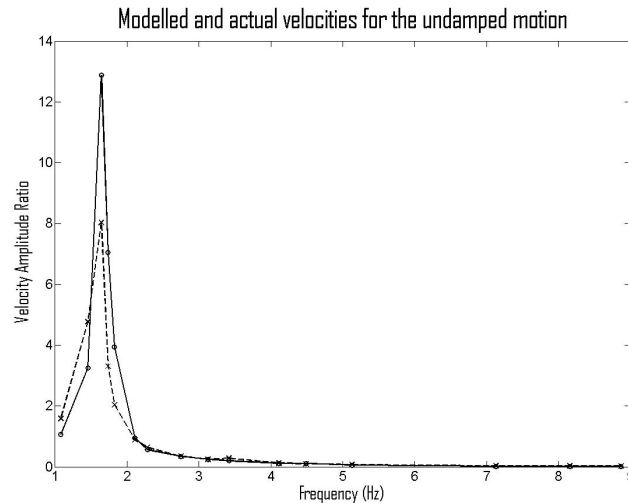
Figure 6.18: A comparison of the modelled and actual undamped motion in the frequency domain. "——-" were the actual measurements and "- - - - ' were the modelled values

of the sprung mass. At higher frequencies the effect of these secondary motions became relatively larger than the desired notion of the system. Over the range of frequencies tested, the model showed a reasonable degree of correlation to the actual measurements.

A similar comparison was performed between the active modelled motion and actual active motion as is illustrated in figure 6.19
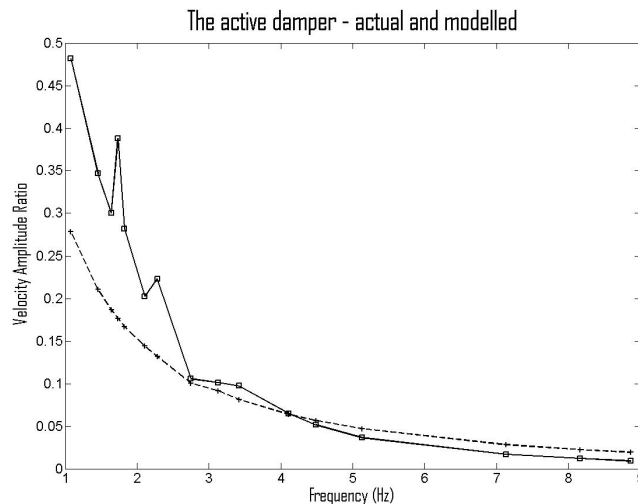
Figure 6.19: A comparison of the modelled and actual actively damped motion in the frequency domain. "———" were the actual measurements and "- - - -" were the modelled measurements.

It should be noted that as the motion of the mass was reduced then the effects of the accelerometer drift become more apparent and that the damper reacted to

this drift. Also at the higher frequencies again the secondary motions become more apparent. There was a spike in the signal at the resonant frequency of the system. At frequencies above 5 Hz the results were more qualitative than quantitative.

A comparison was made between the undamped, the actively e.m. damped and an ideal passively damped system. This is illustrated in figure 6.20. For the passive damper the amplitude of the velocity was greatly reduced near the resonant frequency. However, at frequencies above 2.25 Hz the performance of the damper was worse than in the undamped system.

For the active e.m. damper, compared to the passive damper, the performance was improved at all frequencies tested. In terms of absolute (non-logarithmic) values the worst case for the active damper has 54% of the velocity of the passively damped system. At approximately 9 Hz this reduced to 5%.

For the active damper compared to no damping in the system the reduction in velocity in the 1 Hz region was 55%. In the frequencies around resonance there was a small increase in signal, but the velocity reduction was 97.6%. At higher frequencies the reduction of velocity due to the active damper when compared to the undamped system decreased. As the frequency the advantage of the active system over the undamped system decreases until at 7 Hz the velocities were the same or with in the uncertainties of the measurements.

Summary

The primary aim of the research conducted on the active e.m. damper is to reduce the accelerations experienced by the sprung mass. Other important considerations included the mass and power consumption of the system for use in a lightweight electric vehicle.

Figure 6.20 shows the simulated and experimental results for a undamped suspension system with a pseudo-sinusoidal input compared to an ideal passive system and an active e.m. damper with a Skyhook controller. As expected the undamped passive system shows higher amplitudes near resonance and good attenuation at higher frequencies (above 2 Hz.) There is good correlation between the simulation and the experimental results for the undamped system up to approximately 5 Hz.

The performance of an ideal passive damper was the opposite of the undamped system with a low amplitude near resonance, but poor attenuation above 2 Hz. With automotive suspension systems one ideally wants high damping near the resonant frequency and low damping at frequencies above this. For the ideal passive damper demonstrated in figure 6.20, this should be above 2 Hertz. This highlights the low frequency/high frequency compromise of conventional passive suspension systems.

It should be noted that in this research that above 5 Hz the model does not return a good quantitative result, however the results are still qualitative. At above 5 Hz the signal to noise ratio reduced to the point where the noise strongly interfered

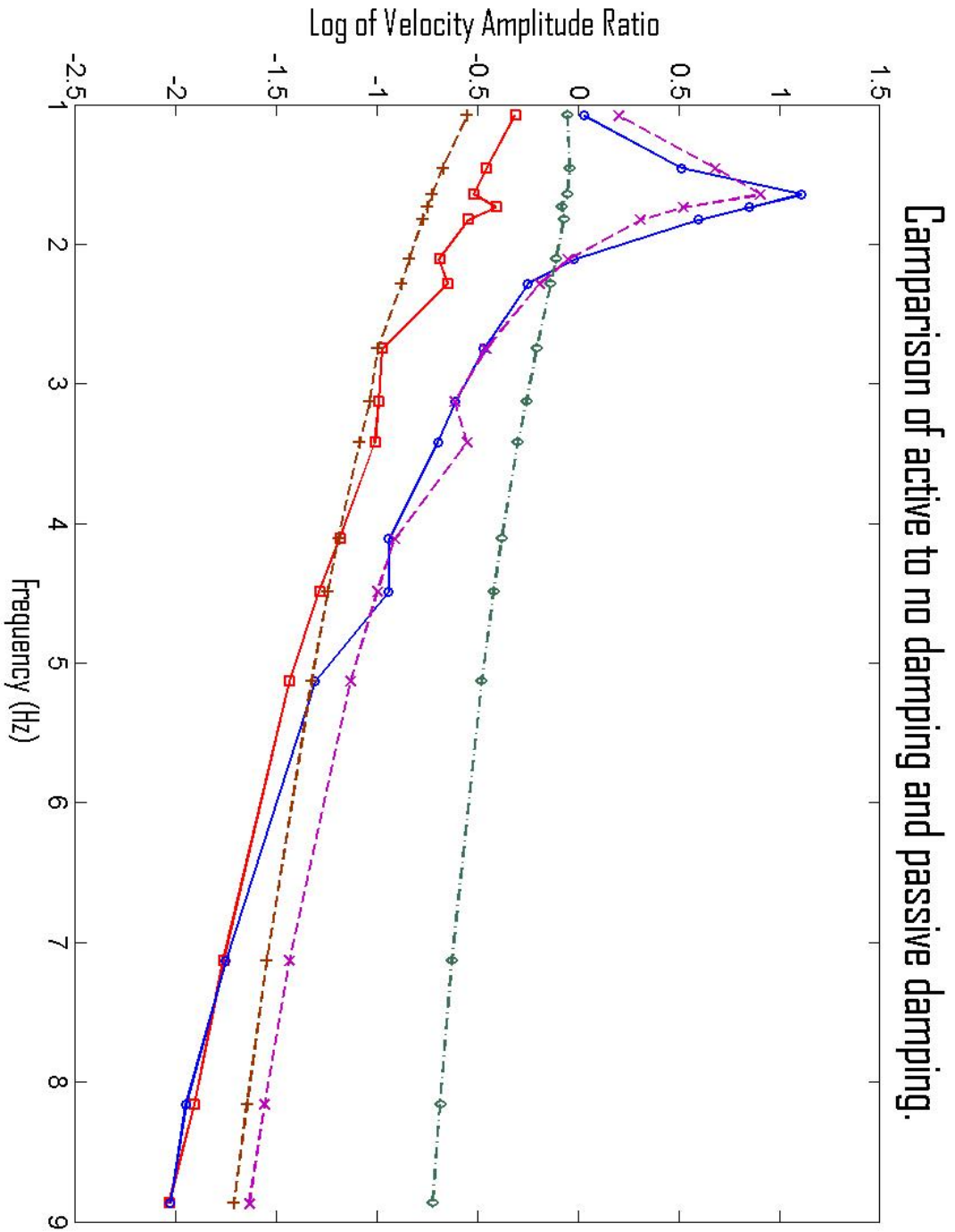Figure 6.20: Active, Passive and No Damping - Frequency Domain. Red '□'s were active experimental. Brown '+'s were active modelled. Blue 'o's were undamped experimental. Purple 'x's were undamped modelled. Green '◇'s were ideal passive modelled.

with the proper control of the active e.m. damper. Also, at frequencies above 5 Hz, primary vibrations in the direction of the damper travel became of similar magnitude as the secondary motions of the sprung mass.

Both the simulated and experimental active e.m. damper, with Skyhook controller, give superior vibration performance compared to the ideal passive damper at all frequencies. There is a good correlation between the simulation and experimental results for the active e.m. damper. This leads to to a high confidence that the model accurately represents the system and can therefore be scaled for real world vehicles.

To obtain the experimental results for the active e.m. damper required the integration of complex componentry and the resolution of many sensor and signal issues that had to be performed in real time. Considering this, the results showed that it is possible to obtain a practical e.m. damper that functions as a full Skyhook damper in the laboratory. The active damper showed a high degree of agreement between experimental results and simulation and the damper exhibited a high degree of authority over the sprung mass. Although very difficult to achieve, this research managed to create Skyhook damping control applied to an active e.m. damper.

6.8   Power consumption

Lightweight electric vehicles have several considerations that are not an issue commercial hydrocarbon fuelled vehicles. Primary amongst these are the extra harshness caused by commercial hydraulic dampers. Another primary consideration is the energy available to the vehicle; the energy storage systems used in electric vehicles have a much lower power density that hydrocarbon based systems.

Therefore, a primary consideration of an active e.m. damper was the power consumed during normal operation. In the VISSIM REALTIME controller, the power demand was determined by the current drawn and the resistance of the coil. In the prototype coil the resistance was measured at 0.22 Ω. The current demanded by the controller was determined by the velocity of the sprung mass relative to an external point. This velocity was multiplied by an externally fixed damping value. Trials showed the most effective damping occurred with the damping value in the range of 100 to 400 Ns/m.

Once the current required was determined, the controller was calibrated so that the output from the DAQ board would produce an output signal of 1 V per Amp of demand. This was then used as an input for a current amplifier. This amplifier was carrying a load of 1 Ω so the current amplifier produced one Amp of output for each Volt of input signal. This was attached directly to the damper coil. The maximum current output was ±6 Amps. If the demand exceeded the available current then the maximum current possible was delivered.

The power consumption of the coil was determined by $P = I^2 R$. The r.m.s values of the power consumption were then recorded. Experimental data was collected

Table 6.5: The r.m.s. power consumption of the prototype damper.

Frequency (Hz)	Power Actual (W)	Power Theory (W)
1.09	0.124	0.055
1.45	0.100	0.058
1.60	0.093	0.058
1.76	0.088	0.058
2.40	0.076	0.055
3.72	0.078	0.046
4.69	0.092	0.034
5.40	0.122	0.028
6.37	0.193	0.028
8.19	0.082	0.020

Table 6.6: The r.m.s. power consumption of the prototype damper at a fixed frequency of 1.45 Hz and varying damper input values.)

Damper Value	Power Actual (W)	Power Model (W)
50	0.094	0.058
100	0.100	0.058
200	0.105	0.058
300	0.1434	0.058
400	0.1781	0.058
500	0.2089	0.058

at frequencies between one and 9 Hz and recorded in table 6.5

In the range between 1 and 4 Hz the theoretical measurements and the experimental measurements were within approximately 1 factor. At above 4 Hz the experimental results were within an order of magnitude of the modelled results. The major cause of this difference conjectured was the accelerometer drift which caused spurious energy demands. This caused large variations in the recorded velocity, even when the mass was motionless. When the mass was being strongly damped the drift signal was on occasion larger than the control signal. This would produce a larger power consumption than was actually required. This accelerometer drift became more apparent above 4 Hz and has an effect larger than at lower frequencies. As could be observed from the theoretical measurements in table 6.5, even with a fixed amplitude input, the power requirement should have reduced at higher frequencies.

For a fixed frequency the power requirements were determined using different damping values. Between the range of damping values of between 100 and 400 Ns/m there was only a small improvement in performance. The vibration apparatus was adjusted to provide a fixed frequency of 1.660 Hz. This frequency was near the resonant frequency of the sprung mass. The experimental and modelled power consumption are given in table 6.6

At lower Damping Values the actual power consumption was within a factor of

the modelled power consumption. Even though the model predicted the same power consumption irrespective of the Damping Value, the experimental damper consumed more power at higher Damper Value settings. A component of this increased power consumption was the damper 'overshooting' the desired damping. This was caused, in part, by the time delay between when the velocity signal enters the controller and the damper signal was enforced. The damper then tried to correct for this new state and could then produce an overshoot in the opposite direction. This ends with a higher power consumption as the controller was always attempting to correct for the velocity that it itself has introduced. It was observed that even with the discrepancies, the power consumption of damper was very low relative to other existing methods of active damping. As low power consumption is vital to the use of an active e.m. damper in a lightweight electric vehicle, further investigation into the use of this damper is a full size vehicle is required.

6.9 Scaling up to a full size car

To determine the feasibility of the active electromagnetic damper as a component of a full size automobile, the two degree of freedom system that was developed in Chapter 5 was used. The two larger magnets used in Chapter 5 were modelled and their fields were determined using the magnet model developed in Chapter 4. This model was then used to determine the forces of a magnet coil system when the magnet was energised to one Ampere. This produced a look up table for use in the damper model.

The car modelled was the University of Waikato Ultracommuter and the values of the suspension system were the same as used in Chapter 5. These are given in table 5.5. The resonant frequency of the sprung and unsprung masses remain the same.

The magnets and coils used in the model were identical to those used previously and are given in table 5.6. The primary difference between the passive damper and the active damper was that the coils were powered to provide active damping.

The effectiveness of the active e.m. damper was determined by the reduction of acceleration in the sprung mass when compared to to a passive damper that was suitable for use in the vehicle. A second major consideration was the power consumption of the damper. As the vehicle was electric powered, a low power consumption was desirable.

A random road profile was constructed using 12 different sine waves ranging from 0.5 Hz to 20 Hz. These were given a phase difference and then summed together. The profile was as illustrated in figure 6.21. This was then used to determine the average accelerations experienced by the passengers of the sprung mass for a passive system, for an active Skyhook damper and an active e.m. damper.

The passive damper and semi-active damper were the same as used for com-
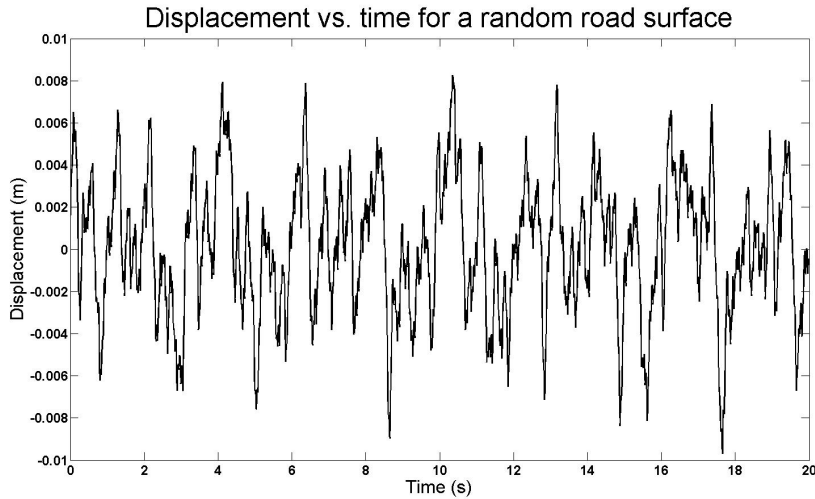
Figure 6.21: A modelled random road surface.

Table 6.7: The two active dampers modelled.

Property	ND3522	ND5550
Number of Magnets	5	1
Number of Coils	6	2
Number of Layers	5	5
Mass (kg)	0.9865	1.3683

parison in Chapter 5. The active damper was modelled using the same N3522 and N5550 magnets that were used in Chapter 5. Two new dampers were modelled, one for each magnet. These dampers were constructed of several coils and one or magnets which travelled axially through the coils, as described in the previous chapter. These dampers are described in table 6.7. The mass given was the mass of the copper wire and the magnets only. This does not include the connections between the vehicle and the magnet, nor the mounting points. Additional mass would be required for the controller and the power switching.

The determination of effectiveness was by comparing the vertical r.m.s. accelerations of the sprung mass of the dampers in the two degree of freedom system that was constructed earlier. As well as an improved acceleration, the active dampers should also be of comparable or lesser mass to the hydraulic passive damper and hydraulic Skyhook damper systems. Further the active e.m. dampers had to have a low power consumption when in use. A comparison of the dampers is given in table 6.8. This was using the same damping coefficient, spring constant and mass values as used in Chapter 5.

The active e.m. damper showed a 61 % reduction in r.m.s acceleration compared to a passive damper with the same damping coefficient. The two active e.m. dampers had very similar accelerations and power consumptions and produced a modelled reduction in r.m.s. acceleration of the sprung mass of 69 % when compared to

Table 6.8: Comparison between a passive, Skyhook and active e.m. damper. Sprung mass = 200kg. unsprung mass = 25 kg.

Damper	R.m.s acceleration (m/s^2)	Power consumption (W)
Passive	0.5597	0
Skyhook	0.2207	0
Active ND3522	0.0640	23
Active ND5550	0.0677	24

the Skyhook damper and 88% when compared to the passive damper. This was a dramatic increase in passenger comfort.

The mass of the copper and the magnets in the damper would be approximately 40 % of the mass the Nissan Pulsar passive damper discussed previously. This would allow extra mass for construction of the connectors and other elements required for a practical damper. The final mass of the damper would be expected to be directly comparable to the mass of a hydraulic passive damper .

The average power consumption was on the order of 24 Watts to achieve this damping. For a vehicle with four wheels, this would produce a total continuous power production on the order of 100 W. In the case of a vehicle such as the University of Waikato's Ultracommuter, this represents an increase of power consumption for lightweight electric vehicle of in the order of 1–2% under normal highway driving conditions. The final power consumption of the vehicle would be directly related to the amplitude of the displacement of the surface that was being traversed. For high quality highway surfaces the power consumption would be less than a corrugated road surface.

6.10 Discussion and conclusions

The use of an electromagnetic active suspension system potentially offers the performance of a fully active hydraulic suspension system with a great reduction in power consumption and mechanical complexity. It was mathematically possible to model the force generated by a coil on a permanent magnet for various currents supplied. This model was tested by examining the maximum force generated by the coil and comparing this to the modelled force. The modelled force was 95% of the measured force. This high degree of agreement in the small scale model proved the theory. Using this theory, it shows that there should be a great reduction in power consumption in normal road operations. To determine if the single degree of freedom damper model was accurate, experimental runs were conducted with a step input. A good relationship was observed between the measured and modelled results.

For the controller, Karnopp's Skyhook was utilised. This used an accelerometer to determine the inertial position and the forces to be generated by the damper.

However, the accelerometer drift was problematic as the accelerometer drift sometimes exceeded the signal being measured. While the use of an Linear Variable Displacement Transducer would produce much reduced noise, this was not a viable option in this case due to the low masses involved. Further research would be required to determine the suitability of an LVDT in a practical automotive application. A simple and fast algorithm was constructed for real time use. This proved effective in this application.

Damping tests were conducting using a vibration rig. The damper was modelled and experimentally measured at frequencies from below the resonant frequency to about 9 Hz. The later frequency was determined by the limits of the experimental apparatus. At all frequencies the active damper showed improved damping performance when compared to a passively damped system. In the frequency range of 1–5 Hz the active damper showed an improved performance when compared to the undamped system. At higher frequencies the performance of the actively damped and the undamped systems approached parity. The amount of authority in the system was high and produced a damping ratios in excess of 1. The actual power consumption of the damper was one to three factors more than was predicted.

The model was then scaled up to produce a quarter car model with two degrees of freedom. This showed that using larger magnets and coils, sufficient power can be produced to create damping authority equal to or in excess of hydraulic dampers. The modelled power consumption would be less than 3% of that used by equivalent active hydraulic dampers. At this low power consumption, it would be practical to use this technology on lightweight electric vehicles.

Chapter 7

Discussion, Conclusions and Recommendations

7.1 Discussion

Introduction

From chapter two it became apparent that there was little information available in regards to lightweight vehicles and in particular lightweight electric vehicles. This lead to several questions: Was it possible to model a passively damped suspension with a linear e.m. element using numerical methods? Was it possible to model an active linear e.m. suspension with a linear e.m. element using numerical methods? Would such a passive system be of practical use in a lightweight electric vehicle? Would such an active system be of practical use in a lightweight electric vehicle?

The objectives of this research was to produce integrated models of a passive and an active electromagnetic damper, then using these models to determine the feasibility of electromagnetic dampers for lightweight electric vehicles, such as constructed by the University of Waikato. Particular areas of interest are in the mass of passive dampers and the mass and power consumption of active dampers.

Modelling was achieved in three parts: the model of the permanent magnet: the models of the dampers and the model of one or two degree of freedom suspension systems.

The Magnet Model

To determine the effectiveness of the passive and active suspension systems proposed it was required to build a model of the permanent magnet. This was then used in the modelled dampers.

Using Maxwell's equation, a numerical model of a magnet was created using the idea of a permanent magnet as a current carrying solenoid. This model was required to produce the magnetic field for a single loop of current at any point. Using this

as a MATLAB function, the magnetic field was determined for a solenoid of 1000 turns. The numerical model constructed produced the magnetic field of the far field, the near field and inside the magnet. By experimental measurement a map of the magnetic field around the magnet was created and compared to a map of the modelled magnetic field. The magnetic fields generated by the magnet as a solenoid and the experimentally measured values agreed to within 91%.

Differences due to the physical limitations of the experimental apparatus had an unreasonably large effect on the comparison between the modelled data and the measured data. To reduce the effect of these anomalous readings two methods were explored. The absolute field strength was summed over all of the points measured in the first method. The modelled absolute field strength was calculated and also summed for the same experimentally measured points. This produced an agreement of 93% between the total values of the modelled and measured fields. However, for several measurements at the ends of the magnet, there was a large discrepancy between the modelled and measured field strength, in part due to difficulty of measurement due to the physical size of the probe previously mentioned. The second method explored the use of the relative differences between the measured and the modelled values. This approach produced an agreement of 91.4%. Using this approach also produced regions where the absolute difference between the measured and absolute field were small yet the percentage difference was over 100 %. This effect was particularly noted where the magnetic field would reverse direction. Removing the most excessive measurements around this region gave a 93.7 % agreement between the measured and experimental values for the magnet. These values too, were within the limitations of the experimental apparatus.

Excluding these anomalous readings the solenoid model of the magnet produced a close approximation of the observed magnetic field. This magnetic field data was then used in producing look up tables for the magnetic field that was used in the magnetic flux in the passive e.m. damper and for the force generated by an active e.m. damper.

The Passive E.M. Damper

To determine whether a passive e.m. damper could provide sufficient damping for use in a practical lightweight electric vehicle, a model of the passive damper first had to be constructed. The theoretical model of the magnet was utilised to determine the flux within a loop of wire created by a magnet. The model was tested experimentally and the flux inside the coil was determined to be 96.6 % of the predicted value. This was then used in a VISSIM model to determine the forces generated by the passive damper, by using Faraday's Law.

A single degree of freedom test rig was constructed and this was tested using a variety of weights as the sprung mass for a step input. The behaviour of the sprung

mass was recorded and the modelled and experimental results were compared. There was a greater than 80 % agreement between the results.

The passive e.m. suspension system was also tested with a psuedo-sine wave input at a variety of frequencies. For frequencies in the range 1-4 Hz there was a close relationship between the modelled and experimental data. At frequencies over 4 Hz, secondary effects dominated and qualitative results were achieved rather than quantitative results.

A good measure of agreement was achieved between the modelled and experimental results in both the time and frequency domains. The passive and active e.m. damper models were used to simulate the two theoretical suspension systems. These two modelled suspension systems were then used to determine if the e.m. dampers could be adapted for use on private automobiles. These two models were tested using a two degree of freedom system and the damping coefficient was determined. This result was then compared to the damping coefficient that was determined using damping theory. It was determined that this damping coefficient was achievable by constructing the dampers of multiple magnets and multiple coils, of which each coil had multiple layers. For a passive e.m. damper using a ND3522 magnet the mass of magnets and copper required was 4.75 kg and for the ND5550 magnet, the mass of magnets and copper required would be 7.61 kg. These weights, before taking into account any fittings required for the structural integrity of the e.m. damper, were greater than were measured for a typical commercial hydraulic damper. It could not determined that the passive e.m. damper offered any significant advantages over commercially available hydraulic passive dampers and for practical purposes the passive e.m. damper offered no advantage over a passive hydraulic damper except for possible specialist applications. While linear passive e.m. dampers may have secondary uses and applications, they are not suitable for use in lightweight electric vehicles.

The Active E.M. Damper

The use of an electromagnetic active suspension system potentially offers the performance of a fully active hydraulic suspension system. This would be achieved with a great reduction in the power consumption and mechanical complexity system. The forces generated by a coil on a permanent magnet were mathematically modelled for various supply currents. The maximum force generated by the coil was modelled and compared to the modelled force. The modelled damper achieved 95% of the maximum force when compare to the measured force. The model showed that the power consumption in a linear e.m. was greatly reduced when compared to a commercial hydraulic active damper system.

To determine the accuracy of model of the single degree of freedom damper, experimental runs were conducted with a step input. A good relationship was observed

between the modelled and measured results.

In the case of the active e.m. suspension, Karnopp's Skyhook ws utilised for the controller. By use of an accelerometer, the inertial velocity and the forces to be generated by the damper were determined. In practical application, the accelerometer drift was problematic and the accelerometer drift could exceed the signal being measured. By use of an Linear Variable Displacement Transducer, the noise could be significantly reduced. However this was not a viable option in this case due to the low masses involved and the size of the forces required to operate an LVDT. Further research would be required to determine the suitability of an LVDT in a full scale automotive application. A simple and fast algorithm to reduce the accelerometer drift was constructed for real time use. This proved effective in this application.

A vibration rig was constructed and used in a series of damping tests. The damping effect of the active e.m. system was modelled and experimentally measured at frequencies from below the resonant frequency to approximately 9 Hz. Limits in the experimental apparatus determined the maximum frequency tested. The active damper showed improved damping performance when compared to a passively damped system for all frequencies tested. In the frequency range of 1–5 Hz, the active damper showed an improved performance when compared to the undamped system. The performance of the actively damped and the undamped systems approached parity at frequencies above 5 Hz. Damping ratios in excess of 1 were produced by the active e.m. damper and the system exhibited a high degree of authority over the sprung mass vibration. The measured power consumption of the damper higher than simulated by one to three factors.

The active e.m. damper model was then scaled up and used in a quarter car model with two degrees of freedom. By using larger magnets and coils, sufficient power could be produced to create a damping authority equal to or in excess of hydraulic dampers. The modelling showed that the power consumption of the active e.m. element would be less than 3% of that used by equivalent active hydraulic dampers and less than 2 % of the power used by a lightweight electric vehicle for propulsion. At this level of power consumption, it would be practical to use this technology on lightweight electric vehicles in the University of Waikato fleet.

7.2   Conclusions

Returning to the original four questions that were posed at the conclusion of the literature review, it is now possible to answer these.

For an integrated model of a simple passive linear e.m. damper consisting of cylindrical coils and cylindrical magnets for use in light weight electric vehicles; there was a good correlation between the model and experimental data.

For determination of the effectiveness of the linear passive e.m. damper for use in lightweight electric vehicles; there was a good correlation between the experimental and modelled results. When scaled up to a lightweight electric vehicle this showed that while a damper could constructed with damping sufficient damping force, it was impractical due to weight considerations.

In the case of an integrated model of a simple active passive linear e.m. damper consisting of cylindrical coils and cylindrical magnets for use in lightweight electric vehicles. a good correlation between modelled and measured results was achieved.

In the determination of the effectiveness of the linear active e.m. damper for use in lightweight electric vehicles; there was a good correlation between the experimental and modelled results. This demonstrated that similar or the same effects as an active hydraulic damper could be achieved with much reduced power consumption and complexity.

7.3 Further work

There are two major areas for future work based upon the low power active linear e.m. damper: improving the accuracy of the model and improving the effectiveness of the damper.

Improving the modelling

To fully test the model of the active e.m. suspension system, full size quarter car should be constructed. This should then be tested on a large scale commercial vibration rig. This research would ensure the scaling up of the mathematical model is accurate. With a model of this scale an LVDT can be used for more accurate input of the position of the sprung mass relative to the unsprung mass.

A full scale suspension system should be constructed for use in the fleet of University of Waikato electric vehicles. This would give real world data on the power consumption and the effectiveness of the damper on highways and during general motoring.

Improving the damper

One of the potential advantages of an active suspension system is the ability to coordinate the actions of all the dampers mounted on the vehicle. By integrating the system with the control system with the vehicle the dampers can be activated to to counter vehicle 'squat', 'nose dive' and 'roll'. This should be researched with the active e.m dampers on a prototype automobile.

Another area that should be researched to improve the real world performance of an actively damped vehicle is the use of vehicle preview with the e.m. dampers in a light weight electric vehicle. As large motions of the wheels produce large power demands in the active damper system, by reducing demand at these times could reduce the vehicles power consumption even further.

Further research could be conducted into the construction of a fully integrated linear active electromagnetic suspension system for the University of Waikato's fleet of electric vehicles. This suspension would co-ordinate the input from the vehicle controls with a road preview system. This currently offers the most effective system with the lowest power consumption.

References

Agutu, W. O. *CHARECTERISZATION OF ELECTROMAGNETIC INDUCTION DAMPER*. Master's thesis, Miami University, Oxford, Ohio (2007).

Akyel, C., S. Babic, and S. Kincic. New and fast procedures for calculating the mutual inductance of coaxial circular coils (circular coil-disk coil). *Magnetics, IEEE Transactions on*, **38(5)**, pp. 2367–2369 (2002).

Akyel, C., S. I. Babic, and M.-M. Mahmoudi. Mutual inductance calculation for non-coaxial circular air coils with parallel axes. *Progress In Electromagnetics Research*, **91**, pp. 287–301 (2009).

Alanoly, J. and S. Sankar. A new concept in semi-active vibration isolation. *Transactions of the ASME: Journal of Mechanisms, Transmissions, and Auomation in Design*, **109**, pp. 242–7 (1987).

Amati, N., A. Canova, F. Cavalli, S. Carabelli, A. Festini, A. Tonoli, and G. Caviasso. Electromagnetic shock absorbers for automotive suspensions: Electromechanical design. In: *Proceedings of ESDA2006*, pp. 131–140. Torino, Italy (2006).

Amati, N., A. Festini, and A. Tonoli. Design of electromagnetic shock absorbers for automotive suspensions. *Vehicle System Dynamics*, **49(12)**, pp. 1913–28 (2011).

Babic, S. and C. Akyel. Magnetic force between inclined circular filaments placed in any desired position. *Magnetics, IEEE Transactions on*, **48(1)**, pp. 69–80 (2012).

Babic, S. I. and C. Akyel. Calculating mutual inductance between circular coils with inclined axes in air. *Magnetics, IEEE Transactions on*, **44(7)**, pp. 1743–1750 (2008).

Barton, M. and Z. Cendes. New vector finite elements for three-dimensional magnetic field computation. *Journal of Applied Physics*, **61(8)**, pp. 3919–3921 (1987).

Bathe, K.-J. *Finite element procedures*. Klaus-Jurgen Bathe (2006).

Besinger, F., D. Cebon, and D. Cole. An experimental investigation into the use of semi-active dampers on heavy lorries. *12th IAVSD Symposium*, **20** (1991).

Browne, A. and J. Hamburb. On road measurement of the energy dissipated in automotive shock absorbers. In: *Symposium on Simulation and Control of Ground Vehicles and Transportation Systems*, volume 2, pp. 167–86 (1986).

Campos, J., L. Davis, F. Lewis, S. Ikenaga, S. Scully, and M. Evans. Active suspension control of ground vehicle heave and pitch motions. In: *Proceedings of the 7th Mediterranean Conference on Control and Automation*, pp. 222–33. Haifa, Israel (1999).

Chaves, M., I. Martins, J. Maia, and J. Esteves. Experimental implementation of an electromagnetic automobile suspension system. In: *Proceedings of the 11th mederterranean Conference on Control and Automation*, p. 5 (2003).

Choi, S. B., Y. T. Choi, E. Chang, S. Han, and C. S. Kim. Control characteristics of a continuously variable er damper. *Mechatronics*, **8**, pp. 143–61 (1996).

Choi, S. B. and W.-K. Kim. Vibration control of a semi-active suspension featuring electrorheological fluid dampers. *Journal of Sound and Vibration*, **234(3)**, pp. 537–46 (1999).

Crosby, M. and D. Karnopp. The active damper: a new concept for shock and vibration control. *Shock and Vibration Bulletin*, **43 part 4**, pp. 119–33 (1973).

Dixit, R. *Sliding mode observation and control for semiactive vehicle suspensions*. Ph.D. thesis, North Carolina State University (2001).

Dixon, J. *The Shock Absorber handbook*. SAE, Warrendale, Pa (1996).

Dixon, J. *Tires, Suspension and Handling*. John Wiley and sons, Warrendale, Pa, second edition (1999).

Duke, M. *Investigation into low power active elements in vehicle suspensions with particular reference to tractor seats*. Ph.D. thesis, South Bank University (1997).

Duke, M. and A. Fow. Comparison of simulation and experimental results of a tractor seat with nonlinear stiffness and dead-band damping. *Journal of vibration and acoustics*, **134(5)** (2012).

Ebrahimi, B., M. Khamesee, and F. Golnaraghi. Design and modelling of a magnetic shock absorber based on eddy current damping effect. *Journal of sound and vibration*, **315**, pp. 875–889 (2008).

Ebrahimi, B., M. Khamesee, and F. Golnaraghi. Eddy current damper feasibility in automobile suspension: modeling, simulation and testing. *Smart Materials and Structures*, **18(1)**, p. 015017 (2009a).

Ebrahimi, B., M. Khamesee, and F. Golnaraghi. A novel eddy current damper: theory and experiment. *Journal of Physics D: Applied Physics,*, **42(7)**, p. 075001 (6 Pages) (2009b).

Ebrahimi, B., M. Khamesee, and M. Golnaraghi. Design of an electromagnetic shock absorber. *ASME 2007 International Mechanical Engineering Congress and Exposition, 11-5 November, Seattle, Washington, USA*, **9**, pp. 2009–14 (2007).

Elbeheiry, E. M. Suboptimal bilinear control methods applied to supressing car vibrations. *Journal of Vibration and Control*, **7**, pp. 276–306 (2001).

Esmailzadeh, E. and F. Fahimi. Optimal adaptive active suspensions for a full car model. *Vehicle Syetm Dynamics*, **27**, pp. 89–107 (1997).

Fialho, I. and G. J. Balas. Road adaptive suspension design using linear parameter-varying gain-scheduling. *IEEE Transactions on Control Systems Technology*, **10(1)**, pp. 249–67 (2002).

Firestone, F. A. A new analogy between mechanical and electrical systems. *Acoustical Society of America*, **4**, pp. 249–67 (1933).

Fodor, M. and R. Redfield. The variable linear transmission for regenerative damping in vehicle suspension control. *Vehicle System Dynamics*, **22**, pp. 1–20 (1993).

Fujiwara, K., T. Adachi, and N. Takahashi. A proposal of finite-element analysis considering two-dimensional magnetic properties. *Magnetics, IEEE Transactions on*, **38(2)**, pp. 889–892 (2002).

Gillespie, T. D. *Fundamentals of Vehicle Dynamics*. Society of Automotive Engineers (1992).

Goldner, R. and P. Zerigian. A preliminary study of energy recovery in vehicles by using regenerative magnetic shock absorbers. Technical report, SAE (2001).

Goldner, R. and P. Zerigian. Electromagnetic linear generator and shock absorber,. US Patent 6952060 (2005).

Graves, K., P. Iovenitti, and D. Toncich. *Electromagnetic energy regenerative vibration damping*. Ph.D. thesis, Swinburne University of Technology (2000a).

Graves, K., P. Iovenitti, and D. Toncich. Electromagnetic regenerative damping in vehicle suspension systems. *International Journal of Vehicle Design*, **24(2-3)**, pp. 182–197 (2000b).

Gupta, A., J. Jendrzejczyk, T. Mulcahy, and J. Hull. Design of electromagnetic shock absorbers. *International Journal of Mechanics and Materials in Design*, **3(3)**, pp. 285–291 (2006).

Gupta, A., T. M. Mulcahy, and J. R. Hull. Electromagnetic shock absorbers. In: *XXI International Modal Analysis Coneference Proceedings , Paper*, volume 181, pp. 3–6 (2003).

Gysen, B., J. Janssen, J. Paulides, and E. Lomonova. Design aspects of an active electromagnetic suspension system for automotive applications. *IEEE Transactions on Industry Applications*, **25(5)**, pp. 1589–97 (2008a).

Gysen, B., J. Paulides, J. Janssen, and E. Lomonova. Active electromagnetic suspension system for improved vehicle dynamics. In: *IEEE Vehicle Power and Propulsion Conference.* Harbin, China (2008b).

Hashiyama, T., T. Furuhashi, and Y. Uchikawa. A study on finding fuzzy rules for semi-active suspension controllers with genetic algorithm. In: *Evolutionary Computation, 1995, IEEE International Conference on*, volume 1, p. 279 (1995).

Hedrick, J. and D. Wormley. Active suspensions for ground transport vehicles em a state of the art review. *ASMA, Applied Mechanics Divison, Nov 30-Dec 5, Houston Texas*, **15**, pp. 21–3 (1975).

Hong, K.-S., S. C. andY.T. Choi, and N. Wereley. Non-dimensional analysis for effectic design of semi-active electrorheological damping control systems. *Proceedings of the Institution of Mechanical Engineers, Part D: Journal of Automobile Engineering*, **217**, pp. 1095–1106 (2002a).

Hong, K.-S., H.-C. Sohn, and J. K. Hedrick. Modified skyhook control of semi-active suspensions : A new model, gain scheduling, and hardware-in-the-loop tuning. *Transactions of the ASME*, **124**, pp. 158–67 (2002b).

Huisman, R. A literauture research into active and semi-active vehicle suspensions with and without preview. Eindhoven (1990).

Ibrahim, I. M. and S. M. El-Demerdash. Investigation of wheeled tractors ride comfort using hydraulic semi-active suspension system. Technical report, International Truck and Bus Meeting and Exposition, Detroit, Michigan. SAE Technical Papers (1999).

Jalili, N. A comparative study and analysis of semi-active vibration-control systems. *Journal of vibration and acoustics*, **124(4)**, pp. 593–605 (2002).

Ji, J., L. Zheng, and Y. n. Li. A comparative study on the control strategies in vehicle suspension. In: *ICMIT 2005: Control Systems and Robotics*, pp. 604211–604211. International Society for Optics and Photonics (2005).

Jiles, D. *Introduction to Magnetism and magnetic materials.* Chapman and Hall/CRC, Boca Raton, second edition (1998).

Jolly, M. and D. Margolis. Regenerative systems for vibration control. *Transactions of the ASME*, **119**, pp. 208–15 (1997).

Kanamori, M. and Y. Ishihara. Finite element analysis of an electromagnetic damper taking into account the reaction of the magnetic field. *JSME international journal. Ser. 3, Vibration, control engineering, engineering for industry*, **32(1)**, pp. 36–43 (1989).

Kanamori, M., Y. Ishihara, and T. Tokadaka. An optimum design technique for a passive electromagnetic damper. *Elektrotechnicky Casopis*, **45(1)**, pp. 3–7 (1994).

Karnopp, D. Active damping in road vehicle suspension systems. *Vehicle System Dynamics*, **12(5)**, pp. 291–316 (1983).

Karnopp, D. Theoretical limitations in active vehicle suspensions. *Vehicle System Dynamics*, **15(1)**, pp. 41–54 (1986).

Karnopp, D. Force generation in semi-active suspensions using modulated dissipative elements. *Vehicle System Dynamics*, **16(5-6)**, pp. 333–43 (1987).

Karnopp, D. Permanent magnet linear motors used as variable mechanical dampers in vehicle suspensions. *Vehicle Systems Dynamics*, **18(4)**, pp. 187–200 (1989).

Karnopp, D., M. Crosby, and R. Harwood. Vibration control using semi-active force generators. *Transactions of the ASME: Journal for Industry for Industry*, **96(2)**, pp. 619–26 (1974).

Kawamoto, Y., Y. Suda, H. Inque, and T. Kondo. Modeling of electrommagnetic damper for automobile suspension. *Journal of System Design and Dynamics,*, **1(3)**, pp. 524–35 (2007).

Kim, H.-J., H. S. Yang, and Y.-P. P. . Improving the vehicle performance with active suspension using road-sensing algorithm. *Computers and Structures*, **80**, pp. 1569–77 (2002).

Kim, J. H. and C. W. Lee. Semi-active damping control of suspension systems for specified operational response mode. *Journal of sound and vibration*, **260(2)**, pp. 307–28 (2003).

Kim, S. Er suspension system with energy generation. *Journal of Intelligent Material Systems and Structures*, **10**, pp. 738–742 (1999).

Kim, S. and Okade. Variable resistance type energy regenerative damper using pulse width modulated step-up chopper. *Journal of Vibration and Acoustics*, **124**, pp. 110–5 (2002).

Kim, Y., W.-G. Hwang, C.-D. Kee, and H.-B. YI. Active vibration control of a suspension system using an electromagnetic damper. *Proceedings of the Institution of Mechanical Engineers*, **215 Part D**, pp. 865–73 (2001).

Kitching, K. J., D. J. Cole, and D. Cebon. Performance of a semi-active damper for heavy vehicles. *Journal of dynamic systems, measurement, and control,*, **122(3)**, pp. 498–506 (2000).

Krasnicki, E. J. Comparison of analytical and experimental results for a semi-active vibration isolator. *The Shock and Vibration Bulletin*, **50(9)**, pp. 69–76 (1980).

Kuns, K. Calculation of magnetic field inside plasma chamber. *UCLA report*, **2(3)**, pp. 1–11 (2007).

Lauwerys, C., J. Swervers, and P. Sas. Linear control of car suspension using nonlinear actuator control. In: *ISMA 2002 International Conference on Noise and Vibration Engineering*, pp. 55–62. Katholieke Universieit Leuven, Leuven, Belgium (2002).

Lauwerys, C., J. Swevers, and P. Sas. Model free control design for a semi-active suspension of a passenger car. *Proceedings of ISMA, Leuven*, pp. 75–86 (2004).

Lee, H.-S. and S.-B. Choi. Control and response characteristics of a magneto-rheological fluid damper for passenger vehicles. *Journal of Intelligent Material Systems and Structures*, **11**, pp. 80–87 (2000).

Liu, J. and K. Liu. A tunable electromagnetis vibration absorber: Characterization and application. *Journal of Sound and Vibration*, **295**, pp. 708–24 (2006).

Longhurst, C. The suspension bible. *Car Bibles* (2006).

Mailat, F., S. Donescu, and V. Chiroiu. On the automotive semi-active suspensions. *Proc. of the Romanian Academy, Series A: Mathematics, Physics, Technical Sciences, Information Science*, **5(1)**, pp. 47–54 (2004).

Maleki, N., A. K. Sedigh, and B. Labibi. Robust model reference adaptive control of active suspension systems. *Opt. Express*, **11(14)**, pp. 1709–13 (2003).

Martins, I., J. Esteves, G. Marques, and F. P. da Silva. Permanent-magnets linear actuators applicability in automobile active suspensions. *IEEE Transactions on Vehicular Technology*, **55(1)** (2006).

Martins, I., J. Esteves, F. P. da Silva, and P. Verdelho. Electromagnetic hybrid active-passive vehicle suspension. In: *IEEE Vehicular Technology Conference*, volume 3, pp. 2273–7 (1999).

Marzbanrad, J., G. Ahmadi, Y. Hoijat, and H. Zohoor. Optimal active control of vehicle suspension systems including time delay and preview for rough roads. *Journal of Vibration and Control*, **8(7)**, pp. 967–991 (2002).

Marzbanrad, J., Y. Hoijat, H. Zohoor, and S. Nikravesh. Optimal preview control design for an active suspension based on a full car model. *Scientia Iranica*, **10(1)**, pp. 23–36 (2003).

Matsuoka, T. and K. Ohmata. A study of a magnetic damper using rare-earth magnets and a pinned displacement magnifying mechanism. *International Journal of applied Electromagnetics and Mechanics*, **13(1-4)**, pp. 263–70 (2002).

Mirzaei, S. A flexible electromagnetic damper. *Electric Machines and Drives Conference, 3-5 May, Antalya*, **2**, pp. 959–62 (2007).

Mirzaei, S., S. Saghaiannejad, V. Tahani, and M. Moallem. Electromagnetic shock absorber. *IEEE International Electric Machines and drives Conference, 2001, Cambridge, MA, USA*, pp. 760–4 (2001).

Nakano, K., Y. Suda, and S. Nakadai. Self-powered active vibration control using a single electric actuator. *Journal of Sound and Vibration*, **260**, pp. 213–35 (2003).

Nakata, T. and N. Takahashi. Direct finite element analysis of flux and current distributions under specified conditions. *Magnetics, IEEE Transactions on*, **18(2)**, pp. 325–330 (1982).

Papagergiou, C. and M. Smith. Labatory experimental testing of inerters. In: *Proceedings of the 44th IEEE Conference on Decision and Control and the European Control Conference*, pp. 3351–6. Seville, Spain (2005).

Paschedag, T., A. Giua, and C. Seatzu. Constrained optimal control: an application to semiactive suspension systems. in control and automation. *MED'06. 14th Mediterranean Conference, IEEE.*, pp. 1–8 (2006).

Phule, P. Magnetorheological (mr) fluids: Principles and applications. *Smart Materials Bulletin*, **2001(2)**, pp. 7–10 (2001).

Rabinow, J. Magnetic fluid shock absorber. US Patent 2667237 (1954). Filed 1948.

Ravaud, R., G. Lemarquand, S. Babic, V. Lemarquand, and C. Akyel. Cylindrical magnets and coils: Fields, forces, and inductances. *Magnetics, IEEE Transactions on*, **46(9)**, pp. 3585–3590 (2010).

Redfield, R. C. Performance of low-bandwidth, semi-active damping concepts for suspension control. *Vehicle System Dynamics*, **20(5)**, pp. 245–67 (1991).

Sammier, D., O. Sename, and L. Dugard. Skyhook and h8 control of semi-active suspensions: Some practical aspects. *Vehicle System Dynamics*, **39(4)**, pp. 279–308 (2003).

Sapinski, B. An experimental electromagnetic induction device for a magnetorheological damper. *Journal of Theoretical and Applied Mechanics*, **46(4)**, pp. 933–47 (2008).

Sharp, R. and S. A. Hassan. The relative performance capabilities of passive, active and semi-active car suspension systems. *Proceedings Institution Mechanical Engineers*, **200(D3)**, pp. 219–228 (1986).

Simanaitis., D. J. Shock absorbers. *Automotive Engineering*, **84(11)**, pp. 34–9 (1976).

Simeu, E. and D. Georges. Modeling and control of an eddy current brake. *Control Engineering Practice*, **4(1)**, pp. 19–26 (1996).

Simon, D. E. and M. E. V. T. Ahmadian. An alternative semiactive control method for sport utility vehicles. *Proceedings of the Institution of Mechanical Engineers, Part D: Journal of Automobile Engineering*, **216(2)**, pp. 129–39 (2002).

Smith, M. The inerter concept and its application. Plenary Lecture, Society of Instrument and Control Engineers (SICE) Annual Conference, Fukui, Japan (2003).

Smith, M. C. Synthesis of mechanical networks: The inerter. *IEEE Transactions on Automatic Control*, **47(10)**, pp. 1648–62 (2002).

Smith, M. C. and F.-C. Wang. Performance benefits in passive vehicle suspensions employing inerters. *Vehicle System Dynamics*, **42(4)**, pp. 235–57 (2004).

Sodano, H., D. J. Bae, J.-S.a nd Inman, and W. K. Belvin. Improved concept and model of eddy current damper. *transactions of the ASME*, **128**, pp. 294–302 (2006).

Strang, W. G. and G. J. Fix. *Analysis of the finite element method*. Prentice-Hall (1973).

Suda, Y., S. Nakadai, and K. Nakano. Hybrid suspension system with skyhook control and energy regeneration. *Vehicle System Dynamics Supplement*, **28**, pp. 619–34 (1998).

Suda, Y. and T. Shiba. A new hybrid suspension system with active control and energy regeneration. *Vehicle System Dynamics Supplement*, **25**, pp. 641–54 (1996).

Systems, D. A. Magneride performance and challenges (2008).

Turkay, S. and H. Akcay. Aspects of achievable performance for quarter-car active suspensions. *Journal of Sound and Vibration*, **311**, pp. 440–60 (2008).

Turnip, A., K. S. Hong, and S. Park. Control of a semi-active mr-damper suspension system: A new polynomial model. *Proceedings, The International Federation of Automatic Control*, pp. 4683–4688 (2008).

Valášek, M., M. Novak, Z. Šika, and O. Vaculin. Extended ground-hook-new concept of semi-active control of truck's suspension. *Vehicle system dynamics*, **27(5-6)**, pp. 289–303 (1997).

Wang, F.-C., M.-F. Hong, and T.-C. Lin. Designing and testing a hydraulic inerter. *Journal of Mechanical Engineering Science*, **225(1)**, pp. 66–72 (2011).

Wang, F.-C. and W.-J. Su. Inerter nonlinearities and the impact on suspension control. In: *2008 American Control Conference*, pp. 3245–50 (2008).

Wendel, G. and G. Stecklein. Regenerative active suspension. Technical Report 882, SAE Special Publications (1991).

Williams, D. E. and W. M. Haddad. Active suspension control to improve vehicle ride and handling. *Vehicle System Dynamics*, **29**, pp. 1–24 (1997).

Williams, R. A. Automotive active suspensions part 2: practical considerations. *Vehicle System Dynamics*, **211(6)**, pp. 427–44 (1997).

Wilson, D. A., R. Sharp, and S. Hassan. The application of linear optimanl control theory to the design of active automotive suspensions. *Vehicle System Dynamics*, **15**, pp. 105–18 (1986).

Winslow, W. Induced fibration of suspensions. *Journal of Apllied Physics*, **20(12)**, pp. 1137–40 (1949).

Yan, G. and L. Zhou. Integrated fuzzy logic and genetic algorithms for multi-objective control of structures using mr dampers. *Journal of Sound and Vibration*, **296(1)**, pp. 368–82 (2006).

Yao, G., F. F. Yap, G. Chen, W. Li, and S. Yeo. Mr damper and its application for semi-active control of vehicle suspension system. *Mechatronics*, **12**, pp. 963–73 (2002).

Yi, K. and B. S. Song. A new adaptive sky-hook control of vehicle semi-active suspensions. *Proceedings of the Institution of Mechanical Engineers, Part D: Journal of Automobile Engineering*, **213(3)**, pp. 293–303 (1999).

Yoshimura, T., A. Kume, M. Kurimoto, and J. Hino. Construction of an active suspension system of a quarter car model using teh concept of slidinng mode control. *Journal of Sound and Vibration*, **239(2)**, pp. 187–99 (2001).

Zhang, Y., T. Mulcahy, and J. H. Hull. Experimental verification of energy-regenerative feasibility for an automotive electrical suspension system. In: *ICVES*, pp. 1–5 (2007).

Zhang, Y., F. Yu, Y. Gu, and X. Zheng. Isolation and energy-regenerative performance experimental verification of automotive electrical suspension. *Journal of Shanghai Jiaotong University*, **42(6)**, pp. 874–877 (2008).

Zhang, Y., F. Yu, K. Huang, and Y. Gu. Permanentmagnet dc motor actuators application in automotive energy-regenerative active suspension. SAE technical Paper 2009-01-0227 (2009).

Zheng, S.-Y., X.-H. Pan, and Z.-F. Ma. Studies on a passive electromagnetic damper. *Journal of Zhejiang University Science A, Suppl. II*, pp. 271–6 (2006).

Zienkiewicz, O., A. Bahrani, and P. Arlett. Solution of three-dimensional field problems by the finite element method. *The Engineer*, **27** (1967).

Zienkiewicz, O., Z. Taylor, and J. Zhu. The finite element method: its basis and fundamentals (2005).

Zienkiewicz, O. C. and R. L. Taylor. *The finite element method: Solid mechanics*, volume 2. Butterworth-heinemann (2000).